JAAVSO

Volume 39
Number 1
2011

The Journal of the American Association of Variable Star Observers

VX Hya: Sudden Change in a Pulsating Star

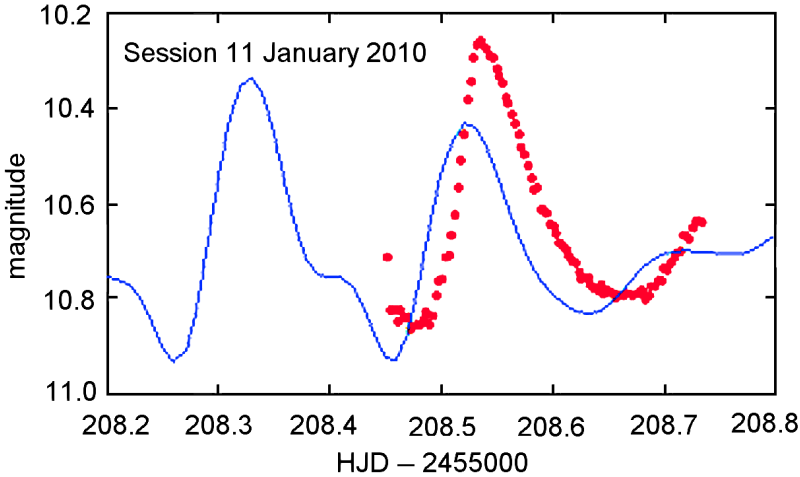

VX Hya light curve for 11 January 2010. The observations are 15 minutes late from the (1,0) pulsation and 40 mn from the (0,1) pulsation of the model.

Also in this issue...

- Studies of "Irregularity" in Pulsating Red Giants
- The Orbital Period of Three Cataclysmic Variables from WASP Data
- The Z CamPaign: Year 1

Complete table of contents inside...

THE AMERICAN ASSOCIATION OF VARIABLE STAR OBSERVERS
FOUNDED 1911

49 Bay State Road
Cambridge, MA 02138
U. S. A.

The Journal of the American Association of Variable Star Observers

ISSN 0271-9053

JAAVSO

The Journal of
The American Association
of Variable Star Observers

Volume 39
Number 1
2011

ISSN 0271-9053

49 Bay State Road
Cambridge, MA 02138
U. S. A.

The *Journal of the American Association of Variable Star Observers* is a refereed scientific journal published by the American Association of Variable Star Observers, 49 Bay State Road, Cambridge, Massachusetts 02138, USA. The *Journal* is made available to all AAVSO members and subscribers.

In order to speed the dissemination of scientific results, selected papers that have been refereed and accepted for publication in the *Journal* will be posted on the internet at the *eJAAVSO* website as soon as they have been typeset and edited. These electronic representations of the *JAAVSO* articles are automatically indexed and included in the NASA Astrophysics Data System (ADS). *eJAAVSO* papers may be referenced as *J. Amer. Assoc. Var. Star Obs., in press,* until they appear in the concatonated electronic issue of *JAAVSO*. The *Journal* cannot supply reprints of papers.

Page Charges

Unsolicited papers by non-Members will be assessed a charge of $15 per published page.

Instructions for Submissions

The *Journal* welcomes papers from all persons concerned with the study of variable stars and topics specifically related to variability. All manuscripts should be written in a style designed to provide clear expositions of the topic. Contributors are strongly encouraged to submit digitized text in MS WORD, LATEX+POSTSCRIPT, or plain-text format. Manuscripts may be mailed electronically to journal@aavso.org or submitted by postal mail to *JAAVSO*, 49 Bay State Road, Cambridge, MA 02138, USA.

Manuscripts must be submitted according to the following guidelines, or they will be returned to the author for correction:

Manuscripts must be:
1) original, unpublished material;
2) written in English;
3) accompanied by an abstract of no more than 100 words.
4) not more than 2,500–3,000 words in length (10–12 pages double-spaced).

Figures for publication must:
1) be camera-ready or in a high-contrast, high-resolution, standard digitized image format;
2) have all coordinates labeled with division marks on all four sides;
3) be accompanied by a caption that clearly explains all symbols and significance, so that the reader can understand the figure without reference to the text.

Maximum published figure space is 4.5" by 7". When submitting original figures, be sure to allow for reduction in size by making all symbols and letters sufficiently large.

Photographs and halftone images will be considered for publication if they directly illustrate the text.

Tables should be:
1) provided separate from the main body of the text;
2) numbered sequentially and referred to by Arabic number in the text, e.g., Table 1.

References:
1) References should relate directly to the text.
2) References should be keyed into the text with the author's last name and the year of publication, e.g., (Smith 1974; Jones 1974) or Smith (1974) and Jones (1974).
3) In the case of three or more joint authors, the text reference should be written as follows: (Smith *et al.* 1976).
4) All references must be listed at the end of the text in alphabetical order by the author's last name and the year of publication, according to the following format:
   Brown, J., and Green, E. B. 1974, *Astrophys. J.*, **200**, 765.
   Thomas, K. 1982, *Phys. Report*, **33**, 96.
5) Abbreviations used in references should be based on recent issues of the Journal or the listing provided at the beginning of *Astronomy and Astrophysics Abstracts* (Springer-Verlag).

Miscellaneous:
1) Equations should be written on a separate line and given a sequential Arabic number in parentheses near the right-hand margin. Equations should be referred to in the text as, e.g., equation (1).
2) Magnitude will be assumed to be visual unless otherwise specified.
3) Manuscripts may be submitted to referees for review without obligation of publication.

Journal of the American Association of Variable Star Observers
Volume 39, Number 1, 2011

Studies of "Irregularity" in Pulsating Red Giants. III. Many More Stars, an Overview, and Some Conclusions
John R. Percy, Emil Terziev 1

VX Hydrae: Observation of a Sudden Change in a Pulsating Star
Michel Bonnardeau, Shawn Dvorak, Rudy Poklar, Gerard Samolyk 10

Recent Maxima of 56 Short Period Pulsating Stars
Gerard Samolyk 23

The Variable Star HD 173637
Arlo U. Landolt 32

CI Cygni 2010 Outburst and Eclipse: An Amateur Spectroscopic Survey—First Results From Low Resolution Spectra
François Teyssier 41

The Orbital Period of Three Cataclysmic Variables From WASP Data
Patrick Wils 60

The Z CamPaign: Year 1
Mike Simonsen 66

The First Historical Standstill of WW Ceti
Mike Simonsen, Rod Stubbings 73

Leo5 is a Z Cam Type Dwarf Nova
Patrick Wils, Tom Krajci, Mike Simonsen 77

Do Eclipsing Variable Stars Show Random Cycle-to-cycle Period Fluctuations?
Seyedyara Mohajerani, John R. Percy 80

Recent Minima of 144 Eclipsing Binary Stars
Gerard Samolyk 94

Times of Minima for Several Eclipsing Binaries and New Ephemerides for V569 Lyrae, V571 Lyrae, and V572 Lyrae
A. Marchini, M. Banfi, M. Cena, G, Corfini, S. Mandelli, G. Marino, R. Papini, D. Premoli, S. Santini, S. Valentini, M. Vincenzi 102

Searching for Orbital Periods of Supergiant Fast X-ray Transients
Maurizio Falanga, Enrico Bozzo, Roland Walter, Gordon E. Sarty, Luigi Stella 110

Anchoring the Universal Distance Scale Via a Wesenheit Template
Daniel J. Majaess, David G. Turner, David J. Lane, Arne A. Henden, Tom Krajci 122

Edward A. Halbach 1909–2011
Gerard Samolyk 141

Table of Contents continued on next page

Abstracts of Papers and Posters Presented at the 99th Annual Meeting of the AAVSO, Held in Woburn, Massachusetts, October 29–30, 2010

The AAVSO Centennial Calendar
Elizabeth O. Waagen 145

The 2010 Eruption of U Scorpii
Ashley Pagnotta 145

The Latest Results on Accreting Pulsating White Dwarfs
Paula Szkody 145

Analyses of "Peculiar" W Virginis Stars in the Milky Way
Doug Welch, Grant Foster 146

RS Sge Observations and Preliminary Analyses
Jerry Horne 147

Revisiting the Unnamed Fleming Variables
Kristine Larsen 147

Multiple Spiral Branches on Late AGB Stars
Qian Wang, Lee Anne Willson 147

Visual Observations of δ Cephei: Time to Update the Finder Chart
David Turner 148

Scientific Literacy of Adult Participants in an Online Citizen Science Project
Aaron Price 148

Leon Campbell and His Fifty Years at Harvard College Observatory
Thomas R. Williams 149

Artificial Intelligence (AI) Approaches for Analyzing Automatically Zillions of Eclipsing Binary Light Curves
Edward F. Guinan 149

A Web Interface for the DASCH Photometry Database
Edward J. Los 150

A Variable Star Database for the iPhone/iPod Touch
John N. Rachlin, Mark G. McGettrick 150

Simple PulseWidthModulation (PWM) LED Source for Linearity Testing of DSLR Camera Sensor
Helmar G. Adler 151

Solar Astronomy: Plasma Motion Detection at Radio Frequencies
Rodney Howe 151

The Water Tank Observatory
John Pazmino 152

Studies of "Irregularity" in Pulsating Red Giants. III. Many More Stars, an Overview, and Some Conclusions

John R. Percy
Emil Terziev
Department of Astronomy and Astrophysics, University of Toronto, Toronto ON Canada M5S 3H4

Received August 4, 2010; revised August 23, 2010; accepted September 6, 2010

Abstract We have analyzed AAVSO visual observations of an additional 85 "irregular" (L-type) pulsating red giants, using Fourier and self-correlation analysis; see *JAAVSO,* **37**, 71 (2009) and *JAAVSO,* **38**, 161 (2010) for details of the methods and previous results. We have categorized the variability of each star (periodic/semiregular, irregular, or not significantly variable), and noted the presence of various spurious effects arising from the visual observing process. Finally, we have suggested which stars should be highest priority for further visual or photoelectric observation, and which could reasonably be dropped from the visual program, and why.

1. Introduction

Cool red giants are all variable in brightness. They are classified in the *General Catalogue of Variable Stars* (*GCVS*, Kholopov *et al.* 1985) as Mira (M), semiregular (SR), or irregular (L). In previous papers (Percy *et al.* 2009, Percy and Long 2010, hereinafter Papers I and II), we showed, through self-correlation and Fourier analysis of AAVSO visual observations, that the L-type variables show a spectrum of behavior, from truly irregular, to semi-periodic. We also found evidence of spurious one-year and one-sidereal-month periods in some of the stars, presumably due to a physiological phenomenon called the Ceraski effect, which arises from the methodology of visual observation. The purpose of the present paper is to extend our analysis to L-type red giants in the AAVSO visual observing program which have fewer observations than those in Papers I and II. All of these stars were presumably placed on the AAVSO visual observing program because they had been found or suspected to be variable, and required study and classification, all of them have already been classified, on some basis, as being or suspected of being irregular (L, Lb, Lc types).

2. Data and analysis

Please see Papers I and II for a description of the visual data, which are taken from the AAVSO International Database, and the two methods of analysis—Fourier (using PERIOD04), and self-correlation—and for examples of Fourier

spectra and self-correlation diagrams. Dr. Matthew Templeton, Science Director, AAVSO Headquarters, kindly provided us with a list of all L-type stars in the database, listed in order of decreasing number of observations. The numbers of observations of the stars in Paper II range from 19,863 down to 3,642. In this paper, the numbers range from 2,683 (AO Cru) down to 249 (NSV 13234). The stars U And, TT Leo, and TY Oph, from Papers I and II, were re-analyzed, with similar results (Table 1).

Some of the stars also had some photoelectric or CCD observations but, for consistency, we used visual data only.

3. Results

The results of the analysis are summarized in Table 1. The columns in Table 1 give: the star name; the variable star type, spectral type, and range (from SIMBAD); the number N of observations; $\Delta m(0)$ and $\Delta m(4000)$; and comments about true or spurious periods. The symbol in brackets after the range is the wavelength band to which the range applies. $\Delta m(0)$ is the intercept on the vertical axis of the self-correlation diagram; it is a measure of the average observational error in the data. $\Delta m(4000)$ is the average Δmag at Δt = 4,000 days in the self-correlation diagram, and is a measure of the variability (including observational error) on time scales of up to this value. The difference between $\Delta m(4000)$ and $\Delta m(0)$ is a measure of the true variability. In the Comments column: Y and M indicate a signal at a period of one year or one sidereal month, respectively. As usual, a colon (:) denotes uncertainty.

The value of $\Delta m(0)$ depends on several factors, including the brightness of the star and the quality of the comparison sequence. For instance: one observer points out that the comparison stars for KK Per are not conveniently situated, which may explain its $\Delta m(0)$ of 0.30—significantly higher than for other sixth-magnitude variables. As always, the quality of the visual data could probably be improved by re-examining the sequences of comparison stars. AAVSO Headquarters has invested considerable time and effort in improving observing charts and comparison star magnitudes in the last decade.

Several stars show a phenomenon that we have occasionally seen in the self-correlation diagrams of stars in Papers I and II (W CMa, WY Gem, TX Per, and DY Vul, for instance): very weak minima at Δt = ~200 + 365 N days, where N is an integer. The amplitudes, however, are less than 0.02 magnitude. We suspect that this is a spurious effect—the Ceraski effect or something similar—related to the method of observation, the lengths of the seasons and of the seasonal gaps, both of which are ~200 days long. In the Comments column of Table 1, we have denoted this by "200/550."

Some stars show real periods. These are denoted by PN(A) where N is the period in days, and A is the amplitude—half the peak-to-peak range. The periods shorter than a few hundred days are probably due to pulsation. Longer periods may

be so-called "long secondary periods"; their nature is still not known (Nicholls *et al.* 2009). Stars considered to be not significantly variable are denoted "nsv"; in practice, this means that the visual amplitude is less than about 0.04 magnitude. Those which are variable but without discernible periodicity are denoted "irr." (irregular).

4. Which irregular red giants should continue to be observed, and how?

There are several thousand stars on the AAVSO visual observing program, including over 900 irregular red variables, according to the list from AAVSO Headquarters. Most have only a handful of observations. Based on the results of this paper, and Papers I and II, we can make recommendations about which stars should continue to be observed, and how (Table 2). These are our recommendations, and not necessarily those of AAVSO staff.

Why observe irregular red variables in the first place? One reason is to confirm that they are variable, and to estimate their amplitude, and to classify them. If they are periodic or semiregular, it is important to determine their period(s), since the period(s), and any changes therein, can provide additional information about the star. Even if the star is not periodic, self-correlation can provide a "profile" of the variability—the amount of variability as a function of time scale—as discussed in Papers I and II.

The advantage of the visual observations in the AAVSO International Database is that they have been made consistently over a long period of time. They can illuminate the stars' variability on time scales from days to decades. This is important in the case of red giants, in which variability is known to occur on these time scales.

A few L-type red giants are known to be complex and interesting. TZ Cyg, for instance, is multi-periodic. It is being analyzed in detail by Dr. Templeton. We did a cursory analysis of this star, but have not included it in Table 1.

We should first point out that, for the stars with the smallest number of observations (a few hundred), the results of the time-series analysis, i.e. the reality, value, and amplitude of any suspected periods, real or spurious, was uncertain. Many more long-term (visual) observations would be required to be sure. We question whether such observations would be worthwhile. Therefore we do not recommend that sparsely-observed L-type red variables (those with less than about 250 observations) should continue to be observed visually, unless there is some exceptional reason to do so.

This having been said, here is what we have found out about irregular red variables in the AAVSO International Database. Note that all of these stars have already been classified as L type.

Some stars show little or no significant variability ("nsv"), and no discernible real period. Visual observation of these stars can be discontinued. Many stars show irregular variability ("irr."), with no discernible real periods. Our analysis

has provided a "profile" of the variability, and it is doubtful that this profile will change. Visual observation of these stars can also be discontinued, though there is always a small chance that the behavior of the star, or properties such as mean magnitude, could change in future.

Some stars show discernible real periods, usually with amplitudes of a few hundredths of a magnitude. Further observations may refine the periods, or provide information about changes in the period or amplitude. In Table 2, we have divided these stars into three groups: (i) higher-priority stars which show definite evidence of periodicity, usually with an amplitude of 0.1 magnitude or more, which could provide useful information about the star—even with visual observations; (ii) medium-priority stars for which there is some evidence for periodicity (albeit usually of low amplitude); and (iii) lower-priority stars which are borderline, and could be dropped from the visual program. These and group (ii) are possible candidates for photoelectric or CCD observing. Our groupings are arbitrary; there is a continuous spectrum of behavior in L-type variables, from strong, large-amplitude periodicity (which definitely warrants continued observation) to weak, low-amplitude, marginal behavior.

Most of the stars with discernible periods have small amplitudes. Using time-series analysis, however, it is possible to extract small-amplitude periods from visual data, e.g. Percy and Palaniappan (2006), who clearly detected low-amplitude rotational variability in AAVSO visual observations of T Tauri stars. Long-term photoelectric photometry would obviously be better but, as noted below, we question the value of long-term photometry for these stars, especially the fainter ones.

Some of the "not significantly variable" stars, and most of the stars in group (iii) may actually be microvariables; the variability of the brighter stars could be studied with photoelectric photometry. The variability of bright small-amplitude red variables, however, has already been well-studied, including by the AAVSO Photoelectric Photometry Program (Percy *et al.* 2008 and references therein). Furthermore, tens of thousands of small-amplitude red variables have already been discovered and studied in survey projects such as MACHO and OGLE. Nevertheless, there is value in continuing to observe bright, periodic, small-amplitude red giants, since these stars can also be studied using other techniques such as spectroscopy and interferometry.

6. Discussion and conclusions

In addition to the spurious one-year and one-month periods discussed in Papers I and II, which we assume are due to the Ceraski effect, we have identified another apparently-spurious, low-amplitude effect: minima in the self-correlation diagram at Δts of ~200 + 365 N days. Many of the stars in Table 1 show one or more of these spurious effects, though it is difficult to confirm them in stars with fewer observations.

In this and Papers I and II, we have analyzed all of the irregular red giants in the AAVSO visual program that have about 250 or more observations. While analysis of stars with fewer observations might conceivably yield some results, that is unlikely, partly because the observations are so sparse, partly because they would have to be sustained over many years, and partly because the stars with more observations tend to be ones for which there is some a priori reason to believe that they may be interesting, for example, they show some evidence of periodicity.

We have also raised some interesting questions about priorities for visual observing of stars in the AAVSO International Database. These are questions that should be considered by AAVSO staff and observers. The question of "which stars to observe" depends on both the scientific value of the observations, on the interests and expertise of the observers, and on the amount of data already accumulated. We will leave it to AAVSO Headquarters to decide on the strategies and priorities for visual and/or CCD observing of these stars.

The analysis of the stars in Table 1 supports the main conclusion of Papers I and II: L-type variable red giants show a continuous spectrum of behavior, from not significantly variable, to irregular, to marginally periodic, to semiregular. The analysis also shows the value of systematic, long-term visual observations of variable stars: for each of the stars in our sample, we have been able to derive some conclusion about its variability, even if the result is a negative one.

8. Acknowledgements

We thank the Natural Sciences and Engineering Research Council of Canada for research support, and the AAVSO observers and headquarters staff, without whose efforts this project would not have been possible. Special thanks to Matthew Templeton and Elizabeth O. Waagen for reading a draft of this paper, and to the referee for useful comments. This research has made use of the SIMBAD database, operated at CDS, Strasbourg, France.

References

Kholopov, P. N. *et al.* 1985, *General Catalogue of Variable Stars*, 4th ed., Moscow.

Nicholls, C. P., Wood, P. R., Cioni, M. R. L., and Soszynski, I. 2009, *Mon. Not. Roy. Astron. Soc.*, **399**, 2063.

Percy, J. R., and Long, J. 2010, *J. Amer. Assoc. Var. Star Obs.*, **38**, 161.

Percy, J. R., Mashintsova, M., Nasui, C. O., Palaniappan, R., Seneviratne, R., and Henry, G. W. 2008, *Publ. Astron. Soc. Pacific*, **120**, 523.

Percy, J. R., and Palaniappan, R. 2006, *J. Amer. Assoc. Var. Star Obs.*, **35**, 290.

Percy, J. R., *et al.* 2009, *J. Amer. Assoc. Var. Star Obs.*, **37**, 71.

Table 1. Results of time-series analysis of L-type red giant variables.

Star	*Type*	*Spectrum*	*Range*	*N*	*Dm (0)*	*Dm (4000)*	*Comments*
AO Cru	Lc	M0Ia/ab	8.5–10.0 (p)	2683	0.38	0.37	200/550; nsv
V930 Cyg	Lb	—	12.9–13.9 (p)	2658	0.44	0.61	P250(0.3)
V1152 Cyg	Lb	M6D	13.0–14.3 (p)	2397	0.16	0.34	200/550; irr.
ψ1 Aur	SRc	K5Iab	4.68–5.02 (V)	2368	0.18	0.27	Y:, P175(0.02), P2000(0.09:)
BO Car	Lc	M4Ib	7.18–8.5 (V)	2160	0.40	0.55	200/550, irr.
V451 Cas	Lb	M5	9.3–10.0 (p)	2059	0.37	0.45	Y:, irr.
KK Per	Lc	M1–3.5Iab	6.6–7.89 (V)	1909	0.30	0.33	nsv
κ Oph	Lb:	K2III	4.1–5.0 (p)	1842	0.16	0.23	Y:, irr.
PR Per	Lc	M1Iab/b	9.8–10.8 (p)	1828	0.32	0.36	Y: P2730 (0.02), irr.
ZZ Cam	Lb	M0–5	8.7–9.3 (p)	1670	0.17	0.21	Y, irr/nsv:
PP Per	Lc	M0–1.5Ia/ab	9.1–10.3 (V)	1610	0.29	0.33	Y:, nsv
V391 Cas	Lb	M4	9.2–10.0 (p)	1526	0.13	0.14	P393(0.02)
RX Cru	Lb:	C(N:)	15–16 (p)	1435	0.28	0.62	P280(0.2:), P548(0.3:)
AS Cep	Lb	M3	11.3–12.9 (p)	1335	0.25	0.35	200/550:, Y:, irr.
BI Cyg	Lc	M4Iab	8.4–9.9 (p)	1329	0.45	0.57	P300(0.03):
HK Lyr	Lb	C6,4(N4)	7.8–9.6 (V)	1289	0.27	0.54	Y, irr.
ε Peg	Lc	K2Ib	0.7–3.5 (V)	1281	0.20	0.27	200/550, irr.
NSV 14213	L	G8	5.6–6.8 (V)	1191	0.15	0.20	Y, P250(0.02):
V939 Her	Lb	MD	7.24–8.02 (Hp)	1167	0.26	0.53	Y:, irr.
UX Cam	Lb	M6	9.5–10.65 (p)	1029	0.23	0.33	P935(0.04)
V338 Aql	L:	M3	11–12.5 (p)	1018	0.21	0.27	P780(0.02), P4000
TZ Cas	Lc	M2Iab	8.86–10.5 (V)	991	0.29	0.43	P3000 ± 500 (0.05)
SY Peg	Lb	M0	9.6–10.0 (V)	962	0.29	0.34	P1600(0.02):
AZ Dra	Lb	M2	8.0–8.9 (p)	948	0.23	0.28	Y:, irr.
HM Aur	Lb	M	11.3–12.4 (p)	938	0.25	0.37	P280(0.05)
FR Per	Lb	C4,5(R3)	12.2–13.4 (p)	919	0.39	0.50	200/550:, irr.
α Sco	Lc	M1.5Iab–b	0.88–1.16 (V)	906	0.17	0.26	Y:, P7000 (0.07):
AA Cam	Lb	M5(S)	9.0–9.6 (p)	865	0.19	0.29	Y:, P650(0.04)
V396 Cen	Lc:	M4Ia–ab/M6	10.0–10.6 (B)	859	0.23	0.46	Y, P6080 (0.08):

Table continued on following pages

Table 1. Results of time-series analysis of L-type red giant variables, cont.

Star	*Type*	*Spectrum*	*Range*	*N*	*Dm (0)*	*Dm (4000)*	*Comments*
V770 Cas	Lb	M2IIIc	7.45–8.13 (Hp)	844	0.21	0.26	Y, P420(0.06), P3450(0.10):
V370 And	SRb	M7III	6.18–7.19 (Hp)	838	0.20	0.44	P120(0.12)
RY Cyg	Lb	C4,8–6,4(N)	8.5–10.3 (V)	836	0.39	0.43	irr.
V TrA	Lb	C5,5(Nb)	10.0–10.7(p)	774	0.17	0.55	Y, irr.
MS Aql	Lb	M4III	10.6–11.2 (p)	733	0.31	0.39	irr.
GO Peg	Lb	M4	8.6–9.3 (p)	707	0.21	0.21	Y, nsv
α Tau	Lb:	K5III	0.75–0.95 (V)	693	0.12	0.18	Y:, irr.
NSV 13857	Lb	M2	6.3–7.08 (B)	678	0.14	0.16	Y, nsv
TV Cyg	Lb:	M0	10.9–11.4 (p)	653	0.11	0.78	irr.
V4018 Sgr	L:	M4d	9.5–13.6 (p)	639	0.37	1.81	Y:, symbiotic
QZ Cyg	Lb	M3	11.2–12.4 (p)	632	0.27	0.32	Y, irr.
U Ant	Lb	C5,3(Nb)	8.8–9.7 (p)	623	0.27	0.69	Y:, irr.
GL And	Lb	K4	9.6–10.2 (p)	616	0.35	0.35	P4050:, irr.
V807 Aql	Lb:	M6.5	13.0–14.0 (p)	615	0.32	0.54	Y:, P160:
X Lup	L:	—	10.4–12.8 (p)	609	0.50	0.90	M, Y, irr. hline
TY Oph	Lb	C5,5(N)	12.7–15.1	564	0.32	0.43	200/550, P5600(0.04)
CY Cyg	Lb	CS(M2p)	10.0–11.7 (p)	559	0.41	0.53	P13.7(0.05:):
UY And	Lb	C5,4(N3)	7.4–12.3 (V)	553	0.30	0.44	irr.
RU Car	Lb	N3	10.9–12.1 (p)	553	0.32	0.34	P400(0.05)
HO Peg	Lb	M8III	8.3–8.7	552	0.13	0.16	Y:, nsv
RW Vir	Lb	M5III	6.72–7.38 (V)	498	0.22	0.31	Y:, P3900(0.05):
AX Cyg	Lb	C4,5(N6)	7.85–8.86 (V)	506	0.37	0.39	M:, P358(0.04):, nsv:
DR Boo	Lb	K0D	8.06–8.60 (Hp)	465	0.15	0.20	P513(0.01), P2030(0.05)
HU Sge	Lb	M0	7.8–8.8 (p)	462	0.15	0.20	200/550:, P1500(0.02):
AC Dra	Lb	M5IIIab	7.14–7.39 (B)	447	0.13	0.22	P380(0.06) (Y?)
DK Boo	Lb	K5D	8.02–8.77 (Hp)	440	0.18	0.21	nsv
NO Aur	Lc	M2SIab	6.10–6.30 (V)	439	0.19	0.30	P325(0.03):, Y:
NSV 436	Lb	M0	8.4–9.1 (p)	436	0.12	0.20	irr

Table continued on next page

Table 1. Results of time-series analysis of L-type red giant variables, cont.

Star	*Type*	*Spectrum*	*Range*	*N*	*Dm (0)*	*Dm (4000)*	*Comments*
FG Boo	Lb	M0D	7.35–8.06 (Hp)	430	0.16	0.40:	P584(0.10)
TT Leo	Lb	M7	10.5–11.7 (V)	429	0.29	0.45	P382(0.05)
V352 Ori	Lb	M7ep	8.5–10.0 (p)	418	0.22	0.28	200/550:, irr.
NSV 4147	L:	—	11.4–12.0 (V)	413	0.18	0.26	200/550, irr.
V1173 Cyg	Lb	M6eaIII	12.3–13.7 (B)	405	0.38	0.55	irr.
V485 Cyg	Lb	M5III	8.9–9.8 (p)	404	0.23	0.40	Y, irr.
UV Cnc	Lb	M4	9.0–10.5 (p)	386	0.27	0.35	P184(0.05), Y
AV Eri	Lb	M2	12.4–13.2 (p)	363	0.3:	1.0:	P120(0.30)
V416 Lac	Lb	M4III	5.05–5.18 (Hp)	354	0.17	0.20	nsv
NQ Cas	Lb	C4,5J(R5)	10.6–11.52 (B)	338	0.22	0.28	irr.
NSV 771	—	M2	11.5–? (p)	337	0.22	0.22	200/550, nsv
XX Cnc	Lb	M4	10.1–11.0 (p)	335	0.36	0.44	irr.
NSV 14284	Lb:	M	11.0–12.0+ (p)	333	0.24	0.44	P125(0.05)
NSV 293	SRS	M4IIIa	5.28–5.50 (V)	327	0.09	0.11	Y, nsv
V2429 Cyg	Lc:	M3	10.4–13.7 (V)	322	0.5	0.5	Y, irr.
SU And	Lc	C6,4(C5II)	8.0–8.5 (V)	310	0.18	0.22	irr.
FR Sct	Z And	M2.5epIab+B	11.6–12.91 (B)	309	0.14	0.20	irr.
LW Cyg	Lb	C5,4(R3)	12.3–14.5+ (B)	299	0.39	0.65	irr.
V727 Sco	Lb:	M1	9.7–10.4 (p)	299	0.18	0.30	200/550, irr.
KP Del	Lb	M5	7.7–8.39 (V)	297	0.19	0.25	Y:, irr.
PV Peg	Lb	—	6.55–7.42 (Hp)	295	0.22	0.30	P120(0.05):
SW Cet	Lb	M7III	9.8–10.9 (p)	294	0.31	0.40	200/550, irr.
EV Peg	Lb	M7	11.5–13.0 (p)	291	0.60	0.65	P235(0.35)
FI Gem	Lb	M6.5	12.8–14.2 (p)	291	0.28	0.45	Y, irr.
FI Vel	L	—	12.6–13.6 (p)	265	0.14	0.50	200/550:, irr.
PX Lyr	L	—	13.0–14.4 (p)	261	0.43	0.65	P400(0.20:), P1450(0.15:)
NSV 2731	L	OB!	11.3–11.7 (p)	253	0.20	0.25	nsv
NSV 13234	L:	K0	9.0–10.2 (V)	249	0.15	0.22	irr. hline

Table 2. Stars recommended by the authors for continued observation, based on the results of this paper, and papers I and II.

Priority Recommendation	*Stars*			
(i) Observe	V370 And	V770 Cas	AV Eri	ST Psc
(Higher Priority)	VW Aql	RX Cru	OP Her	V4018 Sgr
	ψ1 Aur	TZ Cyg	TT Leo	τ4 Ser
	FG Boo	V930 Cyg	EX Ori	CP Tau
	UX Cam	AT Dra	EV Peg	VY UMa
(ii) Observe	V338 Aql	UV Cnc	BI Cyg	PX Lyr
(Medium Priority)	V807 Aql	RU Car	CY Cyg	PV Peg
	HM Aur	TZ Cas	T Lyr	NSV 14284
	UX Cam	AA Cas	X Lyr	
	AA Cam	ST Cep	TU Lyr	
(iii) Observe	HM Aur	AX Cyg	PR Per	DY Vul
(Lower Priority)	NO Aur	BI Cyg	α Sco	NSV 14213
	DR Boo	TY Oph	HU Sge	
	V391 Cas	SY Peg	X TrA	
(iv) Irregular	U Ant	V451 Cas	V2429 Cyg	BL Ori
	SU And	V396 Cen	CT Del	V352 Ori
	UY And	AS Cep	KP Del	ε Peg
	GL And	SW Cet	UW Dra	FR Per
	V Aps	T Cyg	AC Dra:	V727 Sco
	MS Aql	RY Cyg	AZ Dra	FR Sct
	ZZ Cam	SV Cyg	BU Gem	α Tau
	XX Cnc	TV Cyg	FI Gem	V TrA
	W CMa	AX Cyg	GN Her	FI Vel
	RT Car	LW Cyg	V939 Her	RW Vir
	BO Car	QZ Cyg	X Lup	NSV 436
	WW Cas	V485 Cyg	XY Lyr	NSV 4147
	NQ Cas	V1152 Cyg	HK Lyr	NSV 13234
	PY Cas	V1173 Cyg	κ Oph	
(v) Not	SV Aur	AO Cru	HO Peg	NSV 771
Significantly	DK Boo	V449 Cyg	KK Per	NSV 2731
Variable	IZ Cas	WY Gem	PP Per	NSV 13857
	AD Cen	V416 Lac	TX Psc	
	DM Cep	GO Peg	NSV 293	

VX Hydrae: Observation of a Sudden Change in a Pulsating Star

Michel Bonnardeau
116 Jonquille Arzelier, 38650 Chateau-Bernard, France; arzelier1@free.fr

Shawn Dvorak
Rolling Hills Observatory, 1643 Nightfall Drive, Clermont, FL 34711; sdvorak@cfl.rr.com

Rudy Poklar
14084 N. Willow Bend Drive, Tucson, AZ 85737; rfpoklar@aol.com

Gerard Samolyk
P.O. Box 20677; Greenfield, WI 53220; gsamolyk@wi.rr.com

Received April 6, 2010; revised July 12, 2010; accepted August 4, 2010

Abstract Time-series of VX Hya from March 2005 to April 2010 are analyzed. A period jump is discovered to happen in 2008 in all the pulsation modes, being at its strongest for the overtone.

1. Introduction

The δ Scuti star VX Hydrae was studied by Fitch (1966), who found two main pulsations with periods 0.223 day (fundamental) and 0.173 day (overtone), and up to eighteen harmonics and beats. It was also observed by Templeton *et al.* (2009) (hereafter T09), who measured the two main pulsations and up to twenty-three harmonics and beats.

The fundamental pulsation is designated as (1,0) and the overtone as (0,1) with the frequencies n_{10} and n_{01}, respectively. The other pulsations are designated as (i,j) with the frequencies n_{ij}. They are harmonics/beats of the two main pulsations with $n_{ij} = i \times n_{10} + j \times n_{01}$.

2. Discovery of the pulsation change

VX Hya was observed by one of us (MB) with a 203 mm Schmidt-Cassegrain telescope, a Johnson *V* filter and a SBIG ST7E camera (KAF401E CCD). The exposure durations were 200 seconds (a few measurements have 60s). For the differential photometry, the comparison star was TYC 5482-01347/1 with $V = 11.580$ (computed from the Tycho magnitudes owing to Mamajek *et al.* 2002, 2006).

The observations were carried out from 2005 to 2010, with 1,495 measurements

in thirty-two sessions, and are reported in Table 2. Examples of light curves are in Figures 1–4. All the data are in the AAVSO International Database, observer code BZU (along with *B* measurements, not used in this paper).

Following Fitch (1966), the observations are fitted with the function of the time t:

$$V(t) = V_m - 2.5 \log \left[1 + \sum_{i,j} \left(a_{ij} \, sin(2\pi n_{ij} t) + b_{ij} \, cos(2\pi n_{ij} t) \right) \right] \quad (1)$$

where V_m is the non-pulsed part of the brightness and the sum is carried out over the (i,j) pulsations with frequencies n_{ij}.

It is not possible to obtain a good single set of parameters for all the seasons. A good set was obtained for the March 2005–December 2006 observations (see Figures 1 and 2), showing that the pulsations change very little during that period. But this set of parameters does not fit the February 2008–January 2010 data; the observations are late when compared with function (1), and become later and later (see Figures 3 and 4). A change in the pulsations happened between December 2006 and February 2008, making the frequencies smaller (or the periods longer). Up to six pulsations were used for the fit, but the period change is already visible if one uses only the two main pulsations.

3. Analysis of the pulsation change

The observations were fitted with function (1), season by season, the following way:

- the two main pulsations were used: the fundamental (1,0) and the overtone (0,1), two harmonics (2,0) and (0,2), and two beats (1,1) and (–1,1). These six pulsations are those with the greatest amplitudes. There are other pulsations (e.g. T09 detected a total of twenty-five pulsations), but they have smaller amplitudes and are neglected in this study. (Actually an analysis with only the two main pulsations leads to results that are very similar to those shown here);
- for V_m the average magnitude over the season (as Fitch 1966) was used. This approximation is valid because the duration of the observations for a season is much longer than the pulsation periods. Actually, it will be checked that V_m calculated that way is constant over the seasons;
- the a_{ij} and b_{ij} coefficients are then determined by least squares (calculating 12×12 matrixes and inverting them).

Additional observations from the AAVSO International Database were also used, so as to have more data and data that are independently acquired. They were obtained with telescope apertures of 200 to 250mm, SBIG ST7 and ST9

cameras, and the same filter and comparison star as above. The data are from the co-authors SD (observer code DKS), RP (PRX), and GS (SAH), with a total of 10,523 measurements in 60 sessions, and are reported in Table 2 (some of these data were also used by T09). These observations were also fitted the same way as explained above.

The phase of each pulsation is computed by:

$$\phi_{ij} = atan2(a_{ij}, b_{ij}) \quad (2)$$

The frequencies n_{ij} are then adjusted so that the phases ϕ_{ij} vary little over the 2004–2007 seasons. The adopted frequencies are in Table 1. The difference with the frequencies of T09 for 2006 is smaller than 10^{-4} for n_{10} and n_{01} (actually within their uncertainty for n_{10} in 2006), and smaller than 5×10^{-4} for the four harmonic/beat frequencies. The difference with the frequencies for 1955–1959 of Fitch (1966) is smaller than 2×10^{-4} for n_{10} and n_{01}. One can check that the four frequencies $n_{11}...n_{02}$ are harmonics/beats of n_{10} and n_{01} with a precision better than 10^{-4}, for example, $n_{11} = n_{10} + n_{01}$.

The amplitude of each pulsation is computed by:

$$A_{ij} = \sqrt{a_{ij}^2 + b_{ij}^2} \quad (3)$$

The resulting parameters ϕ_{ij} and A_{ij} for each data set are listed in Table 2. The uncertainties in the dates (HJD) of the data sets are the standard deviations of the dates of the measurements. To evaluate the uncertainties on the phases and the amplitudes, V_m is varied by ± 0.01 magnitude and one observes how ϕ_{ij} and A_{ij} change. The uncertainties are found to be the largest for the (–1,1) beat. This is because this pulsation has the longest period ($P_{-11} = 0.76$ day) and the corresponding parameters are then less constrained by the finite data sets.

4. Results

Figure 5 shows the phases as a function of time. There is clearly a sudden phase shift in 2008. The (1,0) pulsation has its phase modified by about 20°, the (0,1) pulsation by 60°, and the phases of the other pulsations change, too. This corresponds to decreases in the pulsation frequencies (and increases in the periods).

A phase shift over time is equivalent to a frequency change. With the time scale of the phase shift being much longer than the pulsation periods, the change Δn_{ij} of the frequency n_{ij} can be computed from the phase shifts $\Delta\phi_{ij}$ as:

$$\Delta n_{ij} = \frac{\Delta\phi_{ij}}{2\pi\Delta t} \quad (4)$$

where Δt is the time interval. The variations of the frequencies, taking the 2005–2006 data set (of observer DKS) as an origin, are computed for the (1,0) and the (0,1) pulsations and the results are shown Table 3 and Figure 6:

- for the pulsation (1,0) there is a jump in the frequency between THJD 4100 and 4500, then the frequency stays constant after a decrease of $-(46.7\pm 2.7)\times 10^{-6}$ day^{-1} (the uncertainty is the standard deviation over 2008–2010);

- for the pulsation (0,1) the frequency jump lasts from THJD 4100 to 4800 with a decrease of at least -100×10^{-6} day^{-1}. It appears that it stays constant thereafter (more observations would be needed here).

That is, the jump for the (0,1) overtone is twice as strong as the jump for the (1,0) fundamental and lasts twice longer.

The other four pulsations are harmonics or beats of the first two. Their phase variations may then be computed from the phase variations of the fundamental and of the overtone, and compared with the observed phase variations. There should be no difference. For example, for the (1,1) pulsation, the computed phase variation is $\Delta\phi_{11}^{\text{comput}} = \Delta\phi_{10} + \Delta\phi_{01}$ and one can check that it is roughly equal to the observed $\Delta\phi_{11}$. The residuals between the observed and computed values are shown Table 3 and Figure 7. They are roughly around 0, the worst being the (–1,1) pulsation, but this one has large error bars, as explained above.

The variation of the amplitudes A_{ij} of the oscillations versus time may be studied, although there is a need for caution because the data come from different observers (with different telescope setups, and so on). This is shown in Figure 8: there is a trend for an increase of the amplitudes before the 2008 period change followed by a decrease. Again, the effect is stronger for the (0,1) overtone (and its (0,2) harmonic) than for the (1,0) fundamental.

For the non-pulsed part of the brightness (V_m), from author MB (observer code BZU) observations only (so as to have homogenous data sets taken with the same setup) a significant variation cannot be detected (standard deviation is 0.014 mag) in 2004–2005 and 2006–2010. There is no variation either (standard deviation is 0.008) from author SD (observer DKS) observations in 2005–2006 and 2008–1010. This both allows checking the validity of the approximation of using an average for the determination of V_m and gives an upper limit on variation on V_m coming from the star.

5. Discussion

These measurements of amplitudes and phases of the oscillations may be compared with those of T09, especially for the 2005–2006 season. The amplitudes M_{ij} of T09 in magnitude are connected to the A_{ij} through:

$$M_{ij} = \frac{2.5}{\text{Log}(10)}\left(A_{ij} - \frac{A_{ij}^{\,2}}{2} + \frac{A_{ij}^{\,3}}{3} - \ldots\right) \qquad (5)$$

T09 lists the magnitudes of the oscillations at $t_{0,2006}$ = 2453807.3515. The evaluation of the amplitudes agrees with theirs within 3 mmag for the two main tones, and within 7 mmag for the four harmonics and beats.

T09 also lists the phases of the oscillations at $t_{0,2006}$. These phases can be recalculated as $2\pi n_{ij} t_{0,2006} + \phi_{ij}$. The agreement is within 2° for the two main tones and within 9° for the four harmonics and beats (modulo 270°, which comes from different models of the oscillations).

The agreement with T09 may be considered as satisfying despite the small differences, especially in view of the small number of harmonics/beats used here.

The increase in amplitude for the overtone (0,1) before 2008 was also detected by T09. The increase for the fundamental (1,0) was not seen by T09 but here the observations are over a longer time and the change is smaller.

The analysis presented here, which is somewhat like an O–C study, is very sensitive to the difference between two data sets. It is more sensitive than, for example, determining the absolute frequency of each data set and taking the difference to search for a variation.

VX Hya is an easy to observe δ Sct star with only one large amplitude overtone. A sudden period jump was discovered that is stronger and lasts longer for the overtone than for the fundamental and that appears to propagate to the harmonics and the beats. Also, the amplitudes of the pulsations got stronger before the period jump. There is a need for a physical explanation of the underlying process and such observations should be helpful to understand how the different tones are coupled.

6. Acknowledgement

The use of the AAVSO International Database and the contributions of data from the co-authors for this amateur research are acknowledged.

References

Fitch, W. S. 1966, *Astrophys. J.*, **143**, 852.
Mamajek, E. E., Meyer, M. R., and Liebert, J. 2002, *Astron. J.*, **124**, 1670.
Mamajek, E. E., Meyer, M. R., and Liebert, J. 2006, *Astron. J.*, **131**, 2360.
Templeton, M. R., Samolyk, G., Dvorak, S., Poklar, R., Butterworth, N., and Gerner, H. 2009, *Publ. Astron. Soc. Pacific*, **121**, 1076.

Table 1. The adopted frequencies (in day^{-1}), after adjustment to minimize the phase shifts for the 2004–2007 seasons (around HJD 2453800).

harmonic	*frequency (d^{-1})*
n_{10}	4.476493
n_{01}	5.789900
n_{11}	10.266397
n_{20}	8.952962
n_{-11}	1.313422
n_{02}	11.579792

Table 2. The parameters that fit the different sets of observations of VX Hya (ϕ the phases in °, A the amplitudes).

Season	2004–2005	2005–2006	2006–2007				2007–2008		2008–2009		2009–2010	
Observer	BZU	DKS	SAH	BZU	PRX	SAH	BZU	PRX+DKS	DKS	BZU	BZU	DKS
No. of sessions	6	16	5	4	11	5	7	4	3	9	6	16
Duration (h)	31.8	111.7	27.1	17.4	46.8	22.2	48.2	16.3	17.6	36.9	27.7	64.5
No. of obs.	248	3098	753	162	1203	626	346	429	712	354	385	3702
HJD–2450000	3445.1 ±2.8	3794.1 ±18.2	4096.0 ±5.9	4096.2 ±1.0	4165.3 ±15.7	4194.8 ±16.4	4507.6 ±2.0	4558.6 ±7.1	4853.4 ±3.3	4873.7 ±37.1	5209.6 ±34.8	5280.0 ±17.4
ϕ_{10} (°)	122.5 ±0.2	124.5 ±0.4	120.0 ±0.5	123.1 ±0.1	122.6 ±0.7	119.2 ±0.6	114.1 ±0.2	110.6 ±1.8	105.3 ±0.4	105.9 ±0.1	102.4 ±0.9	100.3 ±0.7
ϕ_{01}	172.2 ±0.2	173.9 ±0.1	173.5 ±1.1	172.4 ±0.1	172.4 ±0.1	176.9 ±0.7	156.0 ±0.1	154.3 ±1.1	134.5 ±1.2	129.0 ±0.4	114.4 ±0.4	109.5 ±0.3
ϕ_{11}	312.2 ±0.5	316.5 ±0.5	321.6 ±2.6	316.5 ±0.9	312.1 ±0.5	325.8 ±1.1	289.0 ±0.3	288.9 ±2.6	249.3 ±2.0	247.2 ±1.0	224.3 ±0.8	234.9 ±0.8
ϕ_{20}	165.8 ±1.0	167.3 ±0.8	182.3 ±2.8	156.0 ±0.2	166.4 ±1.3	160.5 ±0.8	153.4 ±1.0	162.3 ±1.8	131.5 ±0.6	135.3 ±3.6	141.2 ±0.3	135.6 ±0.8
ϕ_{-11}	206.4 ±3.0	207.3 ±1.1	237.9 ±16.1	206.1 ±3.5	205.4 ±2.0	203.4 ±7.3	196.1 ±0.2	244.1 ±26.4	172.0 ±5.8	162.4 ±4.4	130.5 ±7.0	163.5 ±5.5

Table continued on next page

Table 2. The parameters that fit the different sets of observations of VX Hya (ϕ the phases in °, A the amplitudes), continued.

Season	2004–2005	2005–2006	2006–2007				2007–2008		2008–2009		2009–2010	
Observer	BZU	DKS	SAH	BZU	PRX	SAH	BZU	PRX+DKS	DKS	BZU	BZU	DKS
ϕ_{02}	178.7 ±0.4	184.5 ±1.3	184.1 ±2.2	193.8 ±0.3	178.6 ±1.0	152.0 ±0.8	158.7 ±0.1	141.9 ±0.3	104.9 ±0.7	99.1 ±2.1	61.7 ±0.5	76.6 ±1.2
A_{10}	0.1280 ±0.0020	0.1323 ±0.0011	0.1318 ±0.0001	0.1378 ±0.0001	0.1452 ±0.0009	0.1626 ±0.0019	0.1368 ±0.0012	0.1323 ±0.0059	0.1405 ±0.0022	0.1263 ±0.0001	0.1258 ±0.0004	0.1277 ±0.0008
A_{01}	0.0949 ±0.0008	0.1146 ±0.0006	0.1171 ±0.0004	0.1336 ±0.0009	0.1356 ±0.0011	0.1292 ±0.0041	0.1286 ±0.0008	0.1383 ±0.0075	0.1127 ±0.0006	0.1107 ±0.0002	0.1063 ±0.0008	0.1126 ±0.0002
A_{11}	0.0452 ±0.0005	0.0556 ±0.0004	0.0625 ±0.0003	0.0659 ±0.0005	0.0744 ±0.0003	0.0482 ±0.0004	0.0659 ±0.0003	0.0642 ±0.0026	0.0593 ±0.0009	0.0600 ±0.0040	0.0526 ±0.0004	0.0549 ±0.0002
A_{20}	0.0392 ±0.0005	0.0375 ±0.0004	0.0306 ±0.0016	0.0523 ±0.0022	0.0467 ±0.0012	0.0641 ±0.0007	0.0368 ±0.0006	0.0453 ±0.0035	0.0434 ±0.0009	0.0404 ±0.0029	0.0351 ±0.0003	0.0365 ±0.0012
A_{-11}	0.0358 ±0.0032	0.0372 ±0.0013	0.0248 ±0.0030	0.0529 ±0.0009	0.0557 ±0.0011	0.0524 ±0.0102	0.0450 ±0.0004	0.0290 ±0.0042	0.0535 ±0.0013	0.0359 ±0.0031	0.0511 ±0.0012	0.0335 ±0.0037
A_{02}	0.0248 ±0.0008	0.0252 ±0.0001	0.0422 ±0.0018	0.0333 ±0.0007	0.0404 ±0.0010	0.0392 ±0.0010	0.0341 ±0.0006	0.0522 ±0.0008	0.0284 ±0.0024	0.0220 ±0.0007	0.0275 ±0.0008	0.0299 ±0.0001

Table 3. The frequency variations of the fundamental (1,0) and of the overtone (0,1) of VX Hya from the 2005–2006 season (in $10^{-6}d^{-1}$). The phase residuals between the observed phase variations and the one computed from the frequency variations of (1,0) and (0,1), again taking the 2005–2006 season as the origin (in °).

Season	2004–2005	2005–2006	2006–2007				2007–2008		2008–2009		2009–2010	
Observer	BZU	DKS	SAH	BZU	PRX	SAH	BZU	PRX+DKS	DKS	BZU	BZU	DKS
HJD–2450000	3445.1	3794.1	4096.0	4096.2	4165.3	4194.8	4507.6	4558.6	4853.4	4873.7	5209.6	5280.0
	±2.8	±18.2	±5.9	±1.0	±15.7	±16.4	±2.0	±7.1	±3.3	±37.1	±34.8	±17.4
Δn_{10} ($10^{-6}d^{-1}$)	–15.9	0.0	–41.4	–12.9	–14.2	–36.7	–40.5	–50.5	–50.4	–47.9	–43.4	–45.2
	±5.2	—	±10.9	±4.5	±8.8	±9.2	±3.2	±9.3	±2.8	±3.0	±3.8	±2.7
Δn_{01}	–13.5	0.0	–3.7	–13.8	–11.2	20.8	–69.7	–71.2	–103.3	–115.5	–116.8	–120.4
	±3.1	—	±11.3	±2.2	±1.5	±6.8	±2.6	±6.2	±5.1	±5.7	±4.1	±2.7
$\Delta\phi_{11}$ – (°)	–0.6	0.0	10.0	2.9	–1.0	11.6	0.8	5.9	–8.6	–5.8	–10.6	7.0
$\Delta\phi_{11}^{comput}$	±1.9	±2.0	±5.2	±1.9	±2.1	±3.4	±1.5	±6.5	±4.5	±2.5	±3.1	±2.7
$\Delta\phi_{20}$ –	2.5	0.0	24.0	–8.5	2.9	3.8	6.9	22.8	2.6	5.2	18.1	16.7
$\Delta\phi_{20}^{comput}$	±2.9	±3.2	±5.4	±1.8	±4.2	±3.6	±2.9	±7.0	±2.8	±5.3	±3.7	±3.7
$\Delta\phi_{-11}$ –	–1.2	0.0	26.5	–1.1	–2.3	–12.2	–3.7	42.5	–15.1	–18.6	–39.4	–3.6
$\Delta\phi_{-11}^{comput}$	±4.9	±3.1	±19.3	±5.1	±4.2	±10.1	±2.0	±30.9	±8.8	±6.4	±9.8	±7.9
$\Delta\phi_{02}$ –	–2.4	0.0	0.4	12.3	–2.9	–38.5	10.0	–3.4	–0.8	4.4	–3.8	20.9
$\Delta\phi_{02}^{comput}$	±2.2	±2.9	±5.8	±1.8	±2.4	±3.7	±1.6	±4.0	±4.4	±4.3	±2.6	±3.1

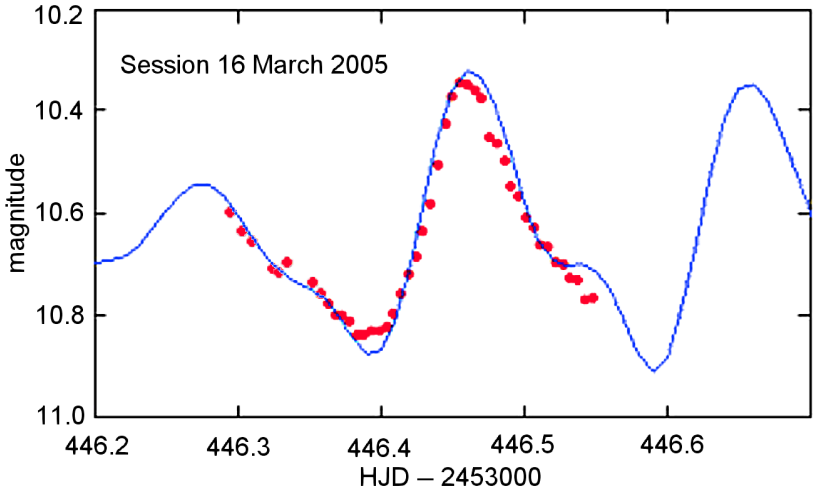

Figure 1. VX Hya light curve for 16 March 2005. The dots are the observations; the line is the model with six pulsations that fits the 2005–2006 observations.

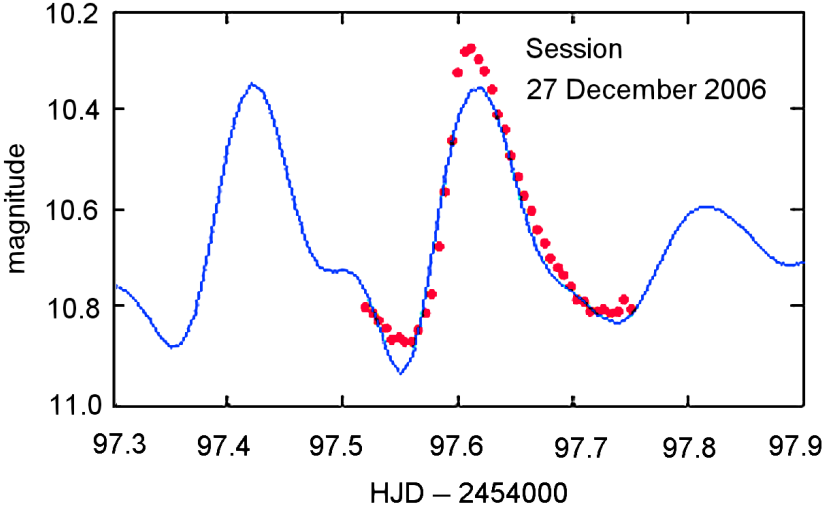

Figure 2. VX Hya light curve for 27 December 2006. The dots are the observations; the line is the model with six pulsations that fits the 2005–2006 observations.

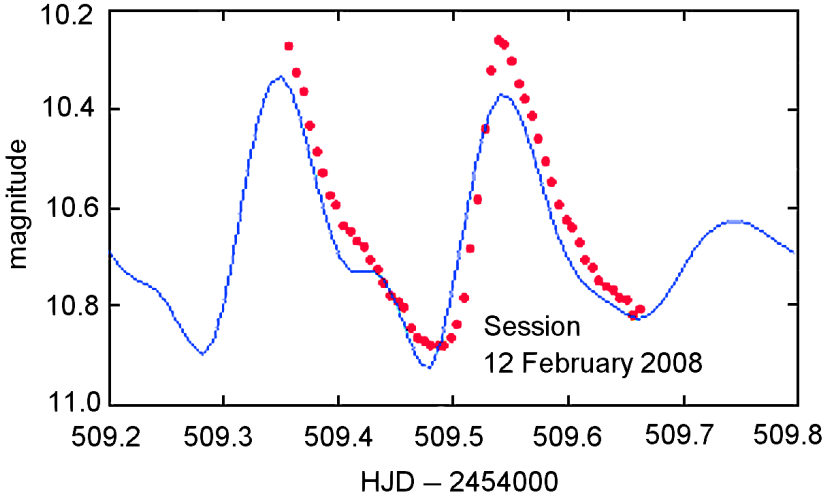

Figure 3. VX Hya light curve for 12 February 2008. The observations are 11 minutes late from the model, that is, the pulsation frequencies decreased.

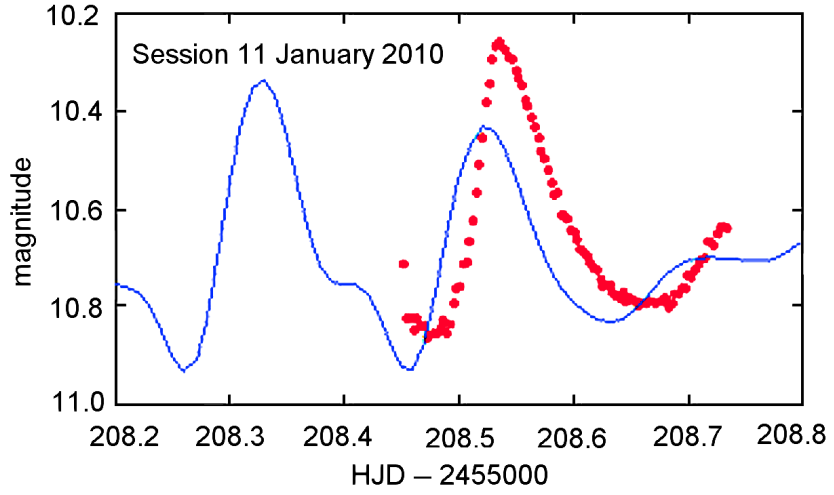

Figure 4. VX Hya light curve for 11 January 2010. The observations are 15 minutes late from the (1,0) pulsation and 40 mn from the (0,1) pulsation of the model.

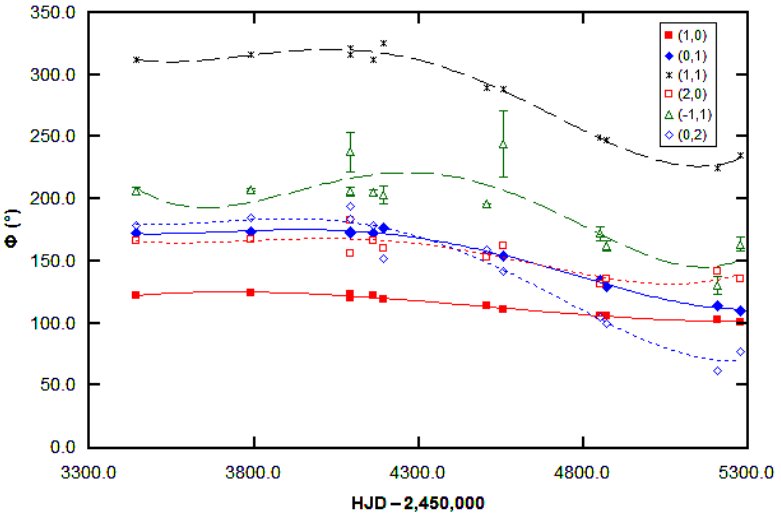

Figure 5. VX Hya phases of the pulsations versus time. From top to bottom: (1,1) pulsation (dashed line); (–1,1) pulsation (dashed line, with large error bars); (0,2) pulsation (dotted line); (0,1) pulsation (full line); (2,0) pulsation (dotted line); (1,0) pulsation (full line).

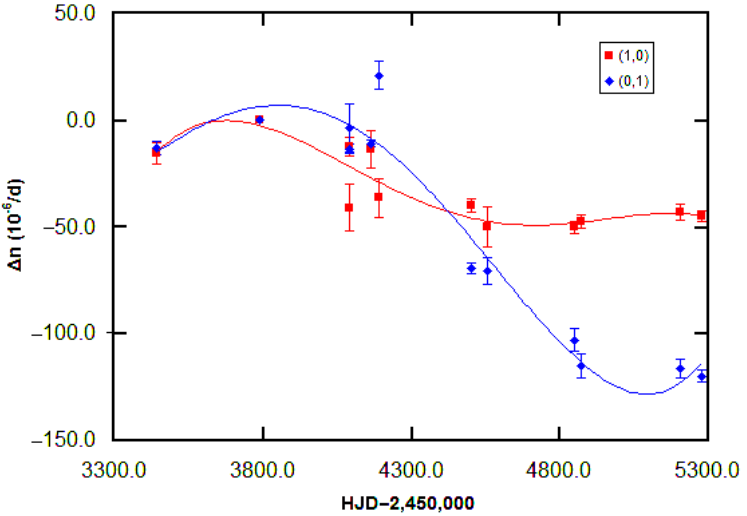

Figure 6. VX Hya frequency variations for the (1,0) fundamental (square symbols) and for the (0,1) overtone (diamond symbols), taking the 2005–2006 observations (HJD = 2,453,800) as 0.

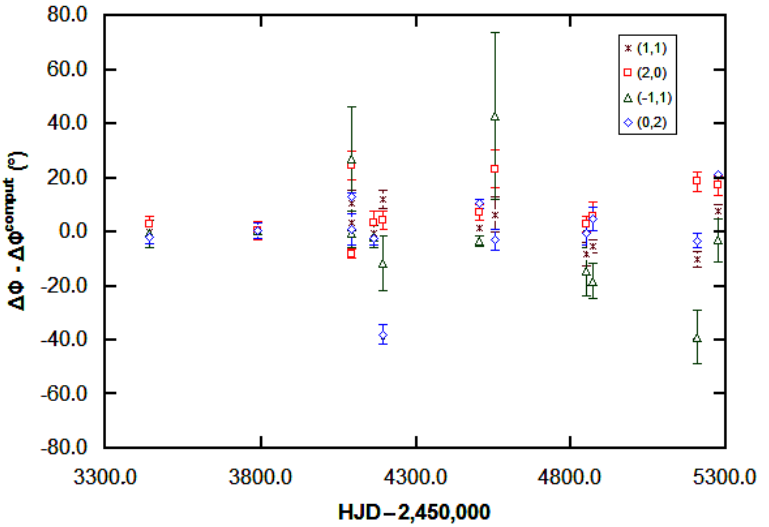

Figure 7. VX Hya. For the harmonics and beats, the residuals between the observed phase variations and the ones computed from the variations of the fundamental and of the overtone, taking the 2005–2006 observations (HJD = 2,453,800) as 0.

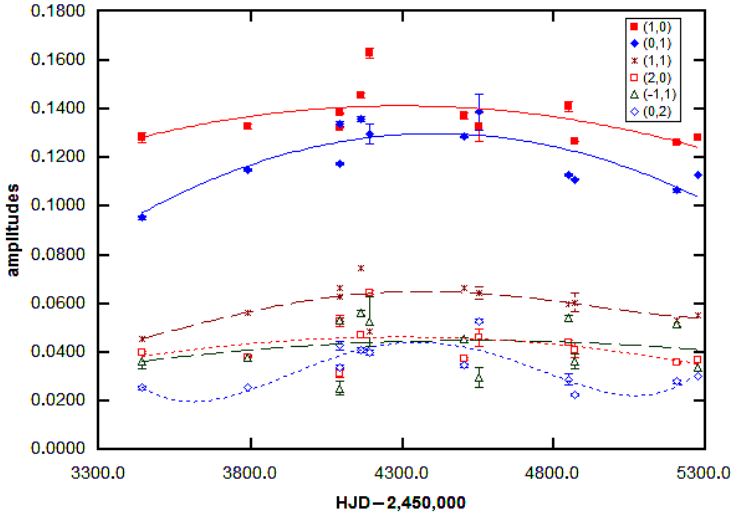

Figure 8. VX Hya amplitudes of the pulsations versus time. From top to bottom: (1,0) pulsation (full line); (0,1) pulsation (full line); (1,1) pulsation (dashed line); (2,0) pulsation (dashed line); (–1,1) pulsation (dashed line, with large error bars); (0,2) pulsation (dotted line).

Recent Maxima of 56 Short Period Pulsating Stars

Gerard Samolyk
P.O. Box 20677, Greenfield, WI 53220; gsamolyk@wi.rr.com

Received January 3, 2011; accepted January 5, 2011

Abstract This paper contains times of maxima for 56 short period pulsating stars (primarily RR Lyrae and δ Scuti stars). This represents a portion of the CCD observations received by the AAVSO Short Period Pulsator (SPP) section in 2010 along with some earlier data.

1. Recent observations

The accompanying list contains times of maxima calculated from CCD observations made by participants in the AAVSO's Short Period Pulsator (SPP) Section. This list will be web-archived and made available through the AAVSO ftp site at ftp://ftp.aavso.org/public/datasets/jsamog391.txt. These observations were reduced by the writer using the PERANSO program (Vanmunster 2007). The error estimate is included.

RR Lyr stars in this list, along with data from earlier AAVSO publications, are included in the GEOS database at: http://rr-lyr.ast.obs-mip.fr/dbrr/dbrr-V1.0_0.php. This database does not include δ Scuti stars.

The linear elements in the *General Catalogue of Variable Stars* (GCVS; Kholopov *et al.* 1985, print version) were used to compute the O–C values for most stars. For a few exceptions where the GCVS elements are missing or are in significant error, light elements from another source are used: DG Hya (Samolyk 2010), AH Leo (Schmidt *et al.* 1995), and VY LMi (Henden and Vidal-Sainz 1997).

References

Henden, A. A., and Vidal-Sainz, J. 1997, *Inf. Bull. Var. Stars*, No. 4535, 1.
Kholopov, P. N., *et al.* 1985, *General Catalogue of Variable Stars*, 4th ed., Moscow.
Samolyk, G. 2010, *Journ. Amer. Assoc. Var. Stars*, **38**, 1239.
Schmidt, E. G., Chab, J. R., and Reiswig, D. E. 1995, *Astron. J.*, **109**, 1239.
Vanmunster, T. 2007, PERANSO period analysis software, http://www.peranso.com

Table 1. Recent times of maxima of stars in the AAVSO RR Lyrae program.

Star	JD(max) Hel. 2400000 +	Cycle	O–C	Observer	Error
SW And	55441.7880	84357	–0.3714	K. Menzies	0.0009
SW And	55527.5863	84551	–0.3753	N. Simmons	0.0020
SW And	55535.5462	84569	–0.3764	K. Menzies	0.0018
SW And	55539.5318	84578	–0.3713	K. Menzies	0.0019
SW And	55550.5834	84603	–0.3767	N. Simmons	0.0011
AC And	54295.4968	41567	0.1794	R. Papini	0.0019
AC And	54302.7574	41581	0.0882	G. Samolyk	0.0035
AC And	54308.5360	41592	0.0904	M. Banfi	0.0025
AC And	54308.5438	41592	0.0982	A. Marchini	0.0027
AC And	54310.6405	41596	0.0944	G. Samolyk	0.0033
AC And	54312.7359	41600	0.0893	G. Samolyk	0.0028
AC And	54329.6257	41632	0.1750	G. Samolyk	0.0019
AC And	54339.6250	41651	0.1969	G. Samolyk	0.0017
AC And	54361.6511	41693	0.1677	G. Samolyk	0.0019
AC And	54363.7675	41697	0.1836	G. Samolyk	0.0021
AC And	54656.8122	42255	0.2075	G. Samolyk	0.0026
AC And	54674.6553	42289	0.1963	G. Samolyk	0.0037
AC And	54676.7764	42293	0.2169	G. Samolyk	0.0024
AC And	54696.7108	42331	0.1965	G. Samolyk	0.0014
AC And	54698.8277	42335	0.2129	G. Samolyk	0.0016
AC And	54708.8218	42354	0.2296	G. Samolyk	0.0023
AC And	54726.6140	42388	0.1675	G. Samolyk	0.0011
AC And	54728.7272	42392	0.1802	G. Samolyk	0.0012
AC And	54768.6363	42468	0.1796	G. Samolyk	0.0017
AC And	55043.7987	42992	0.1756	G. Samolyk	0.0013
AC And	55075.8249	43053	0.1691	G. Samolyk	0.0015
AC And	55085.8152	43072	0.1820	G. Samolyk	0.0020
AC And	55093.7085	43087	0.1984	G. Samolyk	0.0020
AC And	55105.7356	43110	0.1475	G. Samolyk	0.0021
AC And	55115.7214	43129	0.1559	G. Samolyk	0.0014
AC And	55147.7438	43190	0.1456	G. Samolyk	0.0020
AC And	55410.8818	43691	0.1951	G. Samolyk	0.0013
AC And	55415.6989	43701	–0.2391	G. Samolyk	0.0028
AC And	55420.8895	43710	0.2254	G. Samolyk	0.0032
AC And	55427.8152	43724	–0.2007	G. Samolyk	0.0026
AC And	55435.7164	43739	–0.1764	G. Samolyk	0.0031
AC And	55437.8410	43743	–0.1523	G. Samolyk	0.0026
AC And	55460.7234	43786	0.1496	G. Samolyk	0.0039

Table continued on following pages

Table 1. Recent times of maxima of stars in the AAVSO RR Lyrae program, cont.

Star	*JD(max) Hel. 2400000 +*	*Cycle*	*O–C*	*Observer*	*Error*
AC And	55470.7168	43805	0.1656	G. Samolyk	0.0026
TZ Aqr	55478.7002	31390	0.0111	G. Samolyk	0.0019
YZ Aqr	55443.7742	36380	0.0627	R. Sabo	0.0010
TZ Aur	55209.5607	90144	0.0118	K. Menzies	0.0006
TZ Aur	55539.7422	90987	0.0116	K. Menzies	0.0009
TZ Aur	55548.7509	91010	0.0118	K. Menzies	0.0008
TZ Aur	55559.7186	91038	0.0126	R. Poklar	0.0014
TZ Aur	55561.6764	91043	0.0120	K. Menzies	0.0008
BH Aur	55206.5414	27308	–0.0009	K. Menzies	0.0009
BH Aur	55247.5917	27398	0.0014	K. Menzies	0.0006
BH Aur	55257.6246	27420	0.0003	G. Samolyk	0.0013
BH Aur	55467.8834	27881	0.0017	R. Sabo	0.0009
BH Aur	55488.8600	27927	–0.0018	R. Sabo	0.0012
NU Aur	55540.5266	30551	0.2454	K. Menzies	0.0027
NU Aur	55554.5712	30577	0.2652	K. Menzies	0.0022
NU Aur	55555.6441	30579	0.2592	K. Menzies	0.0026
RS Boo	55297.7125	35849	–0.0019	R. Poklar	0.0006
RS Boo	55341.4833	35965	–0.0024	M. Martinengo	0.0008
SW Boo	55257.8089	24705	0.3372	G. Samolyk	0.0015
SW Boo	55261.9191	24713	0.3392	G. Samolyk	0.0016
SW Boo	55311.7289	24810	0.3367	R. Poklar	0.0017
SW Boo	55316.3537	24819	0.3398	P. Damiano	0.0010
SW Boo	55317.3818	24821	0.3408	G. Corfini	0.0012
SW Boo	55336.3811	24858	0.3396	R. Zambelli	0.0012
SW Boo	55336.3813	24858	0.3398	G. Corfini	0.0012
SW Boo	55338.4365	24862	0.3409	G. Corfini	0.0025
SW Boo	55340.4900	24866	0.3403	G. Corfini	0.0013
SW Boo	55354.3562	24893	0.3412	G. Corfini	0.0009
SW Boo	55354.3564	24893	0.3414	R. Zambelli	0.0009
SW Boo	55355.3850	24895	0.3430	G. Corfini	0.0014
SW Boo	55356.4081	24897	0.3390	G. Corfini	0.0011
SW Boo	55358.4654	24901	0.3422	G. Corfini	0.0013
SW Boo	55373.3579	24930	0.3424	G. Corfini	0.0017
SW Boo	55374.3854	24932	0.3428	G. Corfini	0.0011
SW Boo	55375.4117	24934	0.3421	G. Corfini	0.0015
SW Boo	55376.4395	24936	0.3428	R. Zambelli	0.0012
SW Boo	55377.4685	24938	0.3447	R. Zambelli	0.0021
SW Boo	55378.4930	24940	0.3422	G. Corfini	0.0012

Table continued on following pages

Table 1. Recent times of maxima of stars in the AAVSO RR Lyrae program, cont.

Star	JD(max) Hel. 2400000 +	Cycle	O–C	Observer	Error
SW Boo	55391.3322	24965	0.3432	G. Corfini	0.0012
SW Boo	55392.3605	24967	0.3444	G. Corfini	0.0012
SW Boo	55393.3871	24969	0.3440	G. Corfini	0.0009
SZ Boo	55292.7017	52891	0.0087	K. Menzies	0.0013
TV Boo	55260.7479	98065	0.0993	G. Samolyk	0.0031
TV Boo	55294.7927	98174	0.0751	R. Sabo	0.0026
TV Boo	55296.6673	98180	0.0743	G. Samolyk	0.0012
TV Boo	55300.7622	98193	0.1060	R. Poklar	0.0015
TV Boo	55304.7936	98206	0.0741	R. Sabo	0.0027
TV Boo	55316.6695	98244	0.0727	K. Menzies	0.0010
TV Boo	55333.8571	98299	0.0696	R. Sabo	0.0031
TV Boo	55341.6845	98324	0.0830	K. Menzies	0.0011
TV Boo	55356.6805	98372	0.0761	K. Menzies	0.0017
TV Boo	55379.8255	98446	0.0917	R. Sabo	0.0031
TV Boo	55394.8108	98494	0.0742	R. Sabo	0.0029
TW Boo	55212.9285	53209	–0.0615	K. Menzies	0.0016
TW Boo	55291.7037	53357	–0.0628	R. Poklar	0.0014
TW Boo	55323.6399	53417	–0.0630	K. Menzies	0.0011
TW Boo	55407.7421	53575	–0.0599	R. Sabo	0.0030
UU Boo	55264.7859	41977	0.2241	K. Menzies	0.0010
UU Boo	55280.7773	42012	0.2233	K. Menzies	0.0007
UU Boo	55313.6775	42084	0.2252	R. Poklar	0.0017
UU Boo	55329.6712	42119	0.2267	K. Menzies	0.0010
UY Boo	53438.8137	17827	0.6574	J. Bialozynski	0.0012
UY Boo	54206.8829	19007	0.7395	J. Bialozynski	0.0016
UY Boo	54570.7909	19566	0.8299	J. Bialozynski	0.0033
UY Boo	55346.6584	20758	0.9003	G. Samolyk	0.0015
UY Cam	55246.703	73702	–0.091	G. Samolyk	0.003
UY Cam	55544.715	74818	–0.098	R. Poklar	0.003
RW Cnc	55219.5629	28625	–0.3225	R. Papini	0.0020
RW Cnc	55223.9396	28633	–0.3234	G. Samolyk	0.0015
RW Cnc	55238.6993	28660	–0.3380	G. Samolyk	0.0016
RW Cnc	55279.7435	28735	–0.3338	G. Samolyk	0.0017
TT Cnc	52360.6060	22036	0.0680	G. Lubcke	0.0020
TT Cnc	55273.6736	27206	0.1022	K. Menzies	0.0009
TT Cnc	55273.6744	27206	0.1030	G. Samolyk	0.0015
VZ Cnc	55212.8193	85866	0.0169	K. Menzies	0.0009
SS CVn	54219.6332	30505	–0.3549	C. Hesseltine	0.0055

Table continued on following pages

Table 1. Recent times of maxima of stars in the AAVSO RR Lyrae program, cont.

Star	*JD(max) Hel. 2400000 +*	*Cycle*	*O–C*	*Observer*	*Error*
SS CVn	55299.6823	32762	–0.3277	R. Poklar	0.0010
RR Cet	55512.6886	40380	0.0083	R. Poklar	0.0015
RR Cet	55528.7262	40409	0.0081	R. Poklar	0.0019
RZ Cet	55510.6570	42310	–0.1754	R. Poklar	0.0022
XX Cyg	55163.5528	79399	0.0032	N. Simmons	0.0006
XX Cyg	55341.7100	80720	0.0036	G. Samolyk	0.0007
XX Cyg	55341.8435	80721	0.0022	G. Samolyk	0.0007
XX Cyg	55346.6999	80757	0.0035	C. Hesseltine	0.0008
XX Cyg	55346.8341	80758	0.0028	C. Hesseltine	0.0007
XX Cyg	55464.8417	81633	0.0034	R. Sabo	0.0007
XZ Cyg	55344.6625	24046	–2.0457	G. Samolyk	0.0009
XZ Cyg	55357.7457	24074	–2.0301	G. Samolyk	0.0025
XZ Cyg	55372.6672	24106	–2.0430	G. Samolyk	0.0012
XZ Cyg	55377.7971	24117	–2.0468	G. Samolyk	0.0012
XZ Cyg	55378.7308	24119	–2.0465	G. Samolyk	0.0022
XZ Cyg	55384.7913	24132	–2.0531	R. Sabo	0.0026
XZ Cyg	55468.7840	24312	–2.0664	R. Sabo	0.0024
DM Cyg	55345.7976	30399	0.0675	G. Samolyk	0.0013
DM Cyg	55397.8543	30523	0.0615	R. Sabo	0.0006
DM Cyg	55404.5768	30539	0.0663	K. Menzies	0.0009
DM Cyg	55413.8113	30561	0.0638	R. Sabo	0.0012
DM Cyg	55422.6310	30582	0.0665	K. Menzies	0.0007
DM Cyg	55426.8306	30592	0.0675	R. Sabo	0.0011
DM Cyg	55437.7472	30618	0.0677	G. Samolyk	0.0012
DM Cyg	55439.4303	30622	0.0714	R. Papini	0.0014
DM Cyg	55442.7863	30630	0.0685	R. Sabo	0.0009
DM Cyg	55472.5957	30701	0.0678	K. Menzies	0.0005
DM Cyg	55476.3729	30710	0.0663	A. Marchini	0.0007
RW Dra	55386.8275	36145	0.2015	R. Sabo	0.0009
RW Dra	55425.8060	36233	0.2033	R. Sabo	0.0023
XZ Dra	55309.7073	28083	–0.1320	G. Samolyk	0.0022
XZ Dra	55398.8074	28270	–0.1368	R. Sabo	0.0018
XZ Dra	55419.7680	28314	–0.1421	R. Sabo	0.0032
SS For	55486.7463	33946	–0.1394	G. Samolyk	0.0011
RR Gem	55180.4116	34793	–0.4211	M. Martinengo	0.0007
RR Gem	55186.3722	34808	–0.4202	M. Martinengo	0.0009
RR Gem	55191.5335	34821	–0.4239	A. Marchini	0.0005
RR Gem	55199.4812	34841	–0.4224	A. Marchini	0.0008

Table continued on following pages

Table 1. Recent times of maxima of stars in the AAVSO RR Lyrae program, cont.

Star	JD(max) Hel. 2400000 +	Cycle	O–C	Observer	Error
RR Gem	55199.4816	34841	–0.4220	R. Papini	0.0009
RR Gem	55202.6586	34849	–0.4235	R. Poklar	0.0010
RR Gem	55203.4513	34851	–0.4254	N. Ruocco	0.0008
RR Gem	55210.6052	34869	–0.4231	M. Martinengo	0.0011
RR Gem	55212.5902	34874	–0.4247	R. Papini	0.0007
RR Gem	55216.5646	34884	–0.4234	N. Ruocco	0.0008
RR Gem	55218.5495	34889	–0.4250	A. Marchini	0.0007
RR Gem	55220.5348	34894	–0.4263	A. Marchini	0.0005
RR Gem	55250.7333	34970	–0.4234	R. Sabo	0.0008
RR Gem	55491.8817	35577	–0.4425	G. Samolyk	0.0012
RR Gem	55545.5134	35712	–0.4477	A. Marchini	0.0008
RR Gem	55545.5139	35712	–0.4472	M. Martinengo	0.0008
RR Gem	55547.9003	35718	–0.4447	R. Sabo	0.0014
RR Gem	55551.8712	35728	–0.4469	R. Sabo	0.0007
TW Her	55325.8141	84536	–0.0143	G. Samolyk	0.0010
VX Her	55303.7314	73683	0.0132	N. Simmons	0.0007
VX Her	55348.8135	73782	0.0134	G. Samolyk	0.0011
VZ Her	55292.8659	42023	0.0690	K. Menzies	0.0007
VZ Her	55338.6604	42127	0.0694	K. Menzies	0.0007
VZ Her	55381.8161	42225	0.0729	R. Sabo	0.0012
AR Her	54608.7178	27989	–1.2429	G. Samolyk	0.0015
AR Her	55281.7514	29421	–1.2894	G. Samolyk	0.0017
AR Her	55304.7349	29470	–1.3373	G. Samolyk	0.0013
AR Her	55312.7762	29487	–1.2864	R. Poklar	0.0012
AR Her	55367.7131	29604	–1.3428	G. Samolyk	0.0012
DL Her	52559.5619	24257	0.0167	G. Samolyk	0.0023
DL Her	54236.8530	27092	0.0428	J. Bialozynski	0.0025
DL Her	54594.7705	27697	0.0255	J. Bialozynski	0.0026
DL Her	54633.8162	27763	0.0237	G. Samolyk	0.0025
DL Her	54706.5859	27886	0.0232	K. Menzies	0.0015
DL Her	54933.7870	28270	0.0392	G. Samolyk	0.0020
DL Her	55346.7489	28968	0.0449	G. Samolyk	0.0012
DL Her	55395.8386	29051	0.0294	R. Sabo	0.0026
DY Her	55283.8102	146970	–0.0263	K. Menzies	0.0006
DY Her	55303.7278	147104	–0.0253	G. Samolyk	0.0010
DY Her	55316.8056	147192	–0.0270	K. Menzies	0.0008
DY Her	55340.7358	147353	–0.0265	G. Samolyk	0.0008
DY Her	55340.8846	147354	–0.0263	G. Samolyk	0.0009

Table continued on following pages

Table 1. Recent times of maxima of stars in the AAVSO RR Lyrae program, cont.

Star	*JD(max) Hel. 2400000 +*	*Cycle*	*O–C*	*Observer*	*Error*
LS Her	53120.7450	108817	–0.0046	S. Dvorak	0.0020
LS Her	53146.8250	108930	–0.0059	S. Dvorak	0.0020
LS Her	54277.8314	113830	0.0428	J. Bialozynski	0.0019
LS Her	54578.7655	115134	0.0036	J. Bialozynski	0.0026
LS Her	54658.6592	115480	0.0378	K. Menzies	0.0024
LS Her	55303.7160	118275	–0.0129	C. Hesseltine	0.0054
LS Her	55327.7413	118379	0.0084	K. Menzies	0.0024
LS Her	55333.7493	118405	0.0154	K. Menzies	0.0014
LS Her	55336.7713	118418	0.0369	R. Sabo	0.0028
LS Her	55336.7755	118418	0.0411	G. Samolyk	0.0021
LS Her	55354.7437	118496	0.0063	K. Menzies	0.0026
LS Her	55360.7430	118522	0.0046	R. Sabo	0.0022
LS Her	55365.6124	118543	0.0270	K. Menzies	0.0017
LS Her	55367.6725	118552	0.0099	G. Samolyk	0.0023
LS Her	55390.7665	118652	0.0231	R. Sabo	0.0014
LS Her	55396.7288	118678	–0.0156	R. Sabo	0.0012
LS Her	55402.7744	118704	0.0290	R. Sabo	0.0020
LS Her	55407.5764	118725	–0.0160	K. Menzies	0.0021
SZ Hya	54096.8250	24975	–0.1615	G. Samolyk	0.0017
SZ Hya	55242.6641	27108	–0.2558	R. Poklar	0.0023
SZ Hya	55257.7601	27136	–0.2025	G. Samolyk	0.0012
SZ Hya	55263.6638	27147	–0.2085	G. Samolyk	0.0021
SZ Hya	55271.6740	27162	–0.2569	R. Poklar	0.0029
SZ Hya	55271.6753	27162	–0.2556	G. Samolyk	0.0038
SZ Hya	55277.6345	27173	–0.2060	G. Samolyk	0.0014
SZ Hya	55292.6557	27201	–0.2275	R. Poklar	0.0030
UU Hya	54540.6949	28751	0.0115	J. Bialozynski	0.0016
UU Hya	55263.6217	30131	–0.0001	G. Samolyk	0.0015
DG Hya	55271.6146	3841	0.0034	G. Samolyk	0.0018
DG Hya	55286.7012	3861	0.0051	R. Poklar	0.0019
DH Hya	55272.6808	49277	0.0725	R. Poklar	0.0012
DH Hya	55273.6599	49279	0.0736	G. Samolyk	0.0009
RR Leo	55217.8755	26354	0.1005	K. Menzies	0.0006
RR Leo	55261.7583	26451	0.1011	K. Menzies	0.0006
RR Leo	55276.6882	26484	0.1020	R. Poklar	0.0008
RR Leo	55281.6644	26495	0.1019	R. Poklar	0.0011
RR Leo	55521.8901	27026	0.1068	K. Menzies	0.0006
SS Leo	55274.6678	21543	–0.0721	R. Poklar	0.0015

Table continued on following pages

Table 1. Recent times of maxima of stars in the AAVSO RR Lyrae program, cont.

Star	JD(max) Hel. 2400000 +	Cycle	O–C	Observer	Error
ST Leo	55261.8863	57196	–0.0217	G. Samolyk	0.0008
TV Leo	55261.6772	27079	0.1116	G. Samolyk	0.0025
WW Leo	55267.6466	33815	0.0398	R. Poklar	0.0024
AA Leo	55259.7990	26164	–0.0837	G. Samolyk	0.0017
AA Leo	55289.7331	26214	–0.0824	R. Poklar	0.0022
AH Leo	55540.9261	14779	0.0205	K. Menzies	0.0026
AH Leo	55548.8591	14796	0.0247	K. Menzies	0.0032
AH Leo	55554.9205	14809	0.0229	K. Menzies	0.0022
VY LMi	55554.8222	9631	0.0031	K. Menzies	0.0015
U Lep	55199.6639	23814	0.0437	R. Poklar	0.0013
U Lep	55206.6447	23826	0.0468	G. Samolyk	0.0019
SZ Lyn	54879.6191	139007	0.0232	R. Poklar	0.0008
SZ Lyn	54879.7384	139008	0.0220	R. Poklar	0.0006
SZ Lyn	55206.7590	141721	0.0314	G. Samolyk	0.0008
SZ Lyn	55209.6519	141745	0.0314	K. Menzies	0.0005
SZ Lyn	55210.7380	141754	0.0327	G. Samolyk	0.0008
SZ Lyn	55212.6651	141770	0.0313	R. Poklar	0.0009
SZ Lyn	55259.5524	142159	0.0305	G. Samolyk	0.0008
SZ Lyn	55301.6182	142508	0.0296	G. Samolyk	0.0008
SZ Lyn	55301.7401	142509	0.0309	G. Samolyk	0.0008
SZ Lyn	55478.8012	143978	0.0262	G. Samolyk	0.0007
SZ Lyn	55525.8088	144368	0.0252	K. Menzies	0.0010
RR Lyr	55416.5260	22039	–0.0919	L. Corp	0.0037
RR Lyr	55416.5296	22039	–0.0883	L. Corp	0.0044
RR Lyr	55429.5710	22062	–0.0848	L. Corp	0.0020
RR Lyr	55437.4984	22076	–0.0936	L. Corp	0.0028
RR Lyr	55437.5023	22076	–0.0897	L. Corp	0.0027
RR Lyr	55450.5102	22099	–0.1197	L. Corp	0.0031
RR Lyr	55450.5162	22099	–0.1137	L. Corp	0.0016
RZ Lyr	55381.6305	27772	–0.0167	K. Menzies	0.0010
RZ Lyr	55411.7828	27831	–0.0277	R. Sabo	0.0014
AV Peg	55424.7837	29803	0.1305	R. Sabo	0.0009
DF Ser	55305.7747	58474	0.0889	G. Samolyk	0.0012
RV UMa	55197.8988	21626	0.1222	G. Samolyk	0.0010
RV UMa	55257.8057	21754	0.1175	G. Samolyk	0.0018
RV UMa	55273.7269	21788	0.1246	G. Samolyk	0.0011
RV UMa	55295.7218	21835	0.1207	R. Poklar	0.0012
SX UMa	53480.8610	27258	0.1110	V. Petriew	0.0010

Table continued on following page

Table 1. Recent times of maxima of stars in the AAVSO RR Lyrae program, cont.

Star	*JD(max) Hel. 2400000 +*	*Cycle*	*O–C*	*Observer*	*Error*
SX UMa	53483.9320	27268	0.1108	V. Petriew	0.0010
SX UMa	53492.8400	27297	0.1124	V. Petriew	0.0010
SX UMa	53780.9360	28235	0.1319	V. Petriew	0.0010
AE UMa	55199.7092	227808	–0.0021	G. Samolyk	0.0006
AE UMa	55199.8015	227809	0.0042	G. Samolyk	0.0007
AE UMa	55199.8840	227810	0.0007	G. Samolyk	0.0005
AE UMa	55202.6329	227842	–0.0029	G. Samolyk	0.0006
AE UMa	55202.7256	227843	0.0037	G. Samolyk	0.0007
AE UMa	55202.8087	227844	0.0008	G. Samolyk	0.0007

The Variable Star HD 173637

Arlo U. Landolt
Department of Physics and Astronomy, Louisiana State University, Baton Rouge, LA 70803; landolt@phys.lsu.edu

and

Visiting astronomer, Cerro Tololo Inter-American Observatory and Kitt Peak National Observatory, National Optical Astronomical Observatory, which is operated by the Association of Universities for Research in Astronomy, Inc., under contract with the National Science Foundation.

Received August 16, 2010; revised November 5, 2010; accepted November 17, 2010

Abstract *UBV* photometry is presented of the emission line star HD 173637 = V455 Sct, both before and after the star's recognition as being variable in light.

1. Introduction

The star HD 173637 (R.A. = $18^h\ 46^m\ 38.081^s$, Dec. = –07° 55' 55.12", 2000) was included in a list of *UBVRI* photometric standard stars (Landolt 1983). A description containing additional information for HD 173637 was included in an Appendix to that paper. Other names for the star include BD –08 4702, MWC 607, HIP 92128, SAO 142608, AAVSO 1841–08, and ASAS 184638-0755.9. Some years later (Landolt 1993) it was realized that the "e" in the star's spectral classification B0e (Neubauer 1943) should have warned the author concerning the star's appropriateness as a standard star. Emission line stars have a habit of occasionally varying in brightness. An introductory description of such stars is given by Sterken and Jaschek (1996). The most recent spectral type of HD 173637 is B1IV (Morgan *et al.* 1955).

Observations by the author at the CTIO Yale 1.0-m telescope (Landolt 1993) found HD 173637 to be brighter than previously had been known. Therefore, the star no longer should be used as a calibrating standard star. Subsequently, the variable star designation V455 Sct was assigned to HD 173637.

Since the author has standardized multi-color photometry both before and after HD 173637 underwent a change in brightness, it was thought that publication of those data might be useful in future long term studies of the star.

2. Observations

A description of the data obtained for HD 173637 prior to its brightening were published in (Landolt 1983). Those observations were obtained during the

time interval 1978 April 11 through 1981 June 12 UT. The mean error of a single observation for the data for HD 173637 in that paper's Table I*V* was 0.015 in *V*, 0.014 in (*B–V*), and 0.014 in (*U–B*).

Subsequent to data taken prior to the star's brightening, observations were made at the Cerro Tololo Inter-American Observatory's (CTIO) Yale 1.0-m telescope [16], at the CTIO 1.5-m telescope [3], and at Kitt Peak National Observatory's (KPNO) #2 0.9-m telescope [1]. The numbers in brackets provide the number of measures made at each telescope. These data, all obtained with a photoelectric photomultiplier, covered the time interval 1993 June 25 through 2001 October 8.

The data taken prior to brightening were reduced as described in Landolt (1983). All data subsequent to the star's brightening were reduced as described in Landolt (1992). A summary of the observing and reduction philosophy is recorded in Landolt (2007). The error of a single observation, as derived from each night's standard star measurements, is listed in Table 1. These errors are directly applicable to the measurements of HD 173637 since it is of similar brightness as the standard stars.

Recent years saw the beginning of a highly successful All Sky Automated Survey (ASAS) monitoring program at Las Campanas, Chile. Information on the details of the resulting database are in (Pojmański 2002), and at http://www.astrouw.edu.pl/asas/?page=papers. One can find online at http://www.astrouw.edu.pl/asas/?page=aasc the information gleaned from the ASAS database. The star of current interest, HD 173637, appears in the ASAS database, and is identified therein as ASAS 184638-0755.9.

Pojmański (2010) provided a discussion of procedures used in the acquisition and reduction of the data which form the ASAS database. This information is available online at http://www.astrouw.edu.pl/asas/explanations.html. Following advice therein, magnitudes measured through an aperture of six pixels (MAG_4) were chosen for use here. This recommended aperture, for stars of 9th, or brighter, magnitude, corresponded to a 90-arcsec aperture.

3. Discussion

The data published in Landolt (1983), covering the time interval Heliocentric Julian Day (HJD) 2443609.87474 through 2444767.80878, indicated a brightness and color indices for HD 173637 of $V = 9.375$, $(B–V) = +0.236$, $(U–B) = –0.729$, $(V–R) = +0.168$, $(R–I) = +0.187$, and $(V–I) = +0.354$. When next observed (Landolt 1993), it was found to have brightened to $V = 8.944$ (on HJD 2449163.75847 in Table 2 herein), an increase of about 0.4 magnitude. Since then, over the time interval HJD 2449163.75847 through 2452190.56020, according to this author's observations, the star has remained near $V = 8.94 \pm 0.05$, with a slight brightening during 1995 July, near HJD 2449927, to $V = 8.87$. The data indicate that when the star brightens, it becomes redder in (*B–V*) and bluer in (*U–B*). The *V* light curve from the author's data is displayed in Figure 1.

The ASAS light curve shows an overall decline in the brightness of HD 173637 from $V = 8.78$ to 9.45 in the interval HJD 2451962.89437 to 2455136.50915. The five first and five last V magnitude data entries from the ASAS database are shown in Table 3, illustrative of the database content. These V magnitudes were taken from the MAG_4 column in the ASAS tabulation which utilized data taken through a six pixel-wide (90-arc second diameter) aperture. As written by Pojmański (2010), "the V magnitude represents a zero point adjustment, only, of observed instrumental magnitude, to place the observed instrumental magnitude onto the standard photometric system. No color correction was attempted." The third column in Table 3 gives an error for the V magnitude, not for HD 173637 per se, but an average photometric error for the frame. The light curve based on the ASAS database, and illustrated in Figure 2, shows small brightenings or outbursts, occurring at irregular intervals, at times quasi-regular, the largest of which was about 0.3 magnitude, and lasting anywhere from 286 to 1914 days, or so, as measured from beginning of brightening to the end of a slow decline. The ASAS database indicated that HD 173637 varies in brightness with a period of 93.46164 days. No periodicity is evident in either the ASAS or current data. It is likely that this period estimate came from an early, less complete, data sample (Pojmański 2010).

HD 173637 appears in the *Hipparcos Catalogue* (Perryman *et al.* 1997) as HIP 92128. These data cover the approximate Julian Day interval 2447963 to 2449058. The star exhibits an approximate 0.1-magnitude fluctuation in brightness over most of this time frame, rising some 0.25 magnitude near the end of the Hipparcos observing program. These data are summarized in ESA SP-1200, volume 11, page U43, and in ESA SP-1200, volume 8, page 1850. A light curve is shown in ESA SP-1200, volume 12, page C125. Several lines at the beginning and at the end of a subset of the Hipparcos data are given in this paper in Table 4. It should be noted that the Hipparcos times of observation are given in Barycentric Julian Days (BJD).

There is a 75-day overlap of the author's and the ASAS data sets between HJD 2452115.64 and 2452190.56. The overlapping V magnitudes for HD 173637 in the ASAS dataset are some 0.07 magnitude fainter than those in Table 2, most likely a result of the method used to set the zero point of the ASAS data. The data in Table 2 illustrate the brightening from $V \sim 9.4$ to $V \sim 8.9$. The data in Table 3 show recent behavior in the range $8.8 \leq V \leq 9.4$. Hence, HD 173637 has returned to its brightness level of 1978 April 11 UT in recent years, roughly 2005 May to 2009 November.

Figures 1, 2, and 3 provide higher resolution of the photometric behavior of HD 173637. A composite plot of the star's photometric behavior over more than 31 years is given in Figure 4. It should be noted that the Hipparcos data's Barycentric Julian Day time measurements are plotted in Figure 4 as though they were Heliocentric Julian Days, permissible since the time differences of the photometric behavior is greater than the plus or minus four seconds or so difference in a BJD or HJD time measurement.

This author's, the ASAS, and the Hipparcos data all were taken over long periods of time. In contrast, (Gutiérrez-Soto *et al.* 2007) used the COROT satellite to search for short period light variations in selected Be stars, including HD 173637. Their data allowed a search for a short-term periodicity in their 2003 dataset. (Gutiérrez-Soto *et al.* 2007) wrote that they detected "significant peaks in the frequency domain at 1.86 c d^{-1}."

4. Acknowledgements

It is a pleasure to thank the staffs of the KPNO and CTIO for their help in making the observing runs a success. The author thanks G. Pojmański for comments regarding the ASAS survey and database.

This work has been funded by AFOSR grants 77-3218 and 82-0192, and NSF grant AST-0803158.

References

Gutiérrez-Soto, J., Fabregat, J., Suso, J., Lanzara, M., Garrido, R., Hubert, A. -M., and Floquet, M. 2007, *Astron. Astrophys.*, **476**, 927.

Landolt, A. U. 1983, *Astron. J.*, **88**, 439.

Landolt, A. U. 1992, *Astron. J.*, **104**, 340.

Landolt, A. U. 1993, *IAU Circ.*, No. 5822.

Landolt, A. U. 2007, in *The Future of Photometric, Spectrophotometric and Polarimetric Standardization*, ed. C. Sterken, ASP Conf. Proc. 364, Astron. Soc. Pacific, San Francisco, 27.

Morgan, W. W., Code, A. D., and Whitford, A. E. 1955, *Astrophys. J., Suppl. Ser.*, **2**, 41.

Neubauer, F. J. 1943, *Astrophys. J.*, **97**, 300.

Perryman, M. A. C., European Space Agency Space Science Department, and the Hipparcos Science Team 1997, *The Hipparcos and Tycho Catalogues*, ESA SP-1200, ESA Publications Divisionk Noordwiijk, The Netherlands.

Pojmański, G. 2002, *Acta Astron.*, **52**, 397.

Pojmański, G. 2010, personal communication.

Sterken, C., and Jaschek, C. 1996, *Light Curves of Variable Stars. A Pictorial Atlas*, Cambridge Univ. Press, Cambridge, p. 73.

Table 1. RMS errors for nights containing HD 173637 data.

UT (mmddyy)	*V*	*(B–V)*	*(U–B)*	*(V–R)*	*(R–I)*	*(V–I)*
041178	0.010	0.011	0.023	0.004	0.004	0.006
060778	0.004	0.007	0.018	0.005	0.006	0.003
061078	0.006	0.008	0.015	0.003	0.004	0.003
082778	0.004	0.008	0.012	0.003	0.006	0.005
061479	0.008	0.011	0.013	0.004	0.005	0.005
061679	0.009	0.008	0.012	0.002	0.005	0.004
090980	0.010	0.011	0.023	0.003	0.006	0.004
091080	0.007	0.010	0.024	0.002	0.005	0.005
060281	0.006	0.008	0.010	—	—	—
061281	0.005	0.008	0.015	0.012	0.010	0.007
062593	0.015	0.009	0.016	—	—	—
062693	0.007	0.005	0.011	—	—	—
062793	0.007	0.007	0.028	—	—	—
070893	0.009	0.005	0.016	0.006	0.007	0.010
092493	0.009	0.010	0.028	—	—	—
092593	0.010	0.008	0.031	—	—	—
092693	0.011	0.007	0.020	—	—	—
092793	0.007	0.009	0.024	—	—	—
052594	0.006	0.012	0.023	—	—	—
070594	0.009	0.011	0.020	—	—	—
072895	0.006	0.010	0.026	—	—	—
072995	0.006	0.010	0.016	—	—	—
073195	0.004	0.008	0.020	—	—	—
030896	0.009	0.009	0.023	—	—	—
072501	0.007	0.007	0.023	—	—	—
082101	0.008	0.010	0.033:	—	—	—
100801	0.009	0.013	0.033:	—	—	—
ave.	0.0077	0.0089	0.0206	0.0044	0.0058	0.0052
±	0.0024	0.0020	0.0067	0.0030	0.0018	0.0021

Table 2. UBVRI photoelectric photometry of HD 173637.

HJD	*V*	*(B–V)*	*(U–B)*	*(V–R)*	*(R–I)*	*(V–I)*
2443609.87474	9.411	+0.271	–0.666	+0.187	+0.180	+0.367
2443609.87770	9.410	+0.264	–0.646	+0.165	+0.182	+0.347
2443666.83362	9.371	+0.238	–0.751	+0.166	+0.188	+0.354
2443666.83631	9.369	+0.235	–0.744	+0.164	+0.192	+0.357
2443669.79301	9.363	+0.224	–0.738	+0.158	+0.197	+0.354
2443669.79546	9.366	+0.220	–0.738	+0.159	+0.193	+0.351
2443747.59328	9.375	+0.234	–0.727	+0.164	+0.175	+0.338
2443747.59556	9.378	+0.230	–0.719	+0.167	+0.179	+0.344
2444038.81382	9.359	+0.236	–0.712	+0.160	+0.186	+0.346
2444038.81617	9.365	+0.230	–0.712	+0.171	+0.182	+0.353
2444040.81997	9.369	+0.244	–0.727	+0.170	+0.186	+0.355
2444040.82342	9.377	+0.224	–0.710	+0.179	+0.190	+0.369
2444491.60056	9.373	+0.232	–0.723	+0.174	+0.187	+0.361
2444492.60506	9.375	+0.238	–0.739	+0.170	+0.200	+0.369
2444757.84311	9.366	+0.219	–0.671	—	—	—
2444757.84496	9.357	+0.229	–0.680	—	—	—
2444767.80878	9.368	+0.224	–0.736	+0.164	+0.196	+0.360
2449163.75847	8.944	+0.367	–0.832	—	—	—
2449163.77291	8.960	+0.367	–0.831	—	—	—
2449164.63563	9.001	+0.360	–0.838	—	—	—
2449165.70810	8.945	+0.365	–0.827	—	—	—
2449176.79993	8.941	+0.379	–0.751	+0.315	+0.373	+0.687
2449254.55503	8.980	+0.353	–0.817	—	—	—
2449255.49769	8.974	+0.358	–0.867	—	—	—
2449256.50134	9.001	+0.360	–0.838	—	—	—
2449257.51057	8.990	+0.348	–0.841	—	—	—
2449497.82569	9.004	+0.340	–0.841	—	—	—
2449538.67485	8.945	+0.353	–0.826	—	—	—
2449926.69748	8.866	+0.386	–0.791	—	—	—
2449927.59423	8.874	+0.383	–0.835	—	—	—
2449927.59726	8.858	+0.387	–0.823	—	—	—
2449929.51739	8.885	+0.381	–0.821	—	—	—
2450150.90538	8.924	+0.394	–0.806	—	—	—
2452115.64020	8.866	+0.406	–0.800	+0.351	+0.407	+0.758
2452142.61303	8.906	+0.403	–0.792	+0.356	+0.414	+0.770
2452190.56020	8.947	+0.389	–0.786	+0.360	+0.416	+0.781

Table 3. ASAS data on HD 173637.

HJD 2450000.0+	*V*	V_{error}
1962.89437	8.782	0.047
1964.89797	8.792	0.041
1966.89386	8.813	0.038
1978.89188	8.813	0.046
1980.86618	8.790	0.044
—	—	—
—	—	—
—	—	—
5110.58556	9.392	0.074
5122.52506	9.378	0.065
5125.52060	9.358	0.075
5130.52295	9.422	0.083
5136.50915	9.451	0.082

Table 4. Hipparcos data on HD 173637.

BJD 2440000.0+	*V*	V_{error}
7963.25995	9.335	0.017
7963.33452	9.328	0.019
7989.28247	9.296	0.018
7989.29682	9.315	0.017
7989.37138	9.283	0.016
7989.38571	9.280	0.014
8010.43393	9.288	0.015
—	—	—
—	—	—
—	—	—
8932.98104	9.055	0.018
9041.11720	9.002	0.018
9041.13152	8.982	0.022
9058.51581	8.997	0.014
9058.53015	8.992	0.013
9058.68985	8.990	0.015

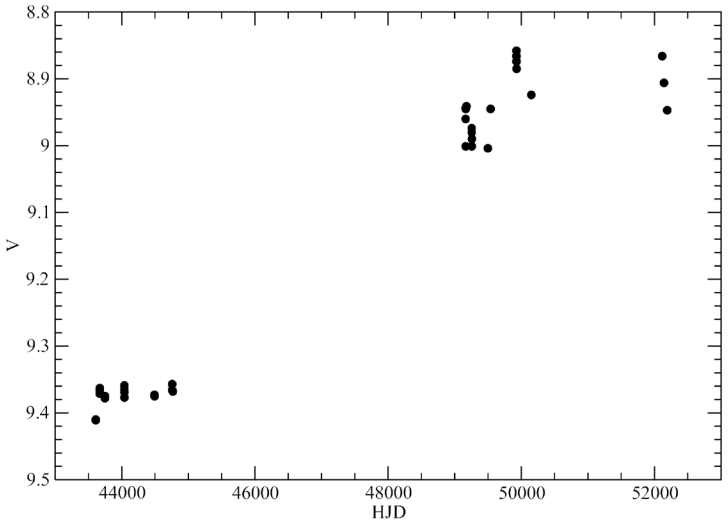

Figure 1. *V* magnitude light curve for HD 173637 based on the author's data in Table 2. To obtain the correct HJD, add 2400000.

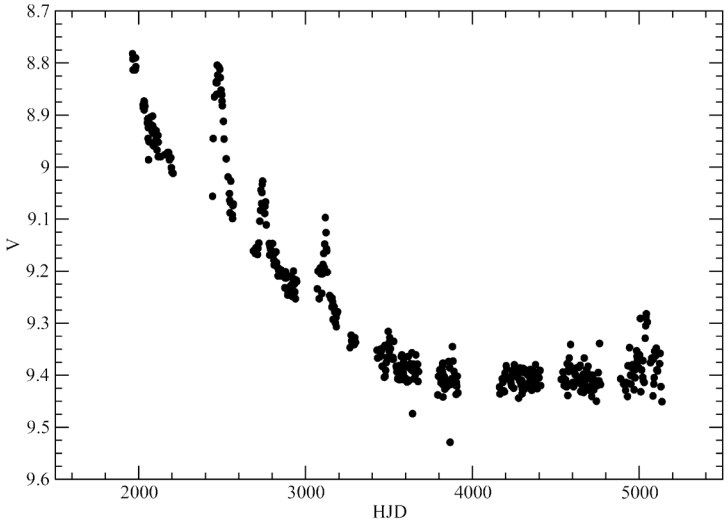

Figure 2. *V* magnitude light curve for HD 173637 based on the ASAS data in Table 3. To obtain the correct HJD, add 2450000.

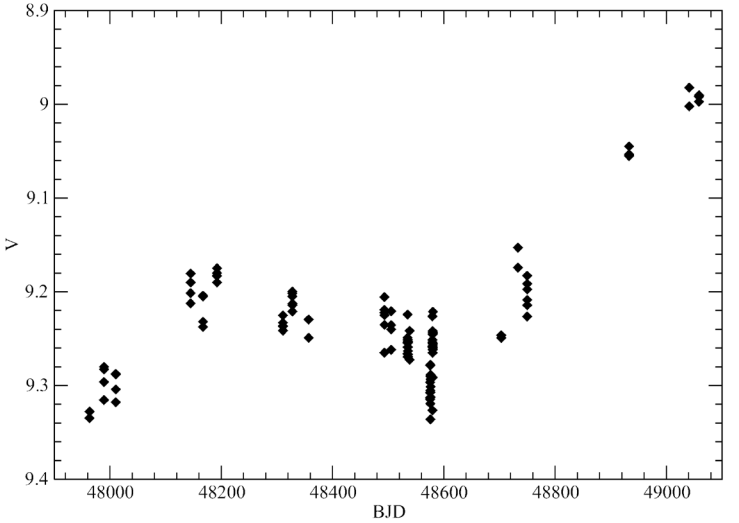

Figure 3. *V* magnitude light curve for HD 173637 based on the Hipparcos data in Table 4. To obtain the correct BJD, add 2400000.

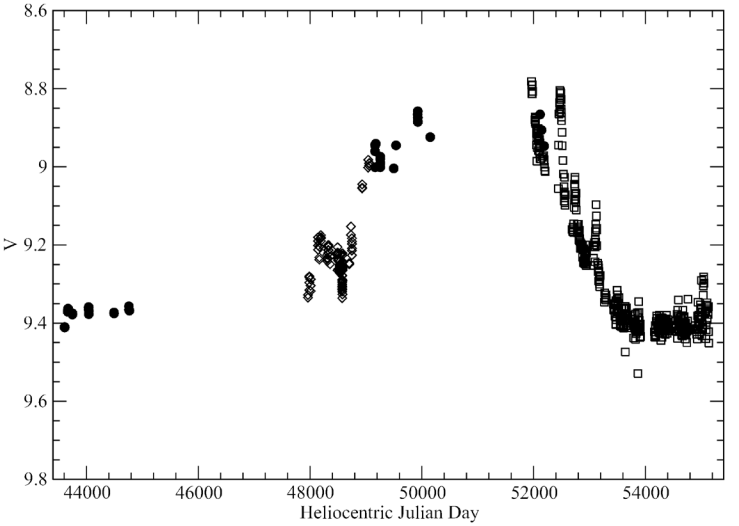

Figure 4. Composite *V* magnitude light curve for HD 173637. The data points from Table 2 (the author's) are plotted with filled circles, from Table 3 (ASAS data) with open squares, and from Table 4 (Hipparcos) with open diamonds. To obtain the correct JD, add 2400000.

CI Cygni 2010 Outburst and Eclipse: An Amateur Spectroscopic Survey—First Results From Low Resolution Spectra

François Teyssier
67 Rue Jacques Daviel, Rouen 76100, France; francois.teyssier@dbmail.com

Received January 10, 2011; revised February 10, 2011; accepted February 11, 2011

Abstract The aim of this document is to present an amateur spectroscopic survey of the 2010 outburst of symbiotic star CI Cygni by Christian Buil, Thierry Garrel, Benjamin Mauclaire, François Teyssier, Eric Sarrazin, and Pierre Dubreuil (ARAS—Astronomical Ring for Access to Spectroscopy). This outburst coincided with an eclipse of the hot component by the late-type giant star. After a brief review of the current knowledge of this system, the campaign is presented. The first results obtained from low-resolution spectra are described: main emission lines (equivalent width and absolute flux) and continuum evolution in comparison with the CCD *V* light curve obtained by AAVSO observers.

1. Introduction

Symbiotic stars are binary systems composed of a cool giant and a hot, luminous white dwarf, surrounded by an ionized nebula. CI Cyg is a symbiotic star containing a cool giant of type M5.5II (Mürset and Schmid 1999) and a compact star. CI Cyg is one of the very few symbiotic systems in which the giant fills or nearly fills its Roche lobe and shows ellipsoidal photometric variations in its light curve, especially in *R* and near-IR bands (Mikołajewska 2003).

From UV observations, Kenyon *et al.* (1991) argued that the compact star should be a $0.5M_{\odot}$ main sequence star surrounded by an extended accretion disk. The high temperature of the hot component (T = 125,000 K) allows the formation of high ionization emission lines (HeII, [Fe VII]) observed in CI Cyg during quiescence. The nature of the hot component is still controversial. On the one hand, Mikołajewska and Kenyon (1992) considered that the evolution during the outburst is best explained by the presence of an unstable thick disk around the main sequence accretor. On the other hand, Mikołajewska (2003) estimates that the quiescent characteristics of the hot component are more consistent with a hot and luminous white dwarf powered by nuclear burning of the accreted hydrogen. During outbursts the temperature is much lower ($T \leq$ 20,000 K). The higher excitation lines thus vanish as the outburst progress. This could be explained by a large expansion in the radius of the accreting star. The expansion of the pseudo-photosphere causes it to cool. The energy peak of the pseudo-photosphere shifts from the far UV to optical range, causing the star to appear in "outburst" (Siviero *et al.* 2009).

At quiescence, the spectrum is dominated by the molecular absorption bands of the cool giant star, Balmer, HeI, and high ionization emission lines (HeII, [Fe VII]) powered by the very hot companion (Figure 1).

Eclipses have been detected in the light curve. The permitted emission lines show a pronounced eclipse effect. The lack of eclipse in forbidden emission lines suggests that they are emitted in a much larger region than the Balmer and Helium lines (Mikołajewka 1985).

As shown in Figure 2, the M giant fills its Roche lobe and transfers material into an extended disk surrounding the hot component. The disk is surrounded by a small He II region and a larger HeI, [OIII] zone. A larger highly ionized region ([FeVII], [NeIII]) has been detected in eclipse studies, but its geometry remains uncertain.

This system shows classical symbiotic outbursts. Those of 1911 and 1937 were minor ones in brightness amplitude and duration. Between 1970 and 1978, CI Cyg underwent an active phase consisting of several optical brightenings with amplitudes up to 2 magnitudes, with 3 maxima occurring in November 1971, November 1973, and August 1975. A sharp minimum, centered on October 4, 1975, was caused by a total eclipse of the outbursting component by the giant star (Figure 3). After a long quiescent state, lasting for three decades, a new series of outbursts began in 2008 (AAVSO 2008).

The 2010 outburst was first detected by Munari *et al.* (2010). This outburst coincides with an eclipse of the hot component.

2. Observations

High and low resolution spectra were acquired by several amateurs in France (Table 1). The fit and dat files can be downloaded from:

http://www.astrosurf.com/aras/CICyg/CI_Cyg.html

68 spectra low and high resolution spectra were acquired between June 30 and December 25, 2010.

A few spectra were acquired using a slitless 100l/mm spectrograph (StarAnalyser) by Eric Sarrazin and Pierre Dubreuil. eShel, Lhires, and Lisa are Shelyak Instruments products. Some samples of spectra at different resolutions are shown in Figures 4a through 4d.

3. Luminosity curve from AAVSO data

The photometric evolution of CI Cygni is presented in Figure 5. Up to July 20, 5-day mean visual data are used (dotted line). The solid line shows the daily-mean CCD-*V* data since July 20. The luminosity increased irregularly for about three months from Vis = 11.2 to a maximum $V = 9.8$ (August 26) with a mean increase of -0.013 mag d^{-1}. This rate shows significant accelerations especially

between July 22 and 31 and between August 16 and 26 with, respectively, –0.032 and – 0.036 mag d^{-1} rates. This almost stage-by-stage rise looks like the Z And outburst in 2000 (Bisikalo *et al.* 2006) though the plateaus are less marked.

The eclipse began on August 26 (JD 2455435) and ended on November 14 (JD 2455515) with a total duration of 80 days, much shorter than the 1975 eclipse duration established at 130 days (Mikołajewska and Mikołajewski 1983). The eclipse ingress is quite linear with minor variations in the slope, with a mean value of 0.035 mag d^{-1}. During the totality, the profile showed a U shape (from September 29 to October 26—JD 2455469 to 2455496) and went through the minimum on October 14 (JD 2455484) at $V = 11.16$. The totality duration was 30 days, also much less than during 1975 (72 days estimated by Mikołajewska and Mikołajewski 1983).

The eclipse egress lasted 16 days, with a mean rate of 0.019 mag d^{-1}, and ended at $V \sim 10.7$. The luminosity has been almost stable since the eclipse ended.

The comparison of profiles (Figures 6a and 6b) shows that the 2010 outburst was much shorter than 2008-2009 and 1975 ones.

The 1975 and 2010 eclipse profiles (Figure 7) have been plotted according to phase computed with the following ephemeris: Min(V) = 2 442 690 + 853.8E, where the epoch is the photocenter of the 1975 eclipse and the period is adopted from Fekel *et al.* (2000).

The minimum luminosity occurs at phase = –0.02, i.e., 18 days before the minimum predicted by the spectroscopic ephemeris. The profile is narrower than for the 1975 eclipse and less symmetric.

4. Spectral evolution

The spectral evolution was studied using low resolution spectra obtained with a 25-cm Schmidt Cassegrain telescope (F/D 10), a Starlight SXV-H9 CCD, and a Lhires III spectrograph with a 150 l/mm grating. The dispersion is 2.14 Å/pixel and the resolution about 800.

The spectra were reduced with standard procedures, including the use of a standard star observation to correct for the wavelength-dependent spectral response.

The spectral evolution is described in Figures 8 and 9.

The outburst progressed from June 30 to August 23. The spectral variation showed the dramatic disappearance of the high excitation lines, especially [FeVII]. The molecular absorption bands strongly weakened; they were partially filled by the emission from the hot components (Figure 8a).

From August 24 (when the eclipse began while the outburst was still in progress), to October 14 (at mid-eclipse), the continuum changed in the reverse way: the absorption bands strengthened (Figure 8b). At mid-eclipse, the continuum was quite the same as at the beginning of the outburst. The high ionization [Fe VII] reappeared slightly, which shows the rise in temperature and the decline of outburst.

The complete evolution is described in Figure 9, in which spectra are in absolute flux.

5. Equivalent width variations

Equivalent widths have been measured on Hα, Hβ, HeI, HeII, and [OIII] lines. The Hα EW was measured directly. For the other lines, a Gaussian fit was used. This allowed the lines to be deblended, notably the [OIII]/HeI lines.

The Ha equivalent width monotonically increased from June 30 to August 18, followed by a sudden decrease of 13% which coincided with a luminosity burst. The monotonic increase then returned up to October 20.

At that time, a new sudden decrease of 14% was detected, eight days after eclipse maximum. From October 20 EW Hα increased again monotonically. This evolution is plotted in Figures 10a through 10d where squares are low spectra values and crosses are values obtained from eShel spectra by Christian Buil.

The general shape of Hβ and Hα EW are similar, with decreases seen in the EW curves at the same time.

The He II λ 4686 EW curve is completely different. The light curve and EW HeII look remarkably similar. HeII is the only line whose EW evolution is clearly correlated with the photometric curve during the eclipse phase.

The [OIII]/He I ratio (Figure 11) was almost stable up to mid-September (~15th), varying from 1.5 to 1.9. It then increased suddenly to a maximum value of 12.6 on October 16 (JD 245586), at phase –0.009, eight days before the predicted date.

The decrease in ratio is nearly linear, with a greater slope (+40% compared to the rising slope), to a minimum of 2.6, slightly greater than the value before eclipse.

6. Line variations in absolute flux

An absolute flux calibration was obtained by scaling the continuum by the CCD-*V* magnitude in the range 530–582 nm (O'Connell 1973). The conversion of *V* magnitude to absolute flux was computed using the Spitzer Science Center Magnitude to Flux Density Converter which overestimates the result by a factor of 1.05 compared with the classical formula: $\log F\lambda = -0.400V - 8.449$ erg × s^{-1} × cm^{-2} × $Å^{-1}$.

The HI, HeI, and HeII absolute flux and luminosity curves look remarkably similar, except that the flux continues to increase after the eclipse ends while the *V* magnitude is almost stable (Figure 12). All these lines show pronounced eclipse effects. The intensity at mid-eclipse is about half the pre-eclipse value for HI lines, 1/6 for HeII λ 4686, and 1/3 for HeI λ 5876. These values are similar to those estimated during the 1975 eclipse (Mikołajewka and Mikołajewski 1983).

The [OIII] λ 5007 flux measurements are more scattered (Figure 13). There is no detectable eclipse effect. The [OIII] emission region is more extended than the HI, HeI, and HeII zone (Mikołajewska and Mikołajewski 1983). The maximum intensity occurred around September 25 (JD 2455465).

7. Continuum variations

At the beginning of the outburst (June 30) the continuum matched correctly with a M5III standard star, HD 221615, from The Indo-U.S. Library of Coudé Feed Stellar Spectra (Figure 14a).

As the outburst progressed the absorption bands reduced. At maximum luminosity, the continuum did not match any earlier spectral type continuum (M3 or M4). A synthetic spectrum was computed consisting of a M5III spectrum and a HI recombination continuum at T = 5,000 K (Osterbrock and Ferland 2006). This is an approximate value which is nevertheless consistent with the value of 7,600K for the nebular emission derived by Skopal (2003) when CI Cyg is in outburst. The result is shown in Fig 14b.

The continuum variations were measured using two TiO indices as defined by Kenyon and Fernandez Castro (1987). TiO1 measures the 6125 Å TiO band while TiO2 measures the 7025 Å TiO band. As illustrated in Figure 15, the two TiO indices are strongly correlated with luminosity *V* curve.

The high degree of correlation is illustrated by the graphs showing TiO index as a function of *V* magnitude (Figures 16a and 16b).

9. Acknowledgements

I would like to thank the AAVSO visual and CCD observers who acquired the photometric data used in this document and especially for CCD measurements: Teofilo Arranz, Emery Erdelyi, Geir Klingenberg, Kenneth Menzies, Stephen Riley, Jari Suomela, Ray Tomlin, Paolo Corelli, Juan-Luis Gonzalez Carballo, Peter Kalajian, Artyom Novichonok, Marzio Rivera, Richard Sabo, Charles Trefzger, Tim Crawford, Keith Graham, David Lane, Martin Nicholson, Douglas Slauson, Andras Timar, and Jani Virtanen.

I gratefully acknowledge Dr. Michael Friedjung (IAP) for his very helpful advice.

References

AAVSO 2008, *AAVSO Special Notice #121* (August 31).

Bisikalo, D. V., Boyarchuck, A. A., Kilpio, E. Yu., Tomov, N. A., and Tomova, M. T. 2006, *Astron. Rep.*, **50**, 722.

Fekel, F. C., Joyce, R. R., Hinkle, K. H., and Skrutskie, M. F. 2000, *Astron. J.*, **119**, 1375.

Kenyon, S. J., and Fernandez Castro, T. 1987, *Astron. J.*, **93**, 938.
Kenyon, S. J., Oliversen, N. A., Mikołajewska, J., Mikołajewski, M., Stencel, R. E., Garcia, M. R., and Anderson, C. M. 1991, *Astron. J.*, **101**, 637.
Munari, U., Siviero, A., Cherini, G., Dallaporta, S., and Valisa, P. 2010, *Astron. Telegram*, Nr. 2732, 1.
Mikołajewska, J., 1985, *Acta Astron.*, **35**, 65.
Mikołajewska, J. 2003, in *Symbiotic Stars Probing Stellar Evolution*, ASP Conference Proceedings, Vol. 303, R. L. M. Corradi, R. Mikołajewska, and T. J. Mahoney, eds., Astronomical Society of the Pacific, San Francisco, p.9.
Mikołajewska, J., and Kenyon, S. J. 1992, *Mon. Not. Roy. Astron. Soc.*, **256**, 177.
Mikołajewska, J., and Mikołajewski, M. 1983, *Acta Astron.*, **33**, 403.
Mürset, U., and Schmid, H. M. 1999, *Astron. Astrophys. Suppl. Ser.*, **137**, 473.
Osterbrok, D. E., and Ferland, G. F. 2006, *Astrophysics of Gaseous Nebulae and Active Galactic Nuclei*, University Science Books, Mill Valley, California.
Skopal, A. 2003, arXiv:astro-ph/0308462v1.
Siviero, A., *et al.* 2009, *Mon. Not. Roy. Astron. Soc.*, **399**, 2139.

Table 1. Observers of high resolution spectra of CI Cyg.

Observer	*Telescope*	*Spectrograph*	*Resolution*	*Approx. Range*	*Nr. spectra*
C. Buil	SC 28cm	eShel	11 000	428–712 nm	16
T. Garrel	SC 21 cm	LHIRES III 2400 l/mm	15 000	650–661 nm	13
B. Mauclaire	SC 21 cm	LHIRES III 2400 l/mm	15 000	652–669 nm	4

Table 2. Observers of low resolution spectra of CI Cyg.

Observer	*Telescope*	*Spectrograph*	*Resolution*	*Approx. Range*	*Nr. spectra*
C. Buil	SC 23 cm	LISA 300 l/mm	1000	390–730 nm	1
F. Teyssier	SC 25 cm	LHIRES III 150 l/mm	800	440–720 nm	34

Table 3. Emission line equivalent width (Å).

Nr.	*Date*	*JD 2450000*	*Phase*	*Ha*	*Hb*	*HeII 4686Å*	*HeI 5876Å*	*[OIII] /HeI*
1	30/06/2010	5378.417	–0.135	124	44.2	50.2	15.2	2.1
2	24/07/2010	5402.393	–0.107	147	54.0	62.4	26.0	1.7
3	02/08/2010	5411.403	–0.097	156	55.1	65.0	27.4	1.6
4	09/08/2010	5417.534	–0.090	167	57.1	64.3	28.9	1.4
5	18/08/2010	5427.390	–0.078	173	57.2	60.3	29.0	1.8
6	23/08/2010	5432.330	–0.072	149	43.0	45.0	26.1	1.7
7	30/08/2010	5439.333	–0.064	172	45.3	53.5	31.2	2.2
8	01/09/2010	5441.426	–0.062	178	48.7	50.4	29.6	1.7
9	04/09/2010	5444.440	–0.058	184	52.7	48.2	30.4	1.9
10	08/09/2010	5448.330	–0.054	194	56.9	47.8	30.4	1.9
11	10/09/2010	5450.335	–0.051	198	57.0	48.0	28.6	1.9
12	17/09/2010	5457.383	–0.043	206	62.6	43.6	30.6	
13	18/09/2010	5458.325	–0.042	210	65.4	30.8	4.3	
14	21/09/2010	5461.396	–0.038	219	67.5	32.9	3.8	
15	22/09/2010	5462.389	–0.037	228	74.1	43.7	31.8	3.8
16	25/09/2010	5465.360	–0.034	234	84.1	41.8	36.0	
17	30/09/2010	5470.300	–0.028	242	87.2	31.6	34.9	6.8
18	07/10/2010	5477.325	–0.020	248	88.5	24.8	33.6	8.9
19	09/10/2010	5479.317	–0.017	248	90.5	23.2	34.3	
20	10/10/2010	5480.300	–0.016	243				
21	12/10/2010	5482.325	–0.014	251	90.3	22.0	35.8	11.9
22	16/10/2010	5486.316	–0.009	261	90.8	19.5	36.4	12.6
23	17/10/2010	5487.301	–0.008	263	89.6	19.9	30.6	
24	20/10/2010	5490.309	–0.004	272	87.0	23.3	32.9	
25	22/10/2010	5492.278	–0.002	248	87.7	22.2	30.9	10.1
26	25/10/2010	5495.271	0.001	239	90.3	23.1	30.7	10.7
27	30/10/2010	5500.291	0.007	234	87.7	20.0	31.4	7.6
28	31/10/2010	5501.285	0.009	229	85.7	21.5	31.5	7.0
29	01/11/2010	5502.275	0.010	229	82.1	20.9	33.9	
30	07/11/2010	5508.244	0.017	239	85.3	26.1	33.5	5.7
31	20/11/2010	5521.273	0.032	254	86.6	34.1	40.0	3.0
32	03/12/2010	5534.290	0.047	305	91.1	44.4	40.1	
33	12/12/2010	5543.252	0.058	327	91.3	46.3	39.6	2.6
34	14/12/2010	5545.213	0.060	317	94.9	45.4	40.3	2.5
35	25/12/2010	5556.250	0.073	350	105.0	64.5	43.2	2.7

Table 4. Emission line absolute flux (10^{-12} erg × cm^{-2} × s^{-1}).

Nr.	*Date*	*JD 2450000*	*Phase*	*Ha*	*Hb*	*HeI 5876Å*	*HeII 4686Å*	*[OIII] 5007Å*
1	30/06/2010	5378.417	–0.135	48	5.1	2.3	5.2	0.6
2	24/07/2010	5402.393	–0.107	65	7.8	4.6	8.1	1.2
3	02/08/2010	5411.403	–0.097	96	8.0	7.6	8.8	1.9
4	09/08/2010	5417.534	–0.090	100		8.9	10.8	2.4
5	18/08/2010	5427.390	–0.078	110	10.5	8.6	10.4	2.8
6	23/08/2010	5432.330	–0.072	128	9.7	10.1	10.9	3.0
7	30/08/2010	5439.333	–0.064	141	11.5	12.4	13.0	
8	01/09/2010	5441.426	–0.062	133	10.1	11.1	9.7	2.9
9	04/09/2010	5444.440	–0.058	134	9.6	10.3	8.5	2.9
10	08/09/2010	5448.330	–0.054	116	11.4	9.4	10.0	3.3
11	10/09/2010	5450.335	–0.051	129	8.4	9.1	6.8	2.9
13	18/09/2010	5458.325	–0.042	84	10.4	6.6	7.0	3.6
15	22/09/2010	5462.389	–0.037	94	10.1	6.4	6.1	4.0
16	25/09/2010	5465.360	–0.034	88	9.1	6.0	4.0	3.8
17	30/09/2010	5470.300	–0.028	72	8.6	4.2	3.1	3.3
18	07/10/2010	5477.325	–0.020	77	6.4	3.7	1.7	2.9
22	16/10/2010	5486.316	–0.009	71	6.6	4.1	1.3	3.5
24	20/10/2010	5490.309	–0.004	77	7.4	4.2	1.8	3.5
25	22/10/2010	5492.278	–0.002	83	6.3	4.3	1.5	3.0
26	25/10/2010	5495.271	0.001	64	6.2	3.9	1.7	3.0
29	01/11/2010	5502.275	0.010	70	7.2	4.4	2.1	3.4
30	07/11/2010	5508.244	0.017	86	7.9	5.3	2.6	3.0
31	20/11/2010	5521.273	0.032	94	9.5	6.6	3.6	2.5
32	03/12/2010	5534.290	0.047	125		8.0	5.2	3.1
33	12/12/2010	5543.252	0.058	138	10.4	8.4	4.4	2.5
34	14/12/2010	5545.213	0.060	140	11.5	8.4	4.4	2.7
35	25/12/2010	5556.250	0.073	160	13.2	10.6	7.1	3.0

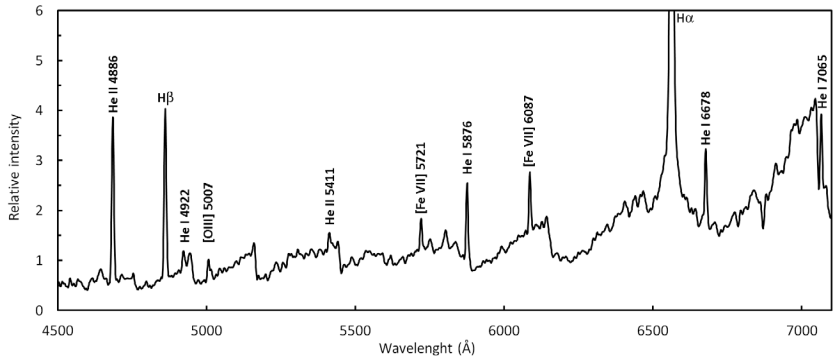

Figure 1. CI Cygni spectrum at the beginning of the outburst (2010 June 30). The Hα line has been truncated in favor of the fainter features.

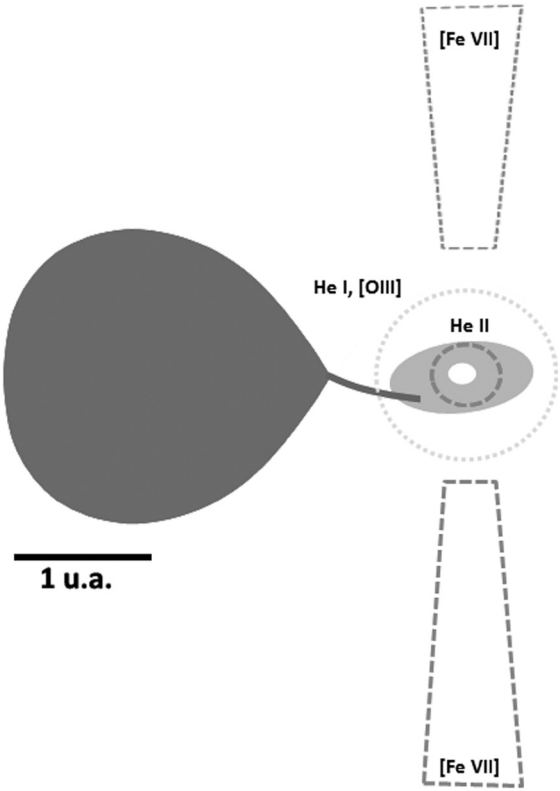

Figure 2. A schematic representation of CI Cyg adapted from Kenyon *et al.* (1991).

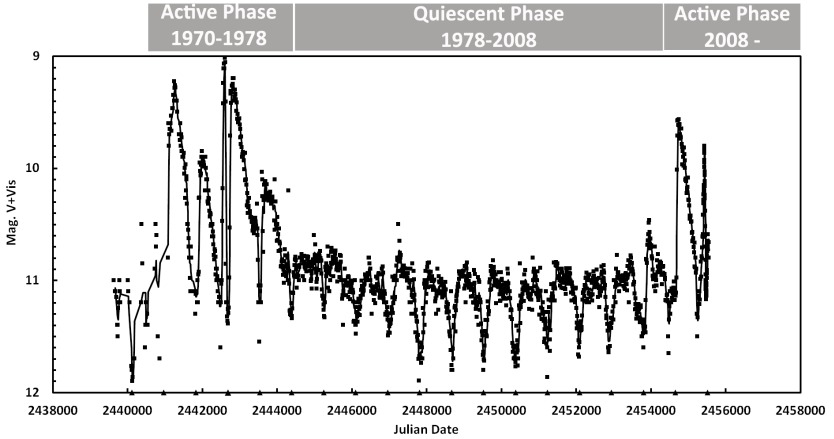

Figure 3. Long term light curve (Visual and CCD-V 10-day mean) from AAVSO observers. Eclipses are marked by triangles.

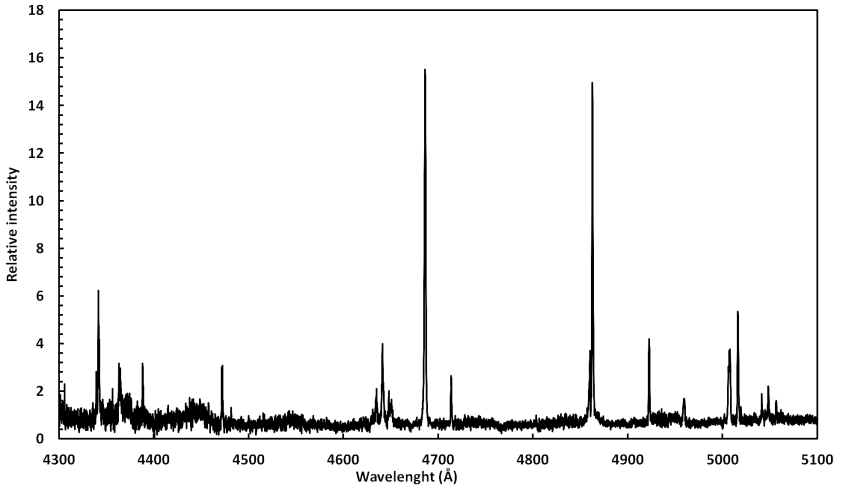

Figure 4a. Part of an eShel spectrum (R = 11000), with line identification by Christian Buil.

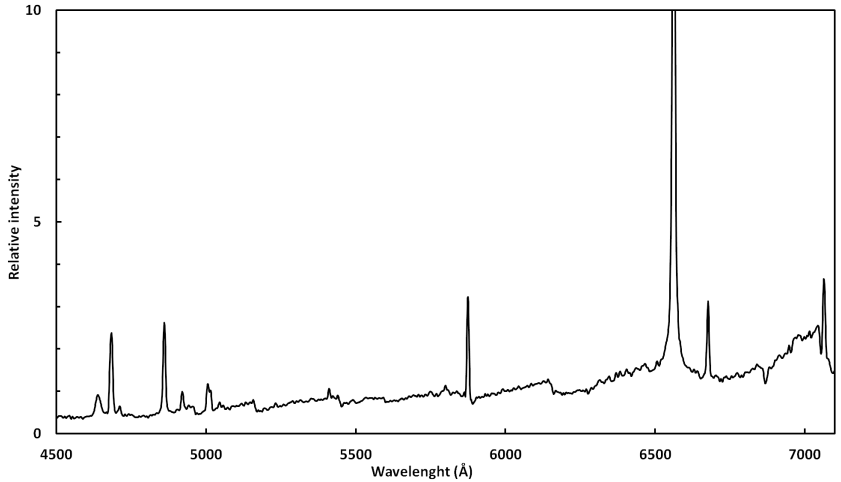

Figure 4b. Low resolution (R = 800) by François Teyssier.

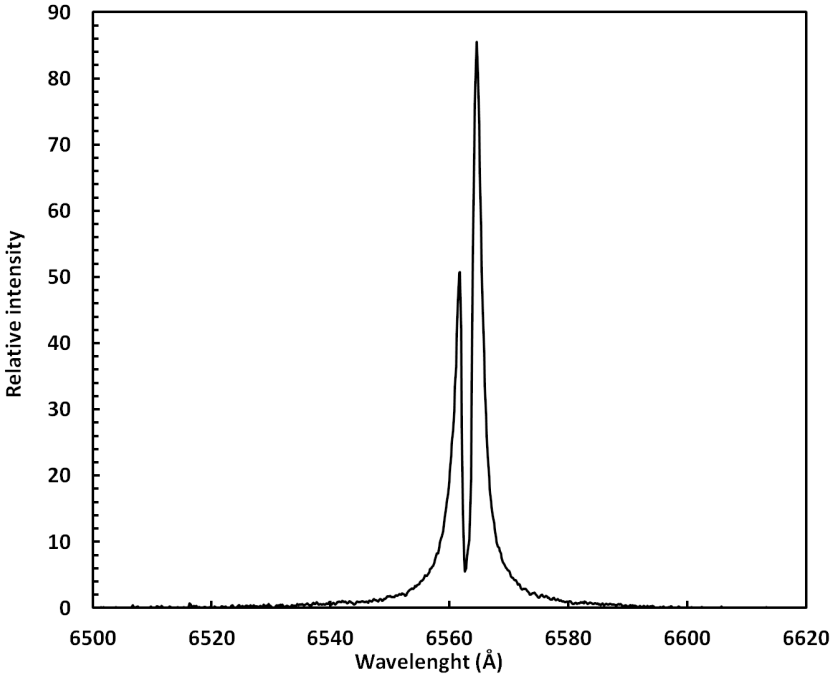

Figure 4c. High resolution spectrum of the Hα line (R = 15000) by Thierry Garrel.

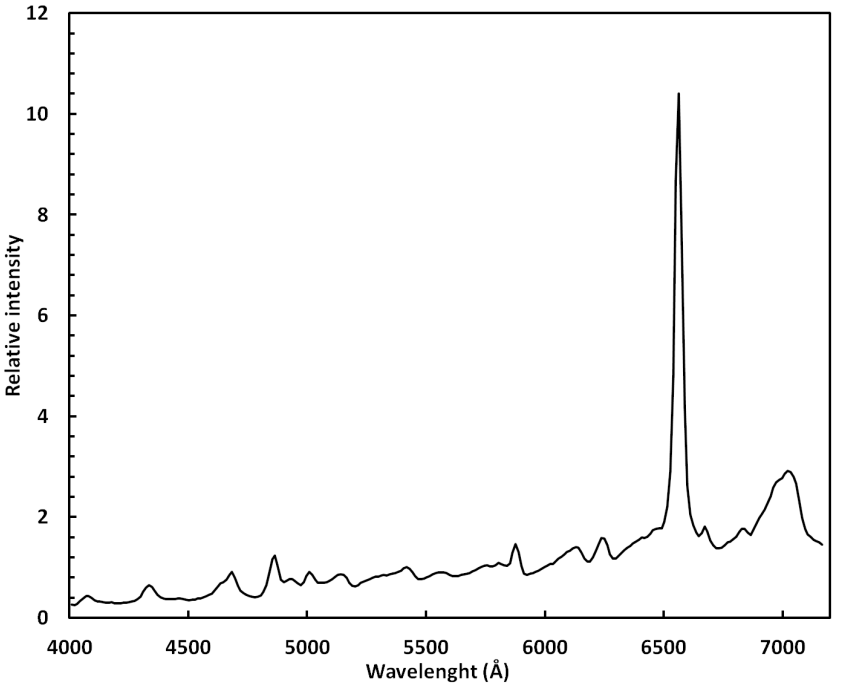

Figure 4d. Very low resolution (slitless Star Analyser) by Eric Sarrazin.

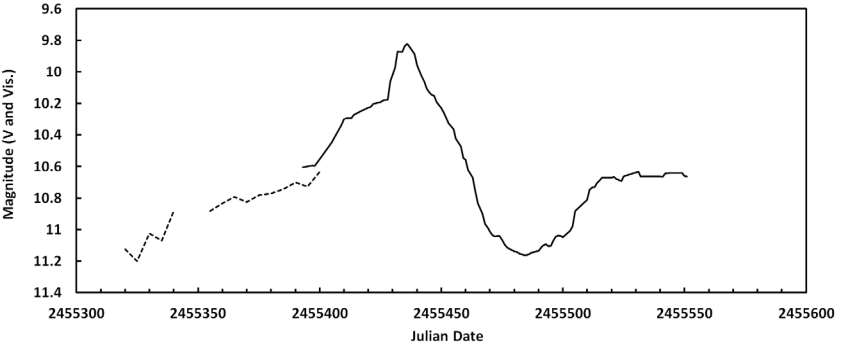

Figure 5. Visual (dotted line) and CCD-V (solid line) light curve from AAVSO data.

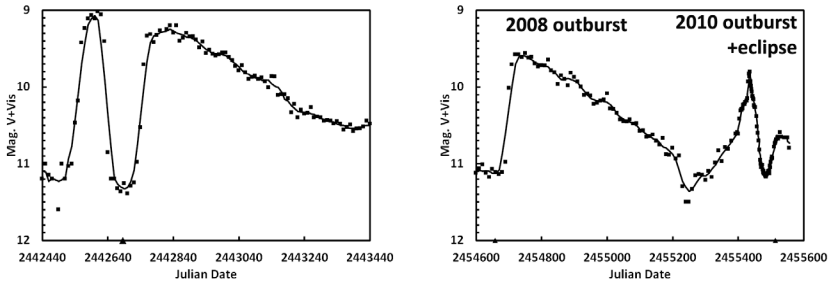

Figure 6. Comparison of 1975 and 2010 outbursts and eclipses photometric profiles. Figure 6a (left): 1975 outburst and eclipse. Figure 6b (right): 2008–2010 outbursts and 2010 eclipse.

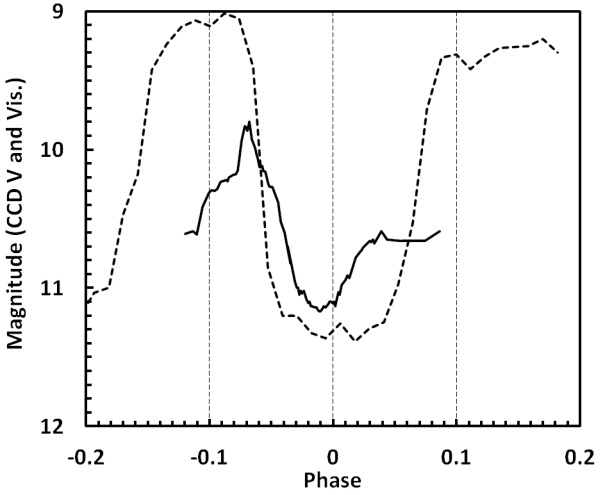

Figure 7. 1975 (dotted line) and 2010 (solid line) eclipse profiles according to phase.

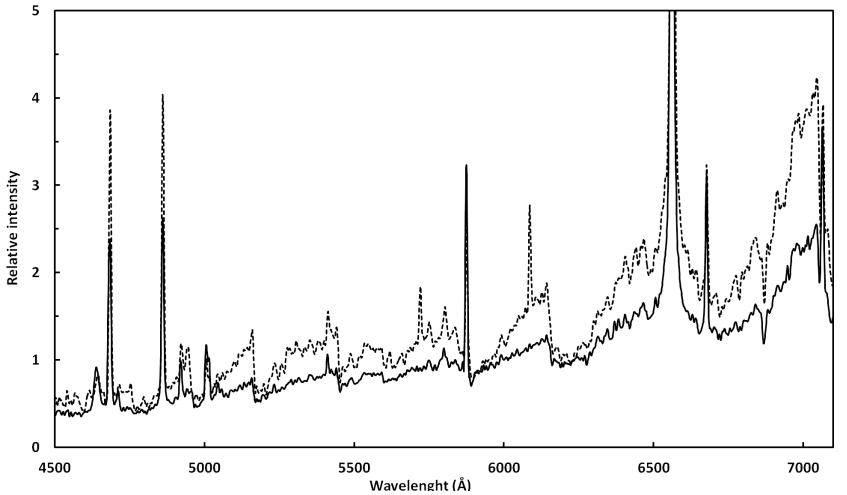

Figure 8a. Spectral evolution of CI Cyg between 2010 June 30 (dotted line) and 2010 August 24 (solid line).

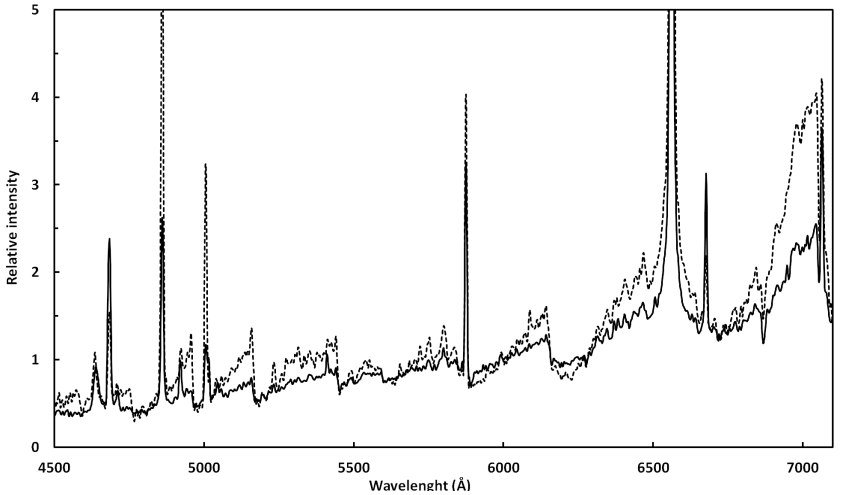

Figure 8b. Spectral evolution between 2010 August 24 (solid line) and 2010 October 14 (dotted line).

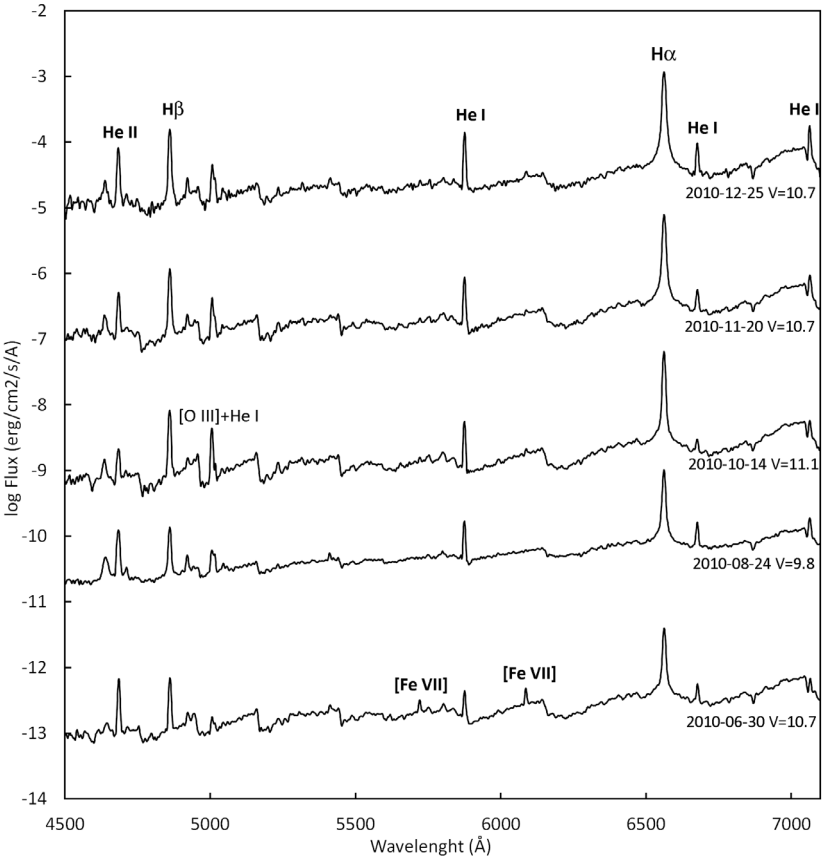

Figure 9. Absolute flux spectral evolution of CI Cyg during the 2010 outburst. For clarity, the spectra are offset in ordinates by 2 units.

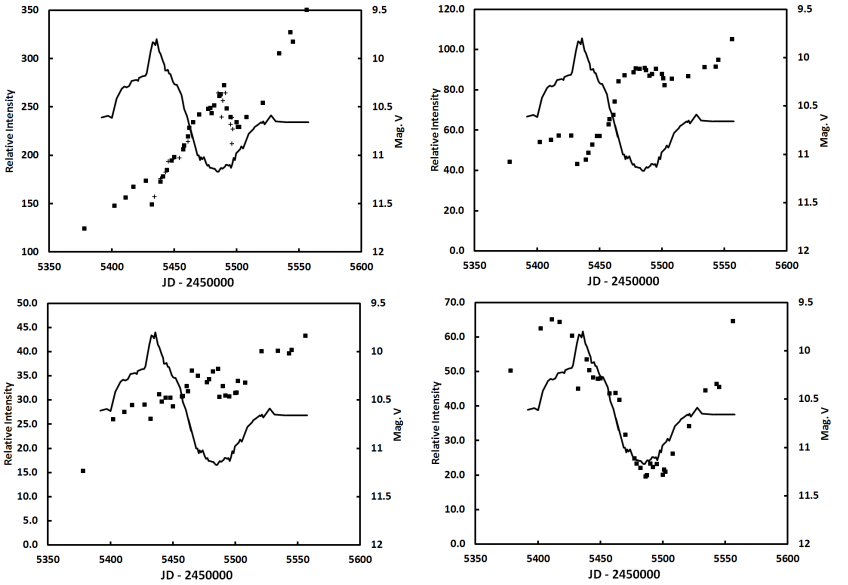

Figure 10. Equivalent widths time series (JD 2450000). Squares for low resolution values, crosses for eShel values (only Hα). Figure 10a (top left): Hα equivalent width. Figure 10b (top right): Hβ equivalent width. Figure 10c (bottom left): HeI λ5876 equivalent width. Figure 10d (bottom right): HeII λ4686 equivalent width.

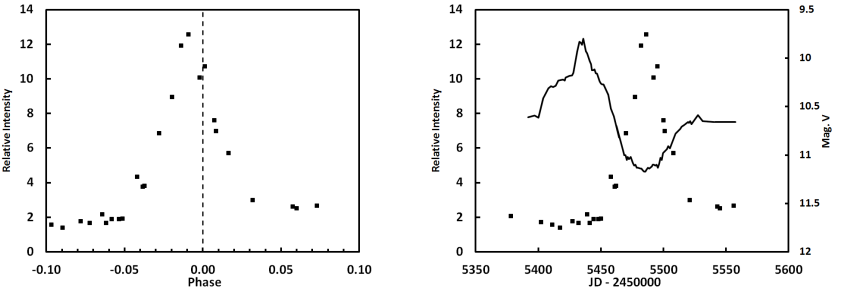

Figure 11a (left). [OIII]/HeI 5016 EW ratio as a function of phase. Figure 11b (right). [OIII]/HeI 5016 EW ratio as a function of JD. CCD-*V* light curve, solid line.

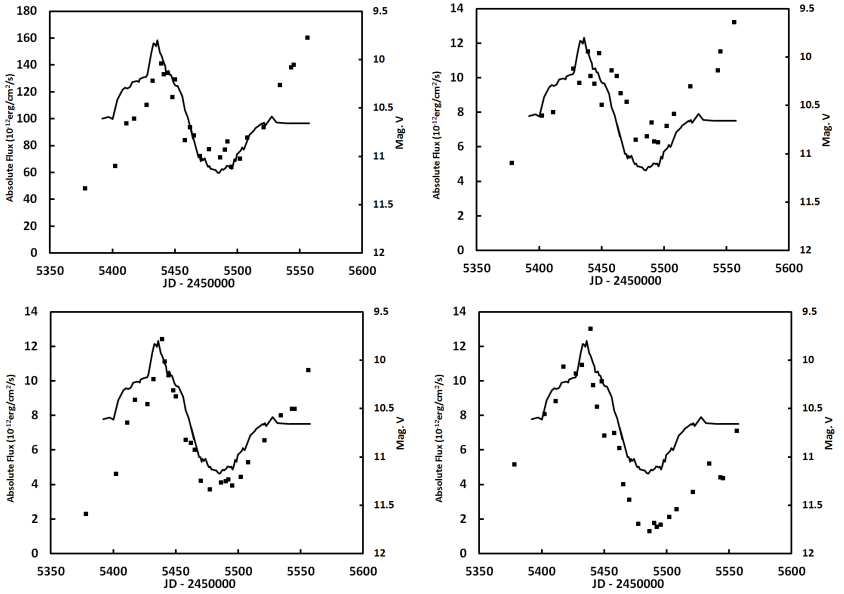

Figure 12. Absolute line flux (erg × $^{s-1}$ × cm^{-2} × Å^{-1}) as a function of time (JD-2450000) and CCD light curve, as solid line). Figure 12a (top left): Hα absolute flux. Figure 12b (top right): Hβ absolute flux. Figure 12c (bottom left): HeI λ 5876 absolute flux. Figure 12d (bottom right): HeII λ4686 absolute flux.

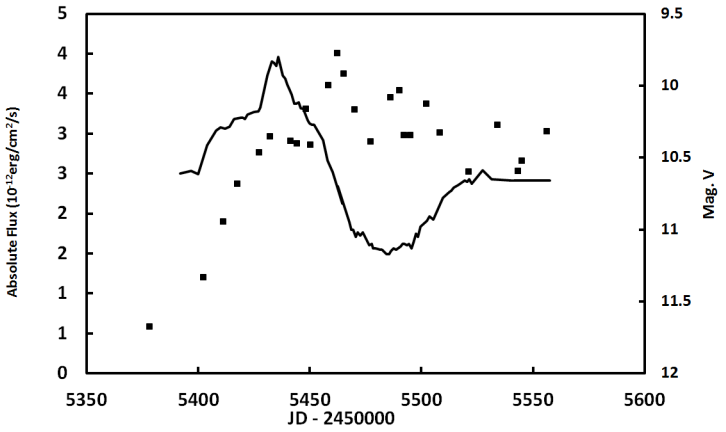

Figure 13. [OIII] l 5007 absolute flux evolution.

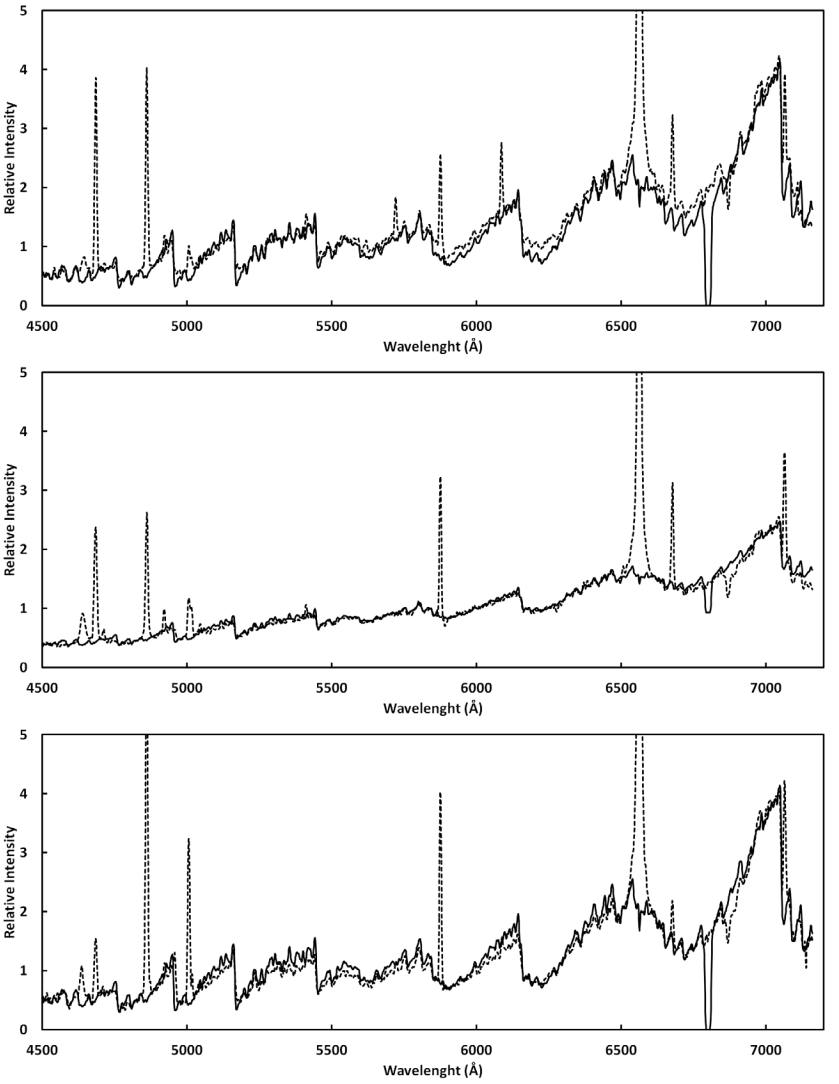

Figure 14. CI Cygni spectra: dotted lines; Comparison spectra: solid lines. Figure 14a (top): Comparison between the 2010 June 30 spectrum (dotted line) and a M5III standard. Figure 14b (middle): At max luminosity (August 24), the continuum matches a synthetic spectrum: M5III composite with a HI recombination continuum (T = 5000 K). Figure 14c (bottom): At mid-eclipse, the continuum again matches a M5 III standard.

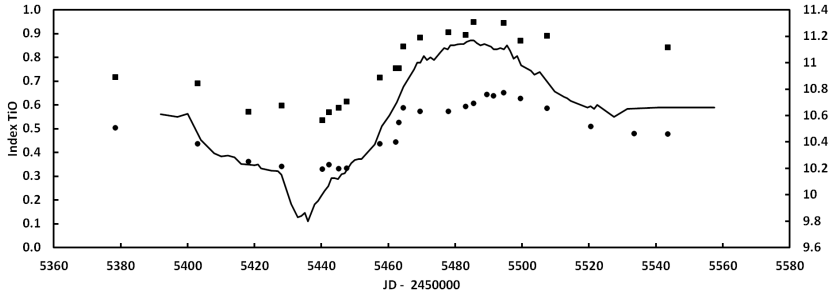

Figure 15. TiO index variation as a function of JD (2450000) and V magnitude (solid line). TiO_1, squares; TiO_2, circles.

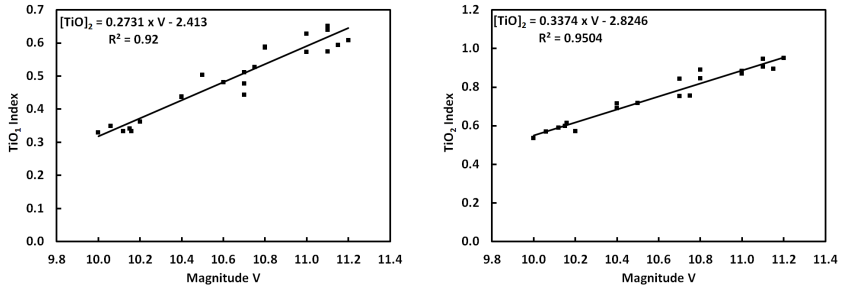

Figure 16a (left): TiO_1 index as a function of V magnitude. Figure 16b (right): TiO_2 index as a function of V magnitude.

The Orbital Period of Three Cataclysmic Variables From WASP Data

Patrick Wils
Aarschotsebaan 31, Hever B3191, Belgium; Vereniging Voor Sterrenkunde, Belgium; patrickwils@yahoo.com

Received November 5, 2010; accepted February 17, 2011

Abstract The publicly available WASP data are analyzed to determine the orbital periods of the cataclysmic variables V378 Peg, SDSS J171456.78+585128.3, and ASAS 150946-2147.7.

1. Introduction

The exoplanet transit survey WASP (Wide Angle Search for Planets) has been taking wide field images since 2004 using two instruments located in La Palma and South Africa.

In the first public data release of the WASP archive all the light curve data and images from 2004 to 2008 from both the Northern and Southern hemisphere instruments were made available (Butters *et al.* 2010). Since these light curves are used to search for exoplanet transits, they can also be used to study other low amplitude variability in stars. Thomas *et al.* (2010) successfully used the data to study the orbital period variations of three cataclysmic variables (CVs). In this study the publicly available WASP data will be used to determine the orbital periods of three other CVs. In the analysis only TAMUZ (Collier Cameron *et al.* 2006) corrected data were used for which the uncertainty on the magnitude is less than 0.1.

2. V378 Peg

V378 Peg = PG 2337+300 has not been studied since its classification by Koen and Orosz (1997) as a cataclysmic variable. The x-ray source 1RXS J234002.7+301808 is probably also related. Koen and Orosz (1997) observed irregular brightness variations of up to 0.3 magnitude with a timescale of a few minutes over a three-hour period.

The WASP data (1SWASP J234004.30+301747.5) show low amplitude variations around magnitude 14.1. A period search using the Phase Dispersion Minimization (PDM) technique of Stellingwerf (1978) shows a sinusoidal light curve with a period of 0.1349 day, with an average amplitude of around 0.15 magnitude, but with a lot of scatter likely caused in part by the irregular variations seen by Koen and Orosz (1997). The 1-day alias of 0.1560 day cannot be entirely excluded to be the real period, but the shorter value seems to be a better fit for

the long wave in the light curve of Koen and Orosz (1997). This variation may be caused by the rotation of the hot spot or the irradiation of the cool companion, but it is also possible that the orbital period is twice the given value, in which case the variation is caused by the ellipsoidal shape of the red dwarf star. Figure 1 shows the phase plot using a period of 0.26985 day, but the phase plot of the longer period is almost indistinguishable from that of the shorter period. Neither can a distinction be made between the minima or maxima in the double period solution. The available photometry from 2MASS (Skrutskie *et al.* 2006) and the Galaxy Evolution Explorer (GALEX; Martin *et al.* 2005) are compatible with a single object with a black body temperature of 12,000 K or higher and do not show the presence of a cool companion. Hence it must be too cool to be detected, and therefore cannot be responsible for the variations seen in the light curve. In that case an orbital period of 0.1349 day is the most likely solution.

3. SDSS J171456.78+585128.3

GUVV-2 J171456.8+585128.3 was discovered to be variable by Wheatley *et al.* (2008) in data from the GALEX satellite, and as SDSS J171456.78+585128.3 = 1RXS J171456.2+585130 it was found to be a CV by Agüeros *et al.* (2009). The latter authors found the spectrum to be that of a K4 star with an invisible companion. Their sparse radial velocity measurements suggested an orbital period of ~10 hours. The WASP data for this object (1SWASP J171456.79+585128.6) show variations around magnitude 14.6 with an amplitude of 0.2 magnitude and a period of about twice the value proposed by Agüeros *et al.* (2009). The data follow the ephemeris:

$$\text{HJD Min I} = 2453260.118\ (14) + 0.83803\ (2)\ E \qquad (1)$$

The light curve in Figure 2 shows a secondary minimum. These variations are very likely caused by the ellipsoidal shape of the K4 star and irradiation or limb darkening effects to account for the different brightness of the minima. The data from the Northern Sky Variability Survey (NSVS; Woźniak *et al.* 2004) are compatible with the orbital period found here (Wils 2009b).

4. ASAS 150946-2147.7

This object was suspected to be a dwarf nova in outburst by Pojmański *et al.* (2009) in data from the All-Sky Automated Survey (ASAS; Pojmański *et al.* 2002). They noted that the object is a blend between two objects. Henden (2009) identified the outbursting object to be identical to 2MASS J15094657-2147462, the brighter of the two objects. Therefore the influence of the fainter object on the brightness of the variable is negligible. According to Uemura *et al.* (2009) ASAS 150946-2147.7 is a candidate black hole X-ray binary based on data from the Swift satellite.

Two outbursts were observed by ASAS, in August 2003 and April 2009. The WASP archive (object 1SWASP J150946.56-214746.5) contains the rising branch of another outburst in July 2006, matching the shape of the ASAS outbursts (see Figure 3). The total outburst amplitude reached just over one magnitude in all cases. These outbursts last less than a month with a slow rise to maximum, taking almost as long as the fade to minimum. This behavior is rather atypical for a dwarf nova and is normally only seen in CVs with an orbital period longer than one day, such as the old nova GK Per (orbital period 1.9968d; Crampton *et al.* 1986), V630 Cas (2.5639d; Orosz *et al.* 2001), and SDSS J204448.92-045928.8 (1.68d; Peters and Thorstensen 2005). Recent outbursts of these dwarf novae have been described by Evans *et al.* (2009), Shears and Poyner (20009), and Wils (2009a), respectively.

Pojmański *et al.* (2009) further detected weak 0.1-magnitude modulations in the ASAS-3 data at quiescence, with a period of 0.351213 or 0.206187 day (these are 1-day aliases of each other). Because of the higher cadence of the WASP observations, they are better suited to distinguish between aliases in this case. A period search of the out-of-outburst data unambiguously revealed the period to be 0.70242 day, exactly twice the longer period found by Pojmański *et al.* (2009). The light curve in Figure 4 shows a double wave varying from magnitude 11.60 to 11.67 with one minimum fainter than the other (secondary minimum at magnitude 11.65), This is likely caused by the changing aspects of an ellipsoidal star during an orbital revolution. An ephemeris for the primary minimum has been calculated as follows:

$$\text{HJD Min I} = 2453880.235\ (11) + 0.70242\ (1)\ E \qquad (2)$$

No phase shifts or period changes were detected after the outburst.

5. Conclusion

The orbital period of V378 Peg cannot be unambiguously determined from WASP data. It is either 0.1349 or 0.1560 day, or twice these values, but the first value is the preferred solution. For SDSS J171456.78+585128.3 the orbital period was found to be 0.83803 day, with two minima and two maxima per orbit caused by the ellipsoidal shape of the red dwarf. The orbital period of ASAS 150946-2147.7 was found to be 0.70242 day, again with two minima and maxima per orbit. Although not as long as the orbital period of GK Per, the outburst behavior of ASAS 150946-2147.7 is similar. Further spectroscopic study should reveal its true nature.

6. Acknowledgements

We have used data from the WASP public archive in this research. The WASP consortium comprises the University of Cambridge, Keele University, University of Leicester, The Open University, The Queen's University Belfast, St. Andrews University, and the Isaac Newton Group. Funding for WASP comes from the consortium universities and from the UK's Science and Technology Facilities Council.

This study made use of NASA's Astrophysics Data System, and the SIMBAD and VIZIER databases operated at the Centre de Données astronomiques de Strasbourg.

References

Agüeros, M. A., *et al.* 2009, *Astrophys. J., Suppl. Ser.*, **181**, 444.
Butters, O. W., *et al.* 2010, *Astron. Astrophys.*, **520**, L10.
Collier Cameron, A., *et al.* 2006, *Mon. Not. Roy. Astron. Soc.*, **373**, 799.
Crampton, D., Fisher, W. A., and Cowley, A. P. 1986, *Astrophys. J.*, **300**, 788.
Evans, P. A., Beardmore, A. P., Osborne, J. P., and Wynn, G. A. 2009, *Mon. Not. Roy. Astron. Soc.*, **399**, 1167.
Henden, A. 2009, vsnet-alert 11172, http://ooruri.kusastro.kyoto-u.ac.jp/mailarchive/vsnet-alert/11172.
Koen, C., and Orosz, J. 1997, *Inf. Bull. Var. Stars*, No. 4539, 1.
Martin, D. C., *et al.* 2005, *Astrophys. J., Lett. Ed.*, **619**, L1.
Orosz, J. A., Thorstensen, J. R., and Honeycutt, K. R. 2001, *Mon. Not. Roy. Astron. Soc.*, **326**, 1134.
Peters, C. S., and Thorstensen, J. R. 2005, *Publ. Astron. Soc. Pacific*, **117**, 1386.
Pojmański, G. 2002, *Acta Astron.*, **52**, 397.
Pojmański, G., Szczygiel, D., and Pilecki, B. 2009, *Cent. Bur. Electron. Telegrams*, No. 1774, 1.
Shears, J., and Poyner, G. 2009, eprint arXiv:0911.1326.
Skrutskie, M. F., *et al.* 2006, *Astron. J.*, **131**, 1163.
Stellingwerf, R. F. 1978, *Astrophys. J.*, **224**, 953.
Thomas, N. L., Norton, A. J., Pollacco, D., West, R. G., Wheatley, P. J., Enoch, B., and Clarkson, W. I. 2010, *Astron. Astrophys.*, **514**, A30.
Uemura, M., *et al.* 2009, Astron. Telegrams, No. 2030, 1.
Wheatley, J. M., Welsh, B. Y., and Browne, S. E. 2008, *Astron. J.*, **136**, 259
Wils, P. 2009a, *Perem. Zvezdy, Prilozh.*, **9**, 19.
Wils, P. 2009b, cvnet-discussion, 1253, http://tech.groups.yahoo.com/group/cvnet-discussion/message/1253.
Woźniak, P. R., *et al.* 2004, *Astron. J.*, **127**, 2436.

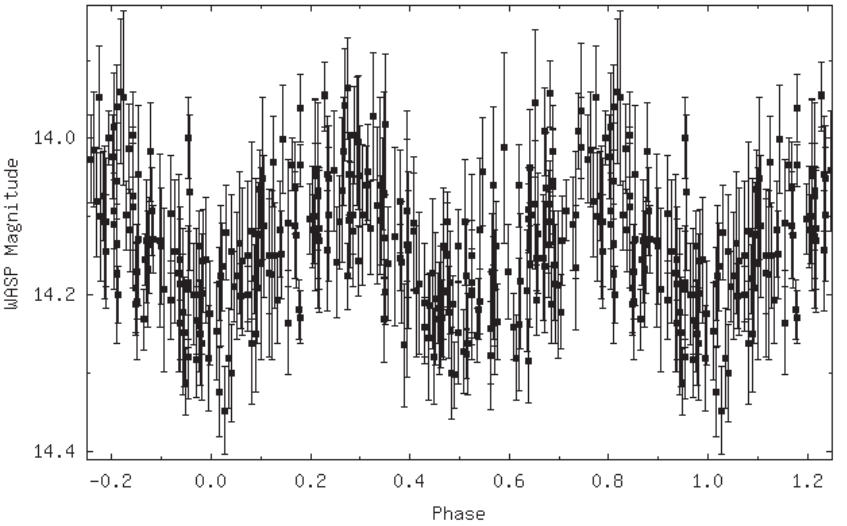

Figure 1. Phase plot of 10-point averages of WASP data of V378 Peg, using a period of 0.26985 day. The error bars represent the standard deviation of the 10-point averages.

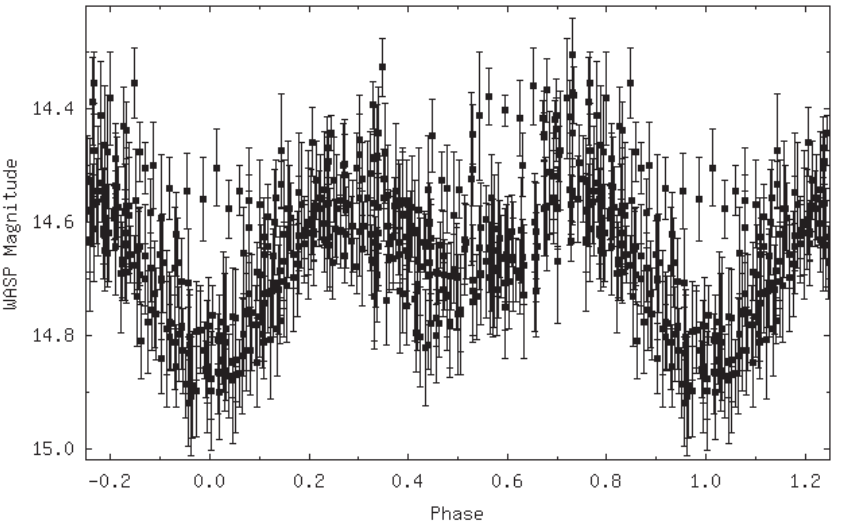

Figure 2. Phase plot of 10-point averages of WASP data of GUVV-2 J171456.8+585128.3, using the ephemeris given in Equation 1. The error bars represent the standard deviation of the 10-point averages.

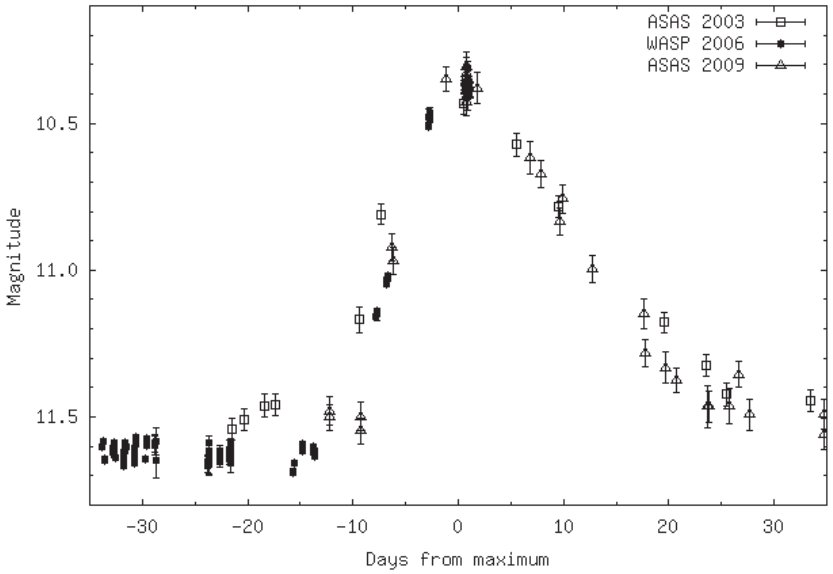

Figure 3. Comparison of the profiles of the three observed outbursts of ASAS 150946-2147.7. Two outbursts were observed in the V band by ASAS (Pojmański 2002), and one was observed unfiltered by WASP (Butters *et al.* 2010). The WASP data are plotted as averages of 10 consecutive points.

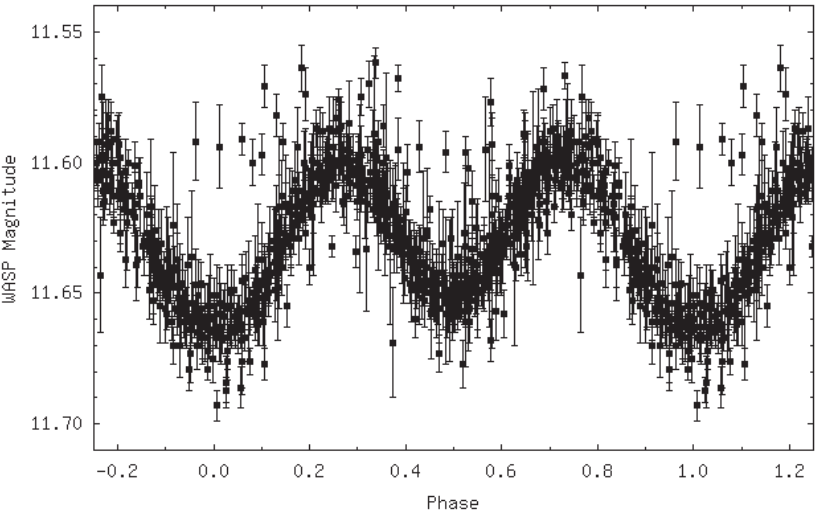

Figure 4. Phase plot of 10-point averages of WASP data of ASAS 150946-2147.7, using the ephemeris given in Equation 2. Only data in quiescence were used. The error bars represent the standard deviation of the 10-point averages.

The Z CamPaign: Year 1

Mike Simonsen
AAVSO, 49 Bay State Road, Cambridge, MA, 02138; mikesimonsen@aavso.org

Received November 29, 2010; accepted December 2, 2010

Abstract The Cataclysmic Variable Section of the American Association of Variable Star Observers (AAVSO) has initiated an observing campaign to study a subset of dwarf novae (DNe), known as Z Cam type (UGZ). We call this program the Z CamPaign. Since there is no strong agreement between the various published catalogues as to which few dozen DNe are actually Z Cam type systems, our primary goal is to accumulate enough data to construct detailed light curves, covering the entire range of variability, to determine unequivocally the 30 Z CamPaign subjects' membership in the UGZ class of DNe. We discuss the organization, science goals, and some early results of the Z CamPaign in detail.

1. Defining Z Cams

U Geminorum-type (UG) variables, also called dwarf novae, are close binary systems in which a dwarf or subgiant K-M star fills the volume of its inner Roche lobe and loses mass to a white dwarf surrounded by an accretion disk. From time to time the system goes into outburst, brightening rapidly by several magnitudes. After several days to a month, or more, it returns to its original state. These dwarf nova outbursts are believed to be caused by thermal instabilities in the disk. Gas accumulates in the disk until it heats up and becomes viscous. This increased viscosity causes it to migrate in toward the white dwarf, heating up even more, eventually causing an outburst (Warner 1995).

Intervals between two consecutive outbursts for a given star may vary, but every star is characterized by a characteristic mean value of these intervals. This mean cycle corresponds to the mean amplitude of the outbursts. Generally speaking, the longer the cycle, the greater the amplitude of the outbursts. According to the characteristics of their light curves, UGs are further subdivided into three types: SS Cyg, SU UMa, and Z Cam. SU UMa type UGs are not relevant to this discussion.

SS Cygni-type variables (UGSS) increase in brightness by 2 to 6 magnitudes in *V* in 1 to 2 days and after several subsequent days return to their original brightness. The cycle times vary considerably, from 10 to several hundreds of days.

Z Camelopardalis-type stars (UGZ) also show cyclic outbursts, but differ from UGSS variables by the fact that sometimes after an outburst they do not return to their quiescent magnitude. Instead they appear to get stuck, for months or even years, at a brightness of about one magnitude fainter than outburst maximum. These episodes are known as standstills. Z Cam cycle times characteristically

range from 10 to 40 days, and their outburst amplitudes are from 2 to 5 magnitudes in *V*, but *standstills are the defining characteristic of the Z Cam stars.*

2. Standstills

If a dwarf nova has a high enough mass-transfer rate, it can resemble a dwarf nova continuously stuck in outburst. This is what nova-like variables are thought to be. One theory explaining Z Cam standstills is that the rate of mass transfer is approximately equal to the critical rate that separates dwarf novae from the nova-like variables (Meyer and Meyer-Hofmeister 1983).

Models can now explain why standstills are about a magnitude fainter than outburst maximum. The gas stream from the mass-losing star heats the disk, and because of this extra source of heat, the critical mass transfer rate at which a standstill occurs is about 40% less than the mass transfer rate during outburst (Stehle *et al.* 2001).

Even with the observations and analyses of recent years, we still know relatively little about standstills. Even the fundamental observational properties of how often they occur or how long they last are not well known. Standstills of Z Cam, the prototypical star of this class, can last between 9 and 1,020 days (Oppenheimer *et al.* 1998). Z Cam was in standstill almost continuously between 1977 and 1981 (AAVSO data). AH Her has been in standstill since June 2009, nine months and counting as of this writing. In contrast, HX Peg has much shorter standstills, from 30 to 90 days long, which can recur yearly (AAVSO data).

Standstills are not static affairs. Szkody and Mattei (1984) showed erratic flare-ups with amplitudes of several tenths of a magnitude in their compilation of the statistics of dwarf nova outbursts. Another well-quoted characteristic of Z Cams is that "standstills are always initiated by an outburst," and "standstills always end with a decline to quiescence" (Hellier 2001). However, there are at least five Z Cam stars that appear to go into outburst from standstill: V513 Cas, IW And, HX Peg, AH Her, and AT Cnc. If this turns out to be an inconvenient truth it provides another challenge in explaining the mechanisms that initiate and end standstills.

3. Science Goals

The science goals of the Z CamPaign are:

1. To determine convincingly which CVs are indeed UGZ and which are imposters. The plan is to analyze the light curves of all the candidates looking for standstill episodes in their light curves. If there are standstills, we will accept them as UGZ. If there are no standstills we will remove them from the list of known Z Cams, and assign another type to them, if possible. If the data are inconclusive, we will concentrate on obtaining

adequate long-term data throughout the range of the variable to make a determination.

2. To improve the overall data available on each of these stars and fill the gaps in the light curves. Since so little is known, even about the well observed Z Cam candidates, we will try to obtain as complete coverage as possible, concentrating on V magnitude observations first, then extending to other bandpasses.

3. To determine if some UGZ actually do go into outburst from standstill, or if perhaps we have just missed the sudden drop to quiescence before the next outburst, leading to the appearance of outburst from standstill behavior.

4. To study and report any other serendipitous discoveries about "UGZ-ness" that come to light as a result of improved coverage.

5. To publish the results in a peer-reviewed journal such as *The Journal of the AAVSO*.

4. Coordinating the campaign

The campaign is coordinated through the Cataclysmic Variable Section of the AAVSO. There is a special campaign page online explaining the details to those interested in observing these stars: https://sites.google.com/site/aavsocvsection/z-campaign. The list of campaign stars can be downloaded in several formats from this web page. The star list is divided into four sub-categories, based on the type and magnitude range.

The first group of stars are confirmed UGZ suitable for continued observation by visual observers throughout their cycles. These are generally the brightest dwarf novae in the campaign and have well sampled light curves, some going back as far as the 1940s. We strongly urge visual observers to continue monitoring these stars for their expected outbursts and standstills as well as unexpected behavior.

The second group of stars are unconfirmed UGZ stars that visual observers should continue to monitor for outbursts and standstills if or when they may occur.

The third group of stars are unconfirmed UGZs that both visual and CCD observers are encouraged to monitor for outbursts, but the standstills are likely to only be visible to CCD observers due to their relative faintness (15th or 16th magnitude). We encourage CCD observers to concentrate on these stars when they are known to be in outburst in particular, so they can monitor the fade from maximum looking for a standstill.

The last group are stars best suited to CCD observers for monitoring for outbursts and standstill behavior. These stars are too faint, even at maximum, for most visual observers to waste valuable time and resources on.

We also take special note of those UGZ that appear to go into outburst from standstill. When one of these stars enters a standstill we will be asking for intensive coverage until the star either goes into quiescence or outburst.

Activity is tracked in near real time as observations come in from AAVSO MyNewsFlash, BAAVSS-Alert, CVnet-Outburst, VSObs-share, and VSNET-outburst email notifications on the Activity at a Glance portion of the section home page: https://sites.google.com/site/aavsocvsection/Home.

5. Early results

The Z CamPaign was launched on September 25, 2009. From increased coverage of some stars and a thorough analysis of the AAVSO light curves we have positively confirmed ten UGZ systems: RX And, TZ Per, Z Cam, AT Cnc, SY Cnc, AH Her, UZ Ser, EM Cyg, VW Vul, and HX Peg. Most of these were known or suspected UGZ.

We have also been able to identify several potential Z Cam imposters. There is no evidence of standstills in their AAVSO light curves going back decades, in most cases. Included in this group are: TW Tri, KT Per, BI Ori, CN Ori, SV CMi, and AB Dra. Some of these stars have been erroneously classified as UGZ for decades in major variable star catalogues.

V344 Ori and V391 Lyr have uncharacteristic long outburst cycles of hundreds of days, and V1363 Cyg is an unusual, unique star, but its light variations are not typical of a UGZ. None of these is a Z Cam. FY Vul has an outburst cycle between 30 and 50 days, but also shows some quasi-periodic variation on shorter time scales, perhaps 15 to 20 days. The amplitude of variation is rather small for a UGZ type dwarf nova. It has been suggested that this star and V1101 Aql may represent a previously unrecognized group of low-amplitude dwarf novae (Kato *et al.* 1999).

As a result of nearly continuous coverage by CCD observers we have uncovered a previously unknown behavior in IW And: repeated outbursts to standstills followed by an other outburst and then a rapid fade to quiescence. This whole process then repeats (see Figure 1). Even more interesting is we have found the same unusual behavior in V513 Cas (see Figure 2).

6. Conclusion

Depending on which catalogue you reference, there are only 30 to 40 Z Cam dwarf novae. If a significant percentage of suspected Z Cams eventually proves not to be Z Cam, the remaining few represent a fairly rare and unique class of stars worthy of further investigation. Z Cam stars are rather ignored for the most part by

amateur and professional alike. This leaves the door to discovery open for those patient and persistent enough to devote time and energy to long-term monitoring of this unique class of cataclysmic variable. We plan to continue this campaign through 2011, modifying the targets list as new information becomes available.

7. Acknowledgements

We acknowledge with thanks the variable star observations from the AAVSO International Database contributed by observers worldwide and used in this research. Several individual observers have been of particular help to this campaign: Gary Poyner, Richard Sabo, George Sjoberg, Tim Crawford, Kenneth Menzies, David Boyd, Bart Staels, Ken Mogul, Keith Graham, and Bill Goff.

References

AAVSO data. 2010, AAVSO International Database (http://www.aavso.org/aavso-international-database).

Hellier, C. 2001, *Cataclysmic Variable Stars*, Springer-Praxis, Chichester, U.K.

Kato, T., Nogami, D., and Baba, H. 1999, *Inf. Bull. Var. Stars*, No. 4766, 1.

Meyer, F., and Meyer-Hofmeister, E. 1983, *Astron. Astrophys.*, **121**, 29.

Oppenheimer, B. D., Kenyon, S. J., and Mattei, J. A. 1998, *Astron. J.*, **115**, 1175.

Stehle, R., King, A., and Rudge, C. 2001, *Mon. Not. Roy. Astron. Soc.*, **323**, 584.

Szkody, P., and Mattei, J. A. 1984, *Publ. Astron. Soc. Pacific*, **96**, 988.

Warner, B. 1995, *Cataclysmic Variables Stars*, Cambridge Univ. Press, Cambridge.

Name	*R.A. (2000)* *h m s*	*Dec. (2000)* *° ′ ″*	*Con-stellation*	*Type*	*Outburst Cycle (d)*	*Range*
V513 Cas	00 18 14.90	+66 18 14.0	Cas	UGZ:	—	15.5–<17.2p
IW And	01 01 08.90	+43 23 26.0	And	UGZ	—	14.2–17.4 p
RX And	01 04 35.50	+41 17 58.0	And	UGZ	(14)	10.3–14 V
TW Tri	01 36 37.00	+32 00 40.0	Tri	UGZ:	(28)	13.3–17.0 p
KT Per	01 37 08.50	+50 57 20.0	Per	UGZ+ZZ	(26)	11.5–15.39V
TZ Per	02 13 50.90	+58 22 53.0	Per	UGZ	(17)	12–15.6 V
PY Per	02 50 00.10	+37 39 23.0	Per	UGZ	—	13.8–16.5 p
BI Ori	05 23 51.80	+01 00 30.0	Ori	UGZ	(20.5)	13.2–16.7 p
CN Ori	05 52 07.80	–05 25 01.0	Ori	UGZ	(15.85)	11–16.2 V
V344 Ori	06 15 19.00	+15 31 00.0	Ori	UGZ:	—	14.2–17.5: p
WZ CMa	07 18 49.20	–27 07 43.0	CMa	UGZ:	(27.1)	14.5–<16.0p
SV CMi	07 31 08.40	+05 58 49.0	CMi	UGZ	(16:)	13.0–16.3 p
BX Pup	07 54 15.60	–24 19 36.0	Pup	UGZ	(18)	13.76–16V
Z Cam	08 25 13.20	+73 06 39.0	Cam	UGZ	(22)	10–14.5V
AT Cnc	08 28 36.90	+25 20 03.0	Cnc	UGZ	(14)	12.3–14.6 p
SY Cnc	09 01 03.32	+17 53 56.0	Cnc	UGZ	—	10.6–14.0 p
AH Her	16 44 10.00	+25 15 02.0	Her	UGZ	(19.8)	10.9–14.7 p
UZ Ser	18 11 24.90	–14 55 34.0	Ser	UGZ	(26.4)	12.0–16.7 p
V391 Lyr	18 21 12.00	+38 47 44.0	Lyr	UGZ:	(100:)	14.0–17.0 p
HS1857+7127	18 57 20.40	+71 31 19.2	Dra	UGZ+E	—	13.9–17.2
V868 Cyg	19 29 04.40	+28 54 26.0	Cyg	UGZ:	(20.38)	14.3–<17.8p
V1505 Cyg	19 29 49.00	+28 32 54.0	Cyg	UGZ:	—	15.2–<17.5p
EM Cyg	19 38 40.10	+30 30 28.0	Cyg	UGZ+E	—	11.9–14.4 p
FY Vul	19 41 40.00	+21 45 59.0	Vul	UGZ:/NL	—	13.4–15.33B
AB Dra	19 49 06.40	+77 44 23.0	Dra	UGZ	(13.4)	11–15.3V
V1363 Cyg	20 06 11.60	+33 42 38.0	Cyg	UGZ:/ UGSU:	—	13.0–<17.6p
VW Vul	20 57 45.10	+25 30 26.0	Vul	UGZ	(30)	13.1–16.27B
V1404 Cyg	21 57 16.40	+52 12 00.0	Cyg	UGZ:	(19.15)	15.7–<17.7p
MN Lac	22 23 04.60	+52 40 58.0	Lac	UGZ:	—	15.1–<18.0p
HX Peg	23 40 23.70	+12 37 42.0	Peg	UGZ	—	12.9–16.62V

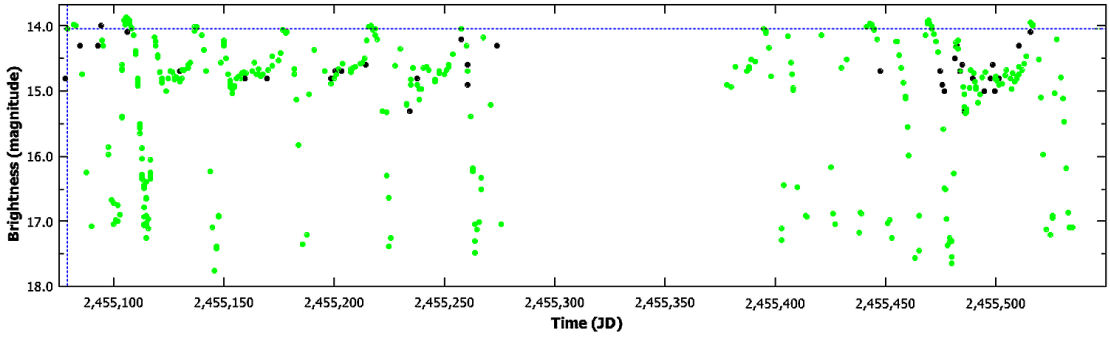

Figure 1. Light curve for IW And, September 1, 2009–March 1, 2010, showing quasi-periodic eclipse-like fadings. Visual observations (dark points), and Johnson *V* observations (lighter points) are shown.

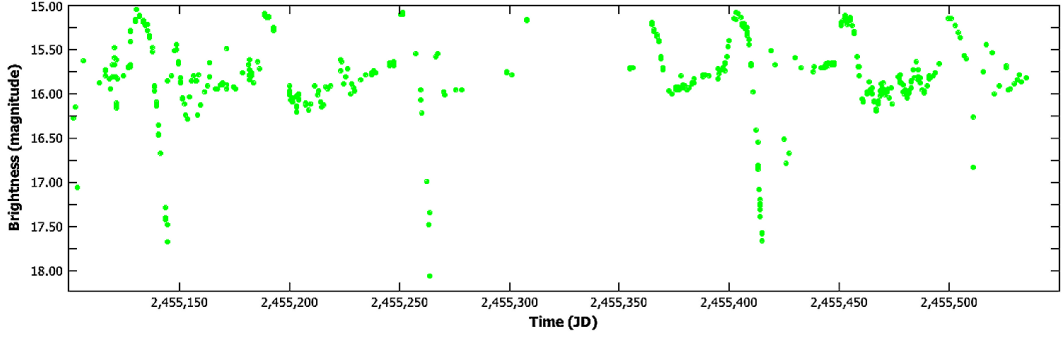

Figure 2. Light curve for V513 Cas, September 1, 2009–September 1, 2010, showing features similar to IW And. Johnson *V* observations are shown.

The First Historical Standstill of WW Ceti

Mike Simonsen
AAVSO, 49 Bay State Road, Cambridge, MA 02138; mikesimonsen@aavso.org

Rod Stubbings
Tetoora Observatory, 2643 Warragul-Korumburra Road, Tetoora Road 3821, Victoria, Australia; stubbo@sympac.com.au

Received November 29, 2010; accepted December 2, 2010

Abstract Z Cam dwarf novae are distinguished from other dwarf novae based on the appearance of so called "standstills" in their long-term optical light curves. It has been suggested previously that WW Cet might be a Z Cam type dwarf nova, but this classification was subsequently ruled out, based on its long-term light curve behavior. Forty years of historical data for WW Cet has shown no evidence of standstills. WW Cet is therefore classified as a UG type dwarf nova in the *General Catalogue of Variable Stars* (GCVS, Samus *et al.* 2007–2009) and the International Variable Star Index (VSX, Watson *et al.* 2006). Beginning in the 2010 observing season, WW Cet has been observed to be in a standstill, remaining more or less steady in the 12th magnitude range. Based on this first ever, historical standstill of WW Cet, we conclude that it is indeed a bona fide member of the Z Cam class of dwarf novae.

1. Introduction

U Geminorum-type (UG) variables, also called dwarf novae, are close binary systems consisting of a dwarf or subgiant K-M star that fills the volume of its inner Roche lobe. This donor star is losing mass to a white dwarf surrounded by an accretion disk. From time to time the system goes into outburst, brightening rapidly by several magnitudes. After several days to a month, or more, it returns to its original state.

These dwarf nova outbursts are thought to be caused by thermal instabilities in the disk. Gas accumulates in the disk until it heats up and becomes viscous. This increased viscosity causes it to migrate in toward the white dwarf, heating up even more, eventually causing an outburst.

Intervals between consecutive outbursts for a given star may vary, but every star is characterized by a characteristic mean value of these intervals. This mean cycle corresponds to the mean amplitude of the outbursts. Generally speaking, the longer the cycle, the greater the amplitude of the outbursts.

According to the characteristics of their light curves, UGs are further subdivided into three types: SS Cyg (UGSS), SU UMa (UGSU), and Z Cam (UGZ). UGSU variables are not relevant to this discussion.

UGSS increase in brightness by 2 to 6 magnitudes in *V* in 1 to 2 days. After several subsequent days, they return to their original brightness. The cycle times vary considerably, from 10 to hundreds of days.

UGZ also show cyclic outbursts, but differ from UGSS variables by the fact that sometimes after an outburst they do not return to their quiescent magnitude. Instead, they appear to get stuck, for months or even years, at a brightness of one to one and a half magnitudes fainter than outburst maximum. These episodes are known as standstills. Z Cam cycle times characteristically range from 10 to 40 days, and their outburst amplitudes are from 2 to 5 magnitudes in *V*, but standstills are the defining characteristic of the Z Cam stars.

2. History

Luyten (Liller 1962a) was the first to mention WW Cet as a variable star. He also suspected it was a cataclysmic variable (CV). Herbig (Liller 1962b) confirmed the CV nature of the star. The first to suggest WW Cet might belong to the Z Cam class of dwarf novae was Paczynski (1963). The system was catalogued as UGZ in the GCVS (Kukarkin *et al.* 1969).

Warner (1987) and Ringwald *et al.* (1996) concluded that since the long-term light curve behavior of WW Cet showed no evidence of standstills it was not a bona fide member of the Z Cam subclass. Both the GCVS (Samus *et al.* 2007–2009) and VSX currently list WW Cet as a UG.

3. Characteristics

A detailed inspection of the AAVSO data shows that WW Cet normally ranges from 16.0V at minimum to 10.5V in outburst. From August 1968 through the end of 2009 its cyclic pattern of outbursts and quiescent stages appears to be as a UGSS star (Figure 1). It has an average cycle time between outbursts of 31.2 days (Samus *et al.* 2007–2009).

The physical characteristics of the star are fairly well known. The orbital period is 0.17587 days (4.22 hours) and the masses of the primary and secondary are known to be 1.05 and 0.393 solar masses respectively. The orbital inclination is 48 degrees (± 11), so WW Cet does not exhibit eclipses (Tappert *et al.* 1997).

It is the longish period, above the period gap, that has led some in the past to suspect WW Cet might be a UGZ. All confirmed UGZ have periods longer than 3 hours. However, this characteristic is not proof of membership in the Z Cam class.

4. The 2010 standstill

There is solid observational evidence in the AAVSO International Database that WW Cet has been in standstill for at least 78 days (Figure 2). The earliest

observation of the 2010 standstill event was reported on September 10, 2010. WW Cet was reported to be magnitude 12.8v. Through November 27, 2010 the star remained 12th magnitude, averaging ~12.4 with fluctuations from 12.9V to 12.0v (Figure 3).

This is 3 to 4 magnitudes in *V* above its typical minimum value and ~1.5 magnitudes in *V* below the average maximum value, almost textbook agreement with the definition of a UGZ standstill. Add to this the fact that its outburst amplitude, cycle time and orbital period all conform to the characteristics of UGZ classification and the evidence for WW Cet as a bona fide Z Cam dwarf nova is overwhelming.

5. Conclusion

We conclude that the behavior of WW Cet in the 2010 observing season represents the first ever recorded standstill of this dwarf novae. Combined with the known characteristics of amplitude, cycle time and orbital period, this standstill confirms WW Cet is a Z Cam dwarf nova.

6. Acknowledgements

We acknowledge with thanks the variable star observations from the AAVSO International Database contributed by observers worldwide and used in this research.

References

Liller, M. H. 1962a, *Harvard Coll. Obs. Announcement Card*, No. 1574

Liller, M. H. 1962b, *Harvard Coll. Obs. Announcement Card*, No. 1576.

Kukarkin, B. V., *et al.* 1969, *General Catalogue of Variable Stars*, 3rd ed., Moscow.

Paczyński, B. 1963, *Publ. Astron. Soc. Pacific*, **75**, 278.

Ringwald, F. A., Thorstensen, J. R., Honeycutt, R. K., and Smith, R. C. 1996, *Astron. J.*, **111**, 2077.

Samus, N. N., *et al.* 2007–2009, *General Catalogue of Variable Stars*, online catalogue, *http://www.sai.msu.su/groups/cluster/gcvs/gcvs.*

Tappert, C., Wargau , W. F., Hanuschik, R. W., and Vogt, N. 1997, *Astron. Astrophys.*, **327**, 231.

Warner, B. 1987, *Mon. Not. Roy. Astron. Soc.*, **22**7, 23.

Warner, B. 1995, *Cataclysmic Variables*, Cambridge Univ. Press, Cambridge.

Watson, C. L., Henden, A. A., Price, A. 2006, in *The Society for Astronomical Sciences 25th Annual Symposium on Telescope Science*, ed. B. Warner, *et al.*, Soc. Astron. Sci., Big Bear, California, 47.

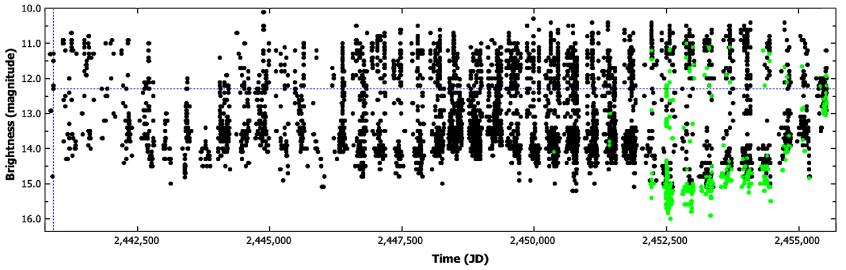

Figure 1. Light curve for WW Cet (1970–2009) using long-term AAVSO data, and demonstrating the UGSS nature of the outburst cycle. Visual observations (dark points), and Johnson *V* observations (lighter points) are shown.

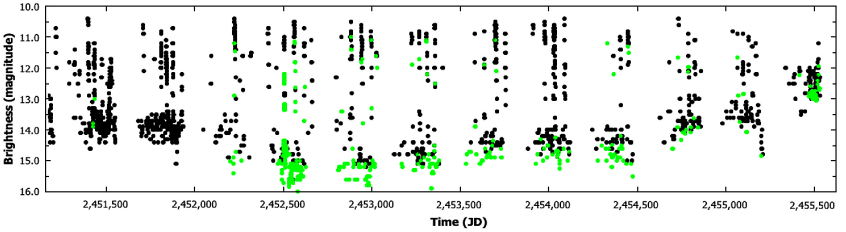

Figure 2. Light curve for WW Cet using AAVSO data from January 1, 1999 to November 27, 2010. The normal UGSS cyclic behavior and the typical range of variation from the prior eleven observing seasons are in stark contrast to the last three months of data, including the 78 days where WW Cet has remained in standstill between 12th and 13th magnitude. Visual observations (dark points), and Johnson *V* observations (lighter points) are shown.

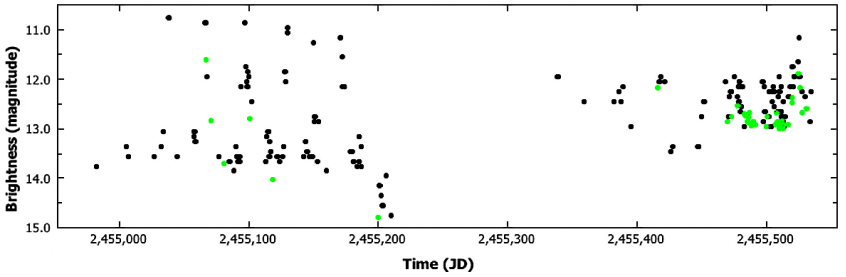

Figure 3. Light curve for WW Cet using AAVSO data from the 2009 observing season (left) showing the UGSS-like outburst cycle, and data from the 2010 observing season showing the first recorded standstill of WW Cet. Visual observations (dark points), and Johnson *V* observations (lighter points) are shown.

Leo5 is a Z Cam Type Dwarf Nova

Patrick Wils
Aarschotsebaan 31, Hever B-3191, Belgium; Vereniging Voor Sterrenkunde, Belgium; patrickwils@yahoo.com

Tom Krajci
Astrokolkhoz, Box 1351, Cloudcroft, NM; tom_krajci@tularosa.net

Mike Simonsen
AAVSO Headquarters, 49 Bay State Road, Cambridge, MA 02138; mikesimonsen@aavso.org

Received March 18, 2011; accepted March 22, 2011

Abstract Photometry of Leo5 = 1H 1025+220 show that it is a dwarf nova of the Z Cam subtype. Two long standstills have been observed in the last five years.

1. Introduction

The Z Cam subtype is a rare class of dwarf novae, characterized by so-called standstills at an intermediate brightness level between the outburst maximum and the quiescent state. These standstills may last for a number of weeks to years, when the object does not change in brightness very much. The orbital periods of Z Cam type dwarf novae have been found to be always above the period gap for cataclysmic variables. Less than forty genuine members of the class are known (Simonsen 2011).

Leo5 = 1H 1025+220 = SDSS J102800.07+214813.5 is a little-studied cataclysmic variable (CV), discovered by Remillard and others (see Downes and Shara 1993) in the course of the HEAO-1 x-ray survey. It was classified as a nova-like variable and confirmed to be a CV spectroscopically by Munari *et al.* (1997), and more recently also by the Sloan Digital Sky Survey (SDSS; Szkody *et al.* 2009). Taylor (1999) found it to be eclipsing with an orbital period of 3.506 hours.

2. Observations

As part of its service to the study of transient objects, the Catalina Real-time Transient Survey (CRTS; Drake *et al.* 2009) publicly provide their data for a number of CVs. For Leo5 data are available from 2005 to the present (Figure 1). These data show a light curve which is typical of a low amplitude (magnitude 15.2–17.7), frequently erupting dwarf nova. On one occasion however, starting early 2008, outbursts seem to have ceased for more than a year, until the end of 2009, with Leo5 at around magnitude 16.2 all the time.

CRTS data are fairly sparse in general (at best one night of four data points each week), so that more frequent observations were called for. These were obtained in *B* and *V* through AAVSOnet starting early 2010. These data, presented in Figure 2, again show the object with frequent outbursts, varying between magnitude 15.5 and 17.5*V*, and spending little time in quiescence. Although there are not enough observations to determine the length of an outburst cycle precisely, it is estimated to be about 20 days. At the start of the 2010–2011 observing season, however, the outbursts had ceased again, and Leo5 was at an intermediate magnitude of 16.2*V*. This standstill has lasted until the present. In hindsight the classification as a nova-like variable may have been partly due to the fact Leo5 is in standstill very often or for extended periods.

3. Conclusion

Leo5 = 1H 1025+220 has been found to be a member of the rare class of Z Cam type dwarf novae, showing frequent and long standstills. Because it is also an eclipsing system, Leo5 may provide more clues to the mechanism causing the standstills.

4. Acknowledgements

This study made use of NASA's Astrophysics Data System, and the SIMBAD and VIZIER databases operated at the Centre de Données astronomiques de Strasbourg (France). The Catalina Real-time Transient Survey is acknowledged for making their data publicly available. The AAVSO data have been obtained through AAVSOnet, the network of robotic telecopes of the AAVSO (Henden 2011).

References

Downes, R. A., and Shara, M. M. 1993, *Publ. Astron. Soc. Pacific*, **105**, 127.
Drake, A. J., *et al.* 2009, *Astrophys, J.*, **696**, 870.
Henden, A. 2011, in *Conf. Proc. Telescopes From Afar*, ed. S. Gajadhar, in press.
Munari, U., Zwitter, T., and Bragaglia, A. 1997, *Astron. Astrophys.*, **122**, 495.
Simonsen, M. 2011, *J. Amer. Assoc. Var. Star Obs.*, **39** (in press).
Szkody, P., *et al.* 2009, *Astron. J.*, **137**, 4011.
Taylor, C. 1999, *SW Sextantis Stars, Superhumps, and Other Phenomena in Cataclysmic Variables*, Ph.D. thesis, Dartmouth College, Hanover, NH.

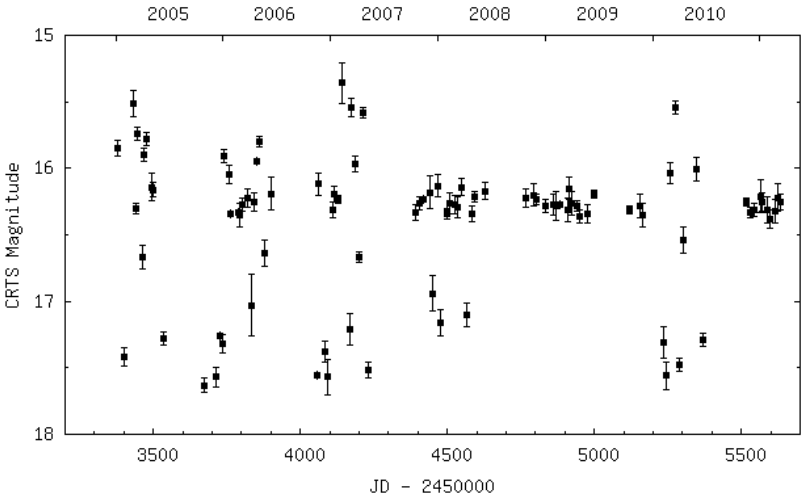

Figure 1. Light curve of Leo5 from the Catalina Real-time Transient Survey.

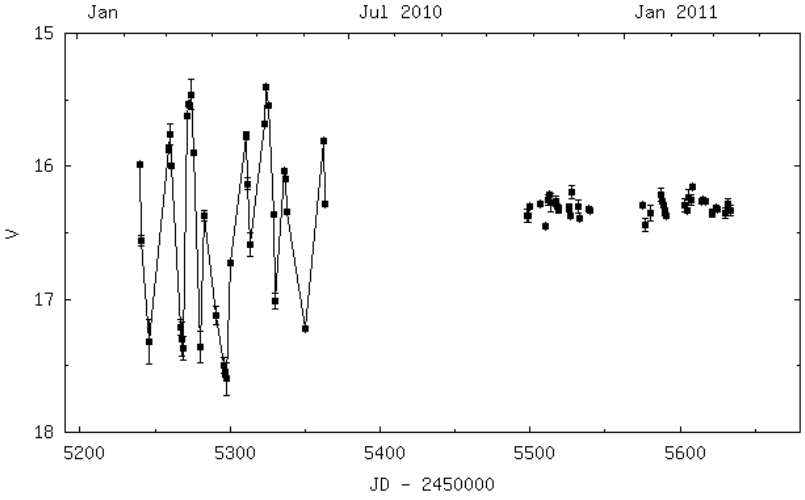

Figure 2. *V* light curve of Leo5 obtained through AAVSONet. The data points from early 2010 have been connected with lines to lead the eye.

Do Eclipsing Variable Stars Show Random Cycle-to-cycle Period Fluctuations?

Seyedyara Mohajerani
John R. Percy
Department of Astronomy and Astrophysics, University of Toronto, Toronto ON Canada M5S 3H4; correspondence should be addressed to Dr. Percy, john.percy@utoronto.ca

Received September 9, 2010; revised October 4, 2010; accepted October 4, 2010

Abstract AAVSO observers and others have measured the times of minima of hundreds of eclipsing binaries over many decades. These times can be used to construct (O–C) diagrams that can be used to refine the periods of the stars, and to look for changes or fluctuations in the periods. We have applied the Eddington-Plakidis (1929) model to the (O–C) data on 100 stars in the AAVSO Eclipsing Binary Program, to determine whether the (O–C) diagrams can be explained by the cumulative effect of random, cycle-to-cycle fluctuations in period. The stars can be divided into three groups: 25–35% showing (O–C) fluctuations due only to measurement errors; 40–50% showing small, random cycle-to-cycle period fluctuations (typically a few times 10^{-4} of a cycle), and 20–30% showing (O–C) variations which do not fit the Eddington-Plakidis model and therefore cannot be explained by the accumulation of random fluctuations. We discuss possible explanations for these three groups.

1. Introduction

For several decades, AAVSO observers and others have systematically recorded the times of minima of eclipsing binaries. These observations have been used to plot (O–C) diagrams (Sterken 2005), which can be used to refine the periods and epochs of the stars, and to look for changes in the periods (e.g. Mallama 1987, who used AAVSO and other observations from amateurs to study period changes in several eclipsing variables). If the period is constant, but not equal to the assumed value, the (O–C) diagram is a straight line with non-zero slope. If an incorrect epoch has been assumed, the intercept on the (O–C) axis is not zero. If the period is changing, the (O–C) diagram is not linear. It is parabolic if the rate of period change is constant.

In many pulsating variables, however, some of the apparent period changes are due to the cumulative effect of random cycle-to-cycle period fluctuations. The formalism for studying these was developed by Eddington and Plakidis (1929), and this formalism, and others, have subsequently been applied to a wide variety of pulsating variables; see Turner *et al.* (2009) for a recent short review. The average fluctuation in period ε is found to be proportional to period

P: $\varepsilon = 0.0136P$ (± 0.0069 s.d.), i.e. $\varepsilon / P = 0.0136$. One possible cause of these fluctuations is the effect of large, random convection cells in the outer layers of the stars.

The signature of these fluctuations in the (O–C) diagram is a random wave-like pattern. Since such patterns are seen in the (O–C) diagrams of many eclipsing binaries (Nelson, undated), it seemed worthwhile to apply the Eddington and Plakidis (1929) algorithm to the data for some of the stars in the AAVSO database. In this way, using this new method of analysis, we can hope to extract some meaningful science from the observations that have been so diligently made.

2. Data and analysis

Times of minima of the stars listed in Tables 1 and 2 were taken from the AAVSO website:

http://www.aavso.org/observed-minima-timings-eclipsing-binaries (groups 1 and 2).

The timings were originally published, in eleven groups of fifty stars, in the *AAVSO Times of Minima of Eclipsing Binaries* series. It is not clear whether there was any bias in selecting the stars in each group, especially the first two groups. We note that group 2 seems to contain more stars with longer periods. In our sample, there is a good distribution of stars with type, range, and period.

Author Mohajerani wrote a computer program in JAVA to implement the algorithm of Eddington and Plakidis (1929). This program was used to generate values of $<u(x)>^2$ as a function of x, the number of elapsed cycles between times of minimum. If the star shows random cycle-to-cycle period fluctuations, the graph of $<u(x)>^2$ as a function of x should be a straight line with slope ε^2, where ε is the average value of the fluctuation, in days, and intercept $2\alpha^2$ where α is the average random observational error in determining the time of minimum, in days. Note that α is the accidental error of observation, and ε is the actual fluctuation in cycle length. Linear least-squares fits were performed on the graphs to determine the slopes and intercepts and their standard errors.

In some stars, the graph is curved upward, and the intercept is negative, which is inconsistent with the model since the intercept is proportional to the square of a real quantity. In this case, it is appropriate to use the value of $<u(1)>^2$ in place of the intercept, to determine α. If no value of $<u(1)>^2$ was available, $<u(2)>^2$ or $<u(3)>^2$ was used. Intercepts determined in this way are marked with an asterisk (*) in the tables.

The referee has correctly pointed out that, in the Eddington-Plakidis algorithm, "a correcting factor is required when x is a considerable fraction of the whole number of periods employed in determining the mean period" (Eddington and Plakidis 1929). In our case, we assume that the periods have been derived from a much larger and longer dataset than we are using. For a few stars, we repeated

the analysis with a smaller maximum value of x. The intercept and slope changed somewhat (perhaps due to curvature in the diagram), but the changes were much smaller than the range of values of the intercept and slope in Table 1.

As we shall discuss in Section 4, it is important to note that the minimum-to-minimum intervals are not necessarily a measure of the orbital period of the binary system at that epoch. For instance, the minima may be distorted by spots or pulsations on the stars, or by light from circumstellar disks or streams.

3. Results

Tables 1 and 2 list the names of the stars, their type according to SIMBAD, the period in days, the approximate magnitudes of maximum and minimum, the slope and its error, the intercept, and the values of α, ε, and ε / P. The types are those used in the *General Catalogue of Variable Stars* (GCVS, Kholopov, *et al.* 1985), and are based on the light curve shape (EA, EB, EW), the state of detachment of the components (DM, SD), the ellipsoidal shape of the components (KW), or the degree of activity (RS: RS CVn). The value of α is the average error in measuring the time of minimum. To assume that this is a fixed value is rather simplistic, since the minima are measured in various ways, by various observers (though the AAVSO Eclipsing Binary program uses a standard method for determining the times of minima). If the slope is negative, then the value of ε is undefined (N/A in Table 1).

Figures 1 and 2 show $<u(x)>^2$ diagrams for two representative stars: ZZ Cep, whose diagram can reasonably be fitted with a straight line, and U Cep, whose diagram cannot.

Most of the $<u(x)>^2$ diagrams can be fitted with a straight line, with a (positive) intercept which is consistent with the expected observational error. Specifically: a histogram of the intercepts shows that slightly more than half are clustered between 2 and 9×10^{-5} with a mean value of about 4×10^{-5}. This corresponds to a value of α of a few times 0.001, which is reasonable: the times of minima are given to the nearest thousandth of a day and, where there are multiple measurements of the same minimum, they tend to differ by a few times 0.001. This value is also consistent with the estimate by Batten (1973), namely, "of order of 10^{-3} to 10^{-4} in the most favorable cases."

Some diagrams cannot be fitted with a straight line; the curve is initially flat, then curves upward (Figure 2). This results in an intercept that is negative, which is unphysical because it is proportional to α^2, where α is a real quantity. Predictably, the (positive) magnitude of the slope is then correlated with the (negative) magnitude of the intercept.

A histogram of the slopes (Figure 3) shows that about a third are clustered between –5 and $+5 \times 10^{-9}$. Although their formal errors generally exclude a slope of zero, we are inclined to assume that these stars have little or no random fluctuations. The rest of the stars have slopes that exceed 10×10^{-9}, and are

likely significant. Almost half fit the Eddington-Plakidis model, with a small but significant slope. About a quarter have significant slopes but do not fit the Eddington-Plakidis model. The distributions of both the intercepts and the slopes were similar for all three types of binaries—EA, EB, and EW.

We looked for correlations between various quantities in Tables 1 and 2. As mentioned, stars with large slopes had large negative intercepts, but this is an artifact of fitting a linear function to non-linear data. The stars with the largest slopes—greater than $\times 10^{-6}$—were: β Lyr (12.94), SW Cyg (4.57), TY Peg (3.09), TX UMa (3.06), XZ Aql (2.14), U CrB (3.45), ST Per (2.65), and U Cep (2.50); the numbers in brackets are the periods in days. Large slopes are associated with longer periods.

Some stars with large ranges (2.5 or greater) and/or faint minima had large slopes and small intercepts, though they tended to be stars that did not fit the Eddington-Plakidis model.

The most interesting correlation was that the stars with the largest slopes tended to be the stars with longest periods. The most extreme case was β Lyr with a period of 12.94 days, and a slope of 1.6×10^{-4}. Other examples are listed above.

The Eddington-Plakidis algorithm assumes that there are fixed values of α and ε. For some stars, the average error of measurement of the times of minima decreases with time, especially as CCD techniques have begun to replace visual techniques. (Almost all of the minima that we analyzed were measured visually.) An inspection of the (O–C) diagrams shows no obvious relation between the properties of the $<u(x)>^2$ diagram and any systematic decreases in the scatter in the corresponding (O–C) diagram (Nelson, undated).

The values of ε / P tend to cluster into two groups: $3–16 \times 10^{-5}$ and $25–45 \times 10^{-5}$. These values are much smaller than in the pulsating variables discussed by Turner *et al.* 2009.

4. Discussion

The results of our study raise several questions: (1) What is the nature and cause of the cycle-to-cycle period fluctuations which are present in some of the stars? (2) Why do many of the stars show no fluctuations, with zero slope in the $<u(x)>^2$ diagram? (3) Why do some stars have $<u(x)>^2$ diagrams which do not fit the Eddington-Plakidis model, but curve upward as in Figure 2?

One way to approach question (3) is to look at the nature of the most extreme cases, those mentioned above. For instance: β Lyr, the most extreme case, is known to have an (O–C) diagram that is highly parabolic, indicative of a large, constant rate of period change (e.g. Wilson and Van Hamme 1999). The same is true of U Cep (e.g. Mansoori 2008). The two stars with the most prominently curved $<u(x)>^2$ diagrams, AB Cas and RT Per, also have (O–C) diagrams with distinct curvature. SW Cyg, TY Peg, TX UMa, and possibly ST Per have (O–C)

diagrams which appear as a broken straight line, indicative of an abrupt period change between two intervals of constant period (Nelson, undated). According to Batten (1973), this is the most common form of period change in eclipsing variables: abrupt changes which are well separated in time. XZ Aql has an (O–C) diagram which appears parabolic, with a possible 36.7-year periodic component. The (O–C) diagram of U CrB appears straight, but van Gent (1982) suggested that there was (one) 160-year cycle present. Such periodic or possibly periodic components would be explainable by the presence of a third star in the system, with a very long orbital period. Many binary systems are actually triple (or more). Apsidal motion, with a time scale of tens of years, is another possible cause (Batten 1973). The (O–C) diagram of Algol (β Per), for instance, shows cycles of 1.8 years due to a third star, 33 years due to apsidal motion, and a time scale of 175 years ("the great inequality") of unknown cause. The (O–C) diagrams that are either parabolic or broken straight lines are assumed to be due to either continuous or episodic mass transfer or loss in the system. We conclude that the stars in our sample whose $<u(x)>^2$ diagrams do not fit the Eddington-Plakidis model are those which, because of the system configuration, undergo continuous or episodic mass transfer or loss.

As for the random cycle-to-cycle period fluctuations seen in many stars, these may be due to random distortions in the light curve minima. Kwee (1958) studied sixteen eclipsing variables, and concluded that there were "small and rapid fluctuations...near the limit of what can be shown by present observations." He drew this conclusion because the residuals in the (O–C) diagram were two to three times larger than the computed mean errors of the observations—typically 0.001 to 0.003 day. He and van Woerden (1957) both attributed such fluctuations to distortions in the light curves.

These distortions of the light curve, during minima, could be due to spots on the eclipsed star, if its rotation period was less than the binary period. This might explain why fluctuations are greater in binaries with longer orbital periods. The distortions could also be due to small oscillations of one of the stars, or due to disks or streams of gas. It is unlikely that they are due to actual changes in the orbital period of the system, caused by mass loss or transfer, because fluctuations of the order of $\times 10^{-4}$ would require much larger mass loss or transfer than is reasonable.

When the seven stars with largest slopes are compared with a sample of stars with slopes close to zero, it turns out that all of the large-slope stars have primaries with spectral type A5 or hotter, whereas the small-slope stars have primaries which are cooler. There is no obvious physical difference between the stars that show small but significant random cycle-to-cycle period fluctuations, and those that do not. Both groups include all types of eclipsing binaries, and a mixture of A, F, and G spectral types.

5. Conclusions

We have analyzed AAVSO timings of the minima of 100 eclipsing variable stars, to look for evidence of random, cycle-to-cycle period fluctuations which may explain some of the features of the (O–C) diagrams of these stars. About 25–35% of our sample show little or no evidence of these; 40–50% show evidence of small but significant fluctuations, and 20–30% show evidence that the main features of their (O–C) diagrams are not due to such fluctuations. We describe some processes which might possibly explain the fluctuations, though the precise cause of the fluctuations in any one star has yet to be determined.

6. Acknowledgements

Author Mohajerani began this project as a participant in the University of Toronto Mentorship Program, which enables outstanding senior high school students to work on research projects at the University. We thank the Natural Sciences and Engineering Research Council of Canada for research support. This project would not have been possible without the sustained efforts of dozens of AAVSO observers, and the help of AAVSO staff. We thank Professors Edward Guinan and Gene Milone for reading a draft of this paper. This research has made use of the SIMBAD database, operated at CDS, Strasbourg, France.

References

Batten, A. H. 1973, *Binary and Multiple Systems of Stars*, Pergamon Press, Oxford.

Eddington, A. S., and Plakidis, S. 1929, *Mon. Not. Royal Astron. Soc.*, **90**, 65.

Kholopov, P. N., *et al.* 1985, *General Catalogue of Variable Stars*, 4th ed., Moscow.

Kwee, K. K. 1958, *Bull. Astron. Inst. Netherlands*, **14**, 131.

Mallama, A. 1987, *J. Amer. Assoc. Var. Star Obs.*, **16**, 4.

Mansoori, D. 2008, *Astrophys. Space Sci.*, **318**, 57.

Nelson, B. undated, http://www.aavso.org/bob-nelsons-o-c-files

Sterken, C. 2005, in *The Light-Time Effect in Astrophysics*, ed. C. Sterken, ASP Conf. Ser. 335, 3.

Turner, D. G., *et al.*, 2009, in *Stellar Pulsation: Challenges for Theory and Observation*, ed. J.A. Guzik and P.A. Bradley, AIP Conf. Ser., 1170, 167.

Van Gent, R. H. 1982, *Astron. Astrophys. Suppl.*, **48**, 457.

Van Woerden, H. 1957, *Leiden Ann.*, **21**, 1.

Wilson, R. E., and Van Hamme, W. 1999, *Mon. Not. Royal Astron. Soc.*, **303**, 736.

Table 1. Analysis of Stars on the AAVSO Eclipsing Binary Program, Group 1.

Name	*Type*	*Period (d)*	*Max*	*Min*	*Range*	*Slope*	*Error*	*Intercept*	*Error*	α	ε	ε/*Period*
RT AND	EA/RS	6.29E–01	9	9.8	0.8 (V)	1.40E–09	5.77E–10	4.16E–05	2.49E–06	4.56E–03	3.74E–05	5.94E–05
WZ AND	EB	6.96E–01	11.2	12	0.8 (V)	7.75E–10	2.75E–09	1.19E–04	1.04E–05	7.71E–03	2.78E–05	4.00E–05
XZ AND	EA	1.36E+00	9.9	12.5	2.6 (V)	4.24E–08	2.10E–09	–4.87E–06	4.34E–06	7.07E–04*	2.06E–04	1.52E–04
AB AND	EW	3.32E–01	9.5	10.5	1 (V)	1.18E–09	2.52E–10	4.81E–05	2.04E–06	4.90E–03	3.43E–05	1.03E–04
CX AQR	EB	5.56E–01	10.6	11.8	1.2 (V)	–6.39E–10	2.26E–10	2.06E–05	1.14E–06	3.21E–03	N/A	N/A
OO AQL	EW/DW	5.07E–01	9.2	9.9	0.7 (V)	1.45E–10	4.37E–10	7.12E–05	2.56E–06	5.97E–03	1.21E–05	2.38E–05
V346 AQL	EA/SD	1.11E+00	9	10.1	1.1 (p)	–1.45E–09	9.57E–10	3.24E–05	2.49E–06	4.02E–03	N/A	N/A
WW AUR	EA/DM	2.53E+00	5.8	6.5	0.7 (V)	1.11E–08	1.16E–08	1.39E–04	1.23E–05	8.33E–03	1.05E–04	4.18E–05
SV CAM	EA/DW/RS	5.93E–01	8.4	9.1	0.7 (V)	7.43E–08	1.48E–09	–8.13E–05	6.79E–06	2.59E–03*	2.73E–04	4.59E–04
RZ CAS	EA/SD	1.20E+00	6.2	7.7	1.5 (V)	1.27E–08	8.74E–10	2.76E–05	2.20E–06	3.71E–03	1.13E–04	9.42E–05
TV CAS	EA/SD	1.81E+00	7.2	8.2	1 (V)	1.94E–08	1.49E–08	1.95E–04	1.89E–05	9.87E–03	1.39E–04	7.69E–05
AB CAS	EA	1.37E+00	10.1	11.9	1.8 (V)	1.07E–07	2.40E–09	–6.63E–05	5.12E–06	3.54E–03*	3.28E–04	2.40E–04
IR CAS	EB	6.81E–01	10.8	12.3	1.5 (p)	6.83E–08	2.34E–09	–2.40E–05	8.83E–06	4.55E–03*	2.61E–04	3.84E–04
IV CAS	EA	9.99E–01	11.2	12.4	1.2 (p)	–3.28E–09	2.13E–09	8.09E–05	5.96E–06	6.36E–03	N/A	N/A
U CEP	EA/SD	2.49E+00	6.8	9.2	2.4 (V)	1.26E–06	1.54E–08	–3.78E–04	1.79E–05	3.00E–03*	1.12E–03	4.49E–04
ZZ CEP	EA/DM	2.14E+00	8.6	9.6	1 (V)	4.62E–09	1.88E–08	2.52E–04	2.41E–05	1.12E–02	6.79E–05	3.17E–05
EG CEP	EB	5.45E–01	9.3	10.2	0. 9 (V)	–2.96E–09	6.90E–10	8.54E–05	3.30E–06	6.54E–03	N/A	N/A
RW COM	EW/KW	2.37E–01	11	11.7	0.7 (V)	9.31E–09	6.03E–10	1.78E–05	7.34E–06	2.99E–03	9.65E–05	4.06E–04
W CRV	EB/KW	3.88E–01	11.2	12.5	1.3 (V)	2.09E–09	5.26E–10	3.56E–05	3.38E–06	4.22E–03	4.57E–05	1.18E–04
ZZ CYG	EA/SD	6.29E–01	10.6	11.7	1.1 (V)	2.85E–08	8.83E–10	–1.19E–05	3.64E–06	1.53E–03*	1.69E–04	2.69E–04
BR CYG	EA	1.33E+00	9.4	10.6	1.2 (V)	2.26E–09	1.63E–09	3.69E–05	3.30E–06	4.30E–03	4.76E–05	3.57E–05

table continued on following pages

Table 1. Analysis of Stars on the AAVSO Eclipsing Binary Program, Group 1, cont.

Name	*Type*	*Period (d)*	*Max*	*Min*	*Range*	*Slope*	*Error*	*Intercept*	*Error*	α	ε	ε/*Period*
CG CYG	EA/SD/RS	6.31E–01	9.7	10.9	1.2 (V)	6.11E–08	1.95E–09	–5.42E–05	7.60E–06	5.30E–03*	2.47E–04	3.92E–04
V387 CYG	EA/K	6.41E–01	11.5	12.3	0.8 (V)	7.85E–10	4.14E–10	2.31E–05	1.62E–06	3.40E–03	2.80E–05	4.38E–05
TY DEL	EA/SD	1.19E+00	9.7	10.9	1.2 (V)	1.77E–07	5.90E–09	–4.96E–05	1.24E–05	2.36E–03*	4.21E–04	3.53E–04
YY DEL	EA	7.93E–01	11.3	12	0.7 (p)	–2.09E–09	1.71E–09	6.49E–05	4.67E–06	5.69E–03	N/A	N/A
FZ DEL	EA/SD	7.83E–01	10.2	11.3	1.1 (p)	6.72E–08	1.84E–09	–5.40E–05	6.14E–06	0.00E+00*	2.59E–04	3.31E–04
Z DRA	EA/SD	1.36E+00	10.8	14.1	3.3 (p)	9.29E–07	2.69E–08	–5.06E–04	5.18E–05	1.41E–03*	9.64E–04	7.10E–04
RZ DRA	EB/SD	5.51E–01	10.1	11	0.9 (V)	6.53E–08	2.28E–09	–5.00E–05	1.12E–05	6.13E–03*	2.56E–04	4.64E–04
AI DRA	EA/SD	1.20E+00	7.1	8.1	1 (V)	1.17E–08	3.79E–09	7.96E–05	7.94E–06	6.31E–03	1.08E–04	9.03E–05
YY ERI	EW/KW	3.21E–01	8.1	8.8	0.7 (V)	1.08E–07	1.76E–09	–1.99E–04	1.58E–05	7.07E–04*	3.29E–04	1.02E–03
SZ HER	EA/SD	8.18E–01	9.9	11.9	2 (V)	–5.54E–08	2.62E–08	5.64E–04	9.09E–05	1.68E–02	N/A	N/A
AV HYA	EB/KE	6.83E–01	10.2	10.8	0.6 (V)	7.96E–08	6.21E–09	4.99E–05	2.32E–05	5.00E–03	2.82E–04	4.13E–04
SW LAC	EW/KW	3.21E–01	8.5	9.4	0.9 (V)	2.08E–08	7.84E–10	8.92E–06	6.71E–06	2.11E–03	1.44E–04	4.49E–04
VX LAC	EA/SD	1.07E+00	10.9	13	2.1 (p)	1.47E–08	8.13E–10	4.93E–08	1.94E–06	1.57E–04	1.21E–04	1.13E–04
Y LEO	EA/SD	1.69E+00	10.1	13.2	3.1 (V)	4.28E–09	1.49E–09	1.77E–05	2.38E–06	2.97E–03	6.54E–05	3.88E–05
EW LYR	EA/SD	1.95E+00	11.2	13.5	2.3 (V)	1.88E–08	7.27E–09	6.35E–05	1.01E–05	5.63E–03	1.37E–04	7.04E–05
ER ORI	EW/KW	4.23E–01	9.3	10	0.7 (V)	2.17E–09	7.04E–10	9.04E–05	4.72E–06	6.72E–03	4.66E–05	1.10E–04
U PEG	EW/KW	3.75E–01	9.2	10.1	0.9 (V)	5.83E–08	2.09E–09	–3.78E–05	1.63E–05	4.95E–03*	2.41E–04	6.44E–04
RT PER	EA/SD	8.49E–01	10.5	11.7	1.2 (V)	1.25E–07	2.31E–09	–9.59E–05	7.65E–06	3.36E–03*	3.54E–04	4.17E–04
XZ PER	EA/SD	1.15E+00	11.4	13.4	2 (p)	3.80E–08	3.94E–09	7.09E–05	9.32E–06	5.95E–03	1.95E–04	1.69E–04
RW TAU	EA/SD	2.77E+00	8	11.6	3.6 (V)	8.00E–07	4.64E–08	–1.47E–04	4.41E–05	0.00E+00*	8.94E–04	3.23E–04
EQ TAU	EW/KW	3.41E–01	10.5	11	0.5 (V)	1.51E–08	9.70E–10	2.32E–05	7.99E–06	3.41E–03	1.23E–04	3.59E–04

table continued on following page

Table 1. Analysis of Stars on the AAVSO Eclipsing Binary Program, Group 1, cont.

Name	*Type*	*Period (d)*	*Max*	*Min*	*Range*	*Slope*	*Error*	*Intercept*	*Error*	α	ε	ε/*Period*
V TRI	EB/SD	5.85E–01	10.7	11.8	1.1 (V)	4.74E–09	6.03E–10	2.26E–05	2.53E–06	3.36E–03	6.89E–05	1.18E–04
X TRI	EA/SD	9.72E–01	8.6	11.3	2.7 (V)	2.49E–08	1.10E–09	5.76E–06	3.00E–06	1.70E–03	1.58E–04	1.62E–04
RV TRI	EA/SD	7.54E–01	11.5	13.3	1.8 (p)	7.73E–08	2.21E–09	–5.21E–05	7.41E–06	2.47E–03*	2.78E–04	3.69E–04
W UMA	EW/KW	3.34E–01	7.8	8.5	0.7 (V)	–5.28E–10	6.07E–10	7.94E–05	4.74E–06	6.30E–03	N/A	N/A
VV UMA	EA/SD	6.87E–01	10.1	10.9	0.8 (V)	–2.08E–09	1.82E–09	7.68E–05	6.45E–06	6.20E–03	N/A	N/A
XZ UMA	EA/SD	1.22E+00	10.1	11.7	1.6 (p)	1.42E–07	5.97E–09	–8.44E–05	1.26E–05	2.83E–03*	3.77E–04	3.08E–04
RU UMI	EB/DW	5.25E–01	10	10.7	0.7 (V)	6.78E–09	1.21E–09	4.50E–05	5.15E–06	4.74E–03	8.24E–05	1.57E–04
BU VUL	EA/SD	5.69E–01	10.6	11.4	0.8 (p)	9.62E–10	2.61E–10	2.40E–05	1.23E–06	3.47E–03	3.10E–05	5.45E–05

Note: Any alpha (α) value with an asterisk (*) is calculated from the $< u(x) >^2$ *value with the smallest x.*

Table 2. Analysis of Stars on the AAVSO Eclipsing Binary Program, Group 2.

Name	*Type*	*Period (d)*	*Max*	*Min*	*Range*	*Slope*	*Error*	*Intercept*	*Error*	α	ε	ε/*Period*
RT AND	EA/RS	6.29E–01	9	9.8	0.8 (V)	1.40E–09	5.77E–10	4.16E–05	2.49E–06	4.56E–03	3.74E–05	5.94E–05
BX AND	EB	6.10E–01	8.87	9.53	0.66 (V)	8.02E–09	3.39E–09	9.35E–05	1.25E–05	6.84E–03	8.96E–05	1.47E–04
XZ AQL	EA/SD	2.14E+00	10.1	11.4	1.3 (p)	2.13E–06	7.68E–08	–7.71E–04	1.06E–04	6.36E–03*	1.46E–03	6.83E–04
V343 AQL	EA/SD	1.84E+00	10.6	12.3	1.7 (p)	2.99E–08	9.44E–09	6.31E–05	1.51E–05	5.62E–03	1.73E–04	9.37E–05
EP AUR	EB	5.91E–01	11.2	11.8	0.66 (V)	–1.18E–08	6.33E–09	3.16E–04	3.13E–05	1.26E–02	N/A	N/A
AL CAM	EA/SD	1.33E+00	10.5	11.3	0.8 (p)	9.07E–08	5.36E–09	–2.98E–05	1.14E–05	4.95E–03*	3.01E–04	2.27E–04
R CMA	EA/SD	1.14E+00	5.7	6.34	0.64 (V)	4.05E–07	2.32E–08	–8.22E–05	5.72E–05	5.66E–03*	6.36E–04	5.60E–04
XZ CMI	EA	5.79E–01	9.7	10.4	0.72 (V)	1.22E–08	3.86E–09	1.08E–04	1.91E–05	7.34E–03	1.10E–04	1.91E–04
RZ CAS	EA/SD	1.20E+00	6.18	7.72	1.54 (V)	1.59E–09	1.11E–08	3.32E–05	4.77E–06	4.07E–03	3.98E–05	3.33E–05
MM CAS	EA/SD	1.16E+00	12	13.1	1.1 (p)	–5.08E–09	8.46E–09	1.81E–04	1.94E–05	9.52E–03	N/A	N/A
OR CAS	EA/SD	1.25E+00	11.4	12.4	1 (p)	2.99E–08	4.46E–09	5.54E–05	1.01E–05	5.27E–03	1.73E–04	1.39E–04
XX CEP	EA/SD	2.34E+00	9.2	10.3	1.12 (V)	–1.26E–08	8.02E–09	1.12E–04	9.69E–06	7.49E–03	N/A	N/A
DV CEP	E	1.16E+00	11.4	12.2	0.8 (p)	1.05E–08	1.82E–09	2.79E–05	3.76E–06	3.74E–03	1.02E–04	8.80E–05
RZ COM	EW/KW	3.39E–01	10.4	11.1	0.71 (V)	2.18E–08	2.29E–09	2.99E–05	1.87E–05	3.86E–03	1.48E–04	4.37E–04
U CRB	EA/SD	3.45E+00	7.66	8.79	1.13 (V)	1.65E–06	9.95E–08	–2.29E–04	9.42E–05	9.55E–03*	1.28E–03	3.72E–04
SW CYG	EA/SD	4.57E+00	9.24	11.8	2.59 (V)	8.13E–06	4.99E–07	–1.37E–03	3.08E–04	3.96E–03*	2.85E–03	6.24E–04
WW CYG	EA/SD	3.32E+00	10	13.3	3.24 (V)	1.21E–07	1.39E–08	4.91E–06	9.84E–06	1.57E–03	3.48E–04	1.05E–04
DK CYG	EW/D	4.71E–01	10.4	10.9	0.56 (V)	1.99E–07	9.35E–09	–2.54E–04	5.81E–05	2.83E–03*	4.46E–04	9.47E–04
KR CYG	EB	8.45E–01	9.19	10	0.81 (V)	–1.11E–08	3.79E–09	5.63E–05	5.24E–06	5.31E–03	N/A	N/A
V477 CYG	EA/DM	2.35E+00	8.5	9.34	0.84 (V)	1.87E–08	6.51E–09	6.05E–05	8.45E–06	5.50E–03	1.37E–04	5.82E–05

table continued on following pages

Table 2. Analysis of Stars on the AAVSO Eclipsing Binary Program, Group 2, cont.

Name	*Type*	*Period (d)*	*Max*	*Min*	*Range*	*Slope*	*Error*	*Intercept*	*Error*	α	ε	ε/*Period*
V704 CYG	EW	5.71E–01	13.6	14.6	1 (p)	5.50E–08	4.80E–09	1.44E–06	2.46E–05	8.49E–04	2.35E–04	4.11E–04
BH DRA	EA/SD	1.82E+00	8.38	9.27	0.89 (V)	5.50E–09	1.23E–08	1.66E–04	1.61E–05	9.11E–03	7.42E–05	4.08E–05
TU HER	EA/SD	2.27E+00	10.9	13.7	2.82 (V)	7.42E–07	4.57E–08	–3.09E–04	5.38E–05	1.59E–03*	8.61E–04	3.80E–04
CT HER	EA/SD	1.79E+00	10.6	11.7	1.1 (p)	3.48E–08	9.95E–09	8.22E–05	1.55E–05	6.41E–03	1.87E–04	1.04E–04
CM LAC	EA/DM	1.60E+00	8.18	9.15	0.97 (V)	4.54E–10	1.71E–09	3.62E–05	3.20E–06	4.25E–03	2.13E–05	1.33E–05
UV LEO	EA/DW	6.00E–01	8.9	9.56	0.66 (V)	1.64E–08	2.41E–09	2.28E–05	1.07E–05	3.38E–03	1.28E–04	2.13E–04
RY LYN	EA/SD	1.43E+00	11.4	13.3	1.9 (p)	1.40E–07	1.07E–08	–1.54E–05	2.10E–05	7.78E–03*	3.74E–04	2.61E–04
FL LYR	EA/DM	2.18E+00	9.27	9.89	0.62 (V)	2.39E–08	8.18E–09	6.41E–05	1.12E–05	5.66E–03	1.54E–04	7.09E–05
BETA LYR	EB	1.29E+01	3.25	4.36	1.11 (V)	1.60E–04	3.96E–05	4.76E–02	7.48E–03	1.54E–01	1.26E–02	9.77E–04
RW MON	EA/SD	1.91E+00	9.26	11.5	2.25 (V)	4.16E–08	5.52E–09	2.26E–05	8.18E–06	3.36E–03	2.04E–04	1.07E–04
U OPH	EA/DM	1.68E+00	5.84	6.56	0.72 (V)	4.76E–08	1.53E–08	1.49E–04	3.02E–05	8.64E–03	2.18E–04	1.30E–04
EQ ORI	EA/SD	1.75E+00	10.2	13.3	3.1 (p)	2.23E–07	1.28E–08	–2.66E–05	1.62E–05	2.47E–03*	4.72E–04	2.70E–04
FL ORI	EA/SD	1.55E+00	11.4	14.6	3.2 (p)	1.92E–08	1.16E–08	1.60E–04	2.34E–05	8.95E–03	1.39E–04	8.94E–05
TY PEG	EA/SD	3.09E+00	10.1	12	1.9 (V)	4.76E–06	3.16E–07	–1.35E–03	2.79E–04	3.77E–03*	2.18E–03	7.05E–04
BB PEG	EW/KW	3.62E–01	10.8	11.5	0.68 (p)	6.29E–09	2.08E–09	1.02E–04	1.63E–05	7.14E–03	7.93E–05	2.19E–04
BX PEG	EW/KW	2.80E–01	11	11.7	0.69 (V)	1.24E–08	1.14E–09	–1.08E–05	1.11E–05	7.07E–04*	1.11E–04	3.97E–04
DI PEG	EA/SD	7.12E–01	9.38	10.5	1.1 (V)	6.39E–09	1.28E–09	3.35E–05	4.75E–06	4.09E–03	8.00E–05	1.12E–04
GP PEG	EA	9.76E–01	10.2	11	0.8 (p)	–9.69E–09	2.10E–08	1.59E–04	2.46E–05	8.92E–03	N/A	N/A
RV PER	EA/SD	1.97E+00	10.3	12.7	2.4 (V)	4.33E–09	3.94E–09	3.06E–05	5.05E–06	3.91E–03	6.58E–05	3.33E–05
ST PER	EA/SD	2.65E+00	9.52	11.4	1.88 (V)	1.42E–06	9.19E–08	–3.49E–04	8.77E–05	3.77E–03*	1.19E–03	4.50E–04
BETA PER	EA/SD	2.87E+00	2.12	3.39	1.27 (V)	5.40E–07	3.80E–08	–7.06E–05	4.35E–05	4.95E–03*	7.35E–04	2.56E–04

table continued on following page

Table 2. Analysis of Stars on the AAVSO Eclipsing Binary Program, Group 2, cont.

Name	*Type*	*Period (d)*	*Max*	*Min*	*Range*	*Slope*	*Error*	*Intercept*	*Error*	α	ε	ε/*Period*
U SGE	EA/SD	3.38E+00	6.45	9.28	2.83 (V)	2.59E–08	7.75E–09	3.53E–05	6.39E–06	4.20E–03	1.61E–04	4.76E–05
V505 SGR	EA/SD	1.18E+00	6.46	7.51	1.05 (V)	1.73E–08	6.02E–09	7.84E–05	1.53E–05	6.26E–03	1.32E–04	1.11E–04
RZ TAU	EW/KW	4.16E–01	10.1	10.7	0.63 (V)	3.02E–08	3.12E–09	1.11E–04	2.23E–05	7.45E–03	1.74E–04	4.18E–04
CT TAU	EW/KW	6.67E–01	10.3	11.1	0.78 (V)	1.10E–08	6.63E–09	1.74E–04	2.74E–05	9.34E–03	1.05E–04	1.57E–04
HU TAU	EA/SD	2.06E+00	5.85	6.68	0.83 (V)	3.93E–08	1.22E–08	1.29E–04	1.79E–05	8.02E–03	1.98E–04	9.65E–05
TX UMA	EA/SD	3.06E+00	7.06	8.8	1.74 (V)	3.63E–06	2.52E–07	–6.11E–04	2.12E–04	2.36E–03*	1.91E–03	6.22E–04
UX UMA	EA/WD+NL	1.97E–01	12.6	14.2	1.58 (V)	3.76E–11	1.87E–11	3.17E–06	3.23E–07	1.26E–03	6.14E–06	3.12E–05
AZ VIR	EW/KW	3.50E–01	10.7	11.4	0.63 (V)	9.79E–09	1.01E–09	2.55E–05	8.14E–06	3.57E–03	9.89E–05	2.83E–04
BO VUL	EA/SD	1.95E+00	10.5	13.3	2.8 (p)	3.41E–07	1.20E–08	–1.13E–04	1.93E–05	1.72E–03*	5.84E–04	3.00E–04
BS VUL	EB/KW	4.76E–01	10.9	11.6	0.7 (V)	–1.27E–09	1.59E–09	9.84E–05	9.79E–06	7.02E–03	N/A	N/A

Note: Any alpha (α) value with an asterisk (*) is calculated from the $< u(x) >^2$ *value with the smallest x.*

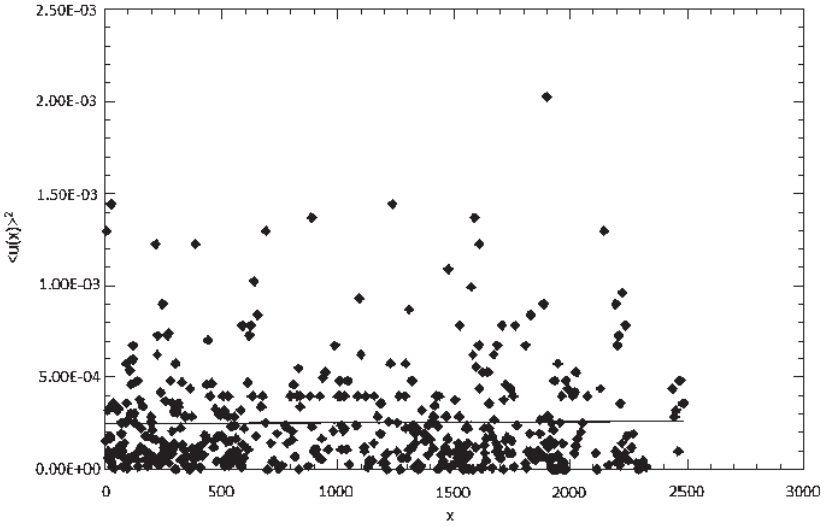

Figure 1. $<u(x)>^2$ diagram for ZZ Cep, a representative variable with no significant random cycle-to-cycle period fluctuations. The diagram is linear and its slope is close to zero.

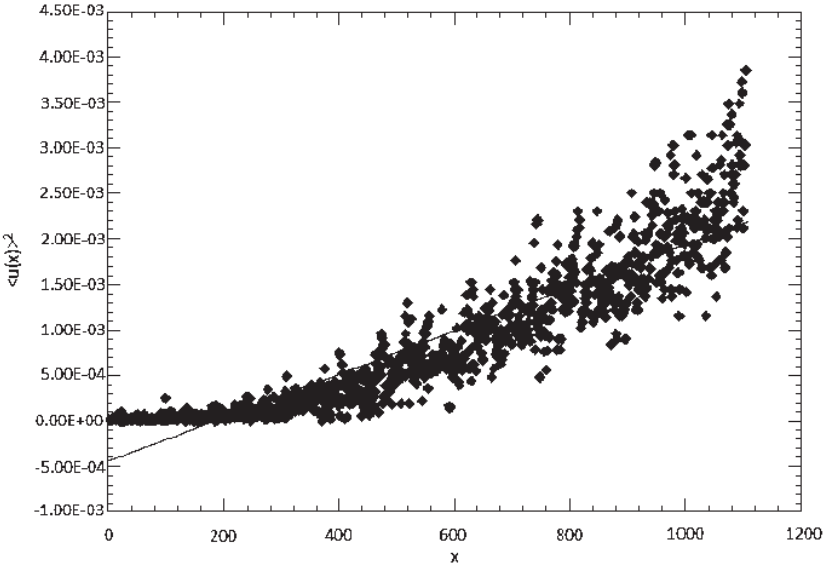

Figure 2. $<u(x)>^2$ diagram for U Cep, one of several variables whose diagram is not a straight line, but curves upward. A linear fit gives a positive slope and a negative intercept.

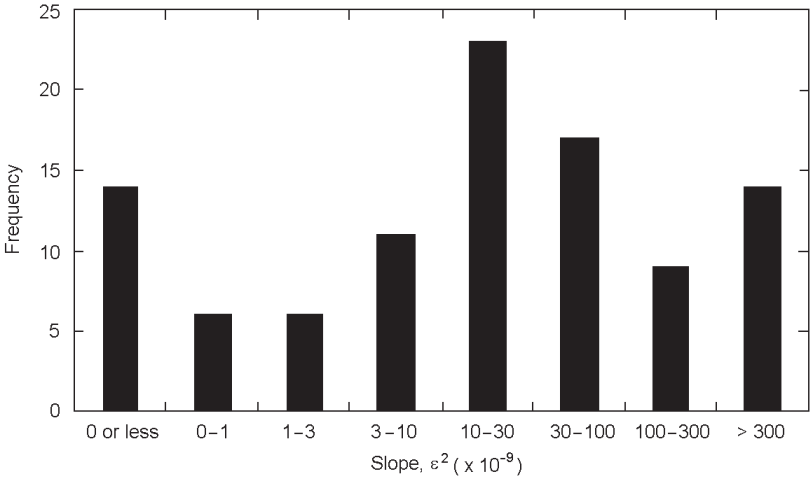

Figure 3. Histogram of slopes of the $<u(x)>^2$ diagrams of the 100 stars in Tables 1 and 2.

Recent Minima of 144 Eclipsing Binary Stars

Gerard Samolyk
P.O. Box 20677, Greenfield WI 53220; gsamolyk@wi.rr.com

Received October 4, 2010; accepted October 4, 2010

Abstract This paper continues the publication of times of minima for eclipsing binary stars from observations reported to the AAVSO Eclipsing Binary Section. Times of minima from observations made from March 2010 through September 2010, along with a few unpublished times of minima from older data, are presented.

1. Recent Observations

The accompanying list contains times of minima calculated from recent CCD observations made by participants in the AAVSO's eclipsing binary program. This list will be web-archived and made available through the AAVSO ftp site at ftp://ftp.aavso.org/public/datasets/gsam2j382.txt. This list, along with eclipsing binary data from earlier AAVSO publications, is also included in the Lichtenknecker database administrated by the Bundesdeutsche Arbeitsgemeinschaft für Veränderliche Sterne e.V. (BAV) at: http://www.bav-astro.de/LkDB/index.php?lang=en. These observations were reduced by the observers or the writer using the method of Kwee and Van Woerden (1956). The standard error is included when available.

The linear elements in the *General Catalogue of Variable Stars* (GCVS, Kholopov *et al.* 1985) were used to compute the O–C values for most stars. For a few exceptions where the GCVS elements are missing or are in significant error, light elements from another source are used: CW Cas (Samolyk 1992a), DV Cep (Frank and Lichtenknecker 1987), Z Dra (Danielkiewicz-Krośniak and Kurpińska-Winiarska 1996), DF Hya (Samolyk 1992b), DK Hya (Samolyk 1990), GU Ori (Samolyk 1985). O–C values listed in this paper can be directly compared with values published in recent numbers of the AAVSO *Observed Minima Timings of Eclipsing Binaries* series.

References

Danielkiewicz-Krośniak, E., and Kurpińska-Winiarska, M., eds. 1996, *Rocznik Astron.* (SAC 68), **68**, 1.

Frank, P., and Lichtenknecker, D. 1987, *BAV Mitt.*, No. 47.

Kholopov, P. N., *et al.* 1985, *General Catalogue of Variable Stars*, 4th ed., Moscow.

Kwee, K. K., and Van Woerden, H. 1956, *Bull. Astron. Inst. Netherlands*, **12**, 327.

Samolyk, G. 1985, *J. Amer. Assoc. Var. Star Obs.*, **14**, 12.

Samolyk, G. 1990, *J. Amer. Assoc. Var. Star Obs.*, **19**, 5.

Samolyk, G. 1992a, *J. Amer. Assoc. Var. Star Obs.*, **21**, 34.
Samolyk, G. 1992b, *J. Amer. Assoc. Var. Star Obs.*, **21**, 111.

Table 1. Recent times of minima of stars in the AAVSO eclipsing binary program.

Star	*HJD(min) 2400000+*	*Cycle*	*O–C (day)*	*Observer*	*Standard Error (day)*
UU And	55380.8209	9238	0.0785	G. Samolyk	0.0002
UU And	55435.8137	9275	0.0783	K. Menzies	0.0001
WZ And	55438.7177	20939	0.0532	K. Menzies	0.0001
WZ And	55454.7183	20962	0.0537	K. Menzies	0.0001
AB And	55405.7635	58140	–0.0254	K. Menzies	0.0001
AB And	55443.4323	58253.5	–0.0263	L. Corp	0.0002
AB And	55443.5987	58254	–0.0259	L. Corp	0.0002
AB And	55458.6991	58299.5	–0.0266	K. Menzies	0.0001
AB And	55459.3632	58301.5	–0.0263	L. Corp	0.0004
AD And	55407.7519	16635	–0.0668	K. Menzies	0.0003
CX Aqr	55442.7177	34154	0.0100	G. Samolyk	0.0001
OO Aql	55385.4336	33095	0.0467	L. Corp	0.0006
OO Aql	55397.5977	33119	0.0478	L. Corp	0.0001
V342 Aql	55438.6670	4754	–0.1670	G. Samolyk	0.0003
V346 Aql	55381.7051	12169	–0.0102	G. Samolyk	0.0001
RY Aur	55260.5973	6227	0.0245	G. Samolyk	0.0001
WW Aur	55261.6609	8838	0.0017	G. Samolyk	0.0001
AP Aur	55282.6051	22549.5	1.2839	G. Samolyk	0.0002
AP Aur	55301.6778	22583	1.2846	G. Samolyk	0.0003
AR Aur	55271.6155	4080	–0.1233	G. Samolyk	0.0003
CL Aur	55277.6120	17929	0.1389	G. Samolyk	0.0002
EP Aur	55277.6534	49015	0.0143	G. Samolyk	0.0002
SS Boo	55345.7302	4555	6.0904	G. Samolyk	0.0009
TU Boo	55259.8104	68438	–0.1336	G. Samolyk	0.0001
TU Boo	55279.7547	68499.5	–0.1330	G. Samolyk	0.0001
TU Boo	55342.3398	68692.5	–0.1352	Y. Ogmen	0.0001
TY Boo	55296.8132	65636	0.0818	G. Samolyk	0.0002
TY Boo	55309.6599	65676.5	0.0840	G. Samolyk	0.0002
TY Boo	55315.6860	65695.5	0.0843	R. Poklar	0.0003
TZ Boo	55261.8482	52594	0.0682	K. Menzies	0.0004
TZ Boo	55301.6695	52728	0.0698	G. Samolyk	0.0001
TZ Boo	55317.7164	52782	0.0699	R. Poklar	0.0002
TZ Boo	55322.6172	52798.5	0.0675	G. Samolyk	0.0005
VW Boo	55301.6839	70484	–0.1785	G. Samolyk	0.0003

Table continued on following pages

Table 1. Recent times of minima of stars in the AAVSO eclipsing binary program, cont.

Star	HJD(min) 2400000+	Cycle	O–C (day)	Observer	Standard Error (day)
ZZ Boo	55305.7841	3353.5	0.0514	G. Samolyk	0.0005
ZZ Boo	55345.7326	3361.5	0.0659	G. Samolyk	0.0007
AD Boo	55273.7333	13379	0.0290	K. Menzies	0.0001
AD Boo	55301.6622	13406	0.0290	G. Samolyk	0.0003
Y Cam	55275.7513	3725	0.3728	R. Sabo	0.0003
SV Cam	55259.6769	21355	0.0529	G. Samolyk	0.0002
EH Cnc	52299.6094	–480	–0.0061	S. Dvorak	0.0002
EH Cnc	52324.6922	–420	–0.0054	S. Dvorak	0.0002
EH Cnc	52383.6357	–279	–0.0047	S. Dvorak	0.0002
EH Cnc	52396.5938	–248	–0.0057	S. Dvorak	0.0001
EH Cnc	52624.8422	298	–0.0040	S. Dvorak	0.0002
BI CVn	50538.688	16070	–0.0129	S. Cook	
BI CVn	52408.7297	20938	–0.0621	S. Dvorak	0.0002
BI CVn	55336.3077	28559	–0.1674	Y. Ogmen	0.0002
R CMa	55262.6374	9660	0.0912	G. Samolyk	0.0002
UU CMa	55259.5743	4921	–0.1064	G. Samolyk	0.0002
AK CMi	55270.7122	21504	–0.0196	R. Poklar	0.0002
AK CMi	55282.5955	21525	–0.0202	G. Samolyk	0.0001
AM CMi	55273.6479	29463.5	0.2082	G. Samolyk	0.0006
RW Cap	55446.6863	3768	–0.5822	G. Samolyk	0.0003
RZ Cas	55298.6586	10122	0.0622	G. Samolyk	0.0001
CW Cas	55379.7944	43114.5	–0.0568	G. Samolyk	0.0002
DZ Cas	55437.7880	34404	–0.1786	G. Samolyk	0.0002
DZ Cas	55445.6368	34414	–0.1787	K. Menzies	0.0002
GT Cas	55436.8067	9397	0.1935	K. Menzies	0.0003
GT Cas	55439.7958	9398	0.1928	K. Menzies	0.0003
GT Cas	55448.7651	9401	0.1927	K. Menzies	0.0002
IR Cas	55436.6255	19205	0.0084	G. Samolyk	0.0001
IS Cas	55437.7450	14478	0.0655	K. Menzies	0.0001
IS Cas	55461.6850	14491	0.0658	K. Menzies	0.0001
OR Cas	55436.7186	9012	–0.0233	K. Menzies	0.0001
OX Cas	55422.8423	5685.5	0.0489	K. Menzies	0.0010
PV Cas	55440.7044	8691	–0.0336	K. Menzies	0.0002
U Cep	55336.6685	4330	0.1697	G. Samolyk	0.0001
SU Cep	55367.7122	32219	0.0052	G. Samolyk	0.0002
WZ Cep	55346.7168	65412.5	–0.0976	G. Samolyk	0.0002
DK Cep	55409.6919	22131	0.0344	K. Menzies	0.0001
DL Cep	55346.7256	13125	0.0545	G. Samolyk	0.0003

Table continued on following pages

Table 1. Recent times of minima of stars in the AAVSO eclipsing binary program, cont.

Star	*HJD(min) 2400000+*	*Cycle*	*O–C (day)*	*Observer*	*Standard Error (day)*
DV Cep	55345.6940	7386	–0.0049	G. Samolyk	0.0001
EG Cep	55444.7483	23595	0.0137	N. Simmons	0.0001
EG Cep	55445.8368	23597	0.0130	G. Samolyk	0.0001
GW Cep	55442.6137	53501.5	–0.0506	C. F. Rivero	0.0004
GW Cep	55442.6140	53501.5	–0.0503	C. F. Rivero	0.0003
GW Cep	55443.5698	53504.5	–0.0510	C. F. Rivero	0.0005
GW Cep	55443.5702	53504.5	–0.0506	C. F. Rivero	0.0002
RW Com	55280.6585	64287	–0.0137	K. Menzies	0.0001
RZ Com	55290.6751	60422	0.0434	R. Poklar	0.0001
RZ Com	55310.6469	60481	0.0433	K. Menzies	0.0001
SS Com	55263.7549	73307	0.7091	G. Samolyk	0.0002
CC Com	55279.6445	71350.5	–0.0149	G. Samolyk	0.0002
U CrB	55336.7986	11178	0.1203	G. Samolyk	0.0002
RW CrB	55304.6558	20034	–0.0004	G. Samolyk	0.0002
W Crv	55296.7558	40324	0.0184	G. Samolyk	0.0001
W Crv	55298.6960	40329	0.0182	R. Poklar	0.0001
W Crv	55304.7114	40344.5	0.0184	G. Samolyk	0.0001
W Crv	55345.6533	40450	0.0177	N. Simmons	0.0001
RV Crv	55303.6924	19102.5	–0.0748	G. Samolyk	0.0004
RV Crv	55346.6599	19160	–0.0743	G. Samolyk	0.0007
V Crt	55261.8404	19749	–0.0028	C. Hesseltine	0.0001
Y Cyg	55379.8023	15327.5	0.0921	G. Samolyk	0.0003
Y Cyg	55424.7483	15342.5	0.0931	N. Simmons	0.0003
WW Cyg	55337.7938	4509	0.0874	K. Menzies	0.0001
ZZ Cyg	55356.7573	16475	–0.0555	K. Menzies	0.0001
BR Cyg	55304.8539	10330	0.0008	G. Samolyk	0.0001
CG Cyg	55338.7760	25214	0.0647	K. Menzies	0.0001
CG Cyg	55381.6923	25282	0.0634	G. Samolyk	0.0001
CG Cyg	55436.6029	25369	0.0648	K. Menzies	0.0001
DK Cyg	55408.6297	36986	0.0852	K. Menzies	0.0004
KR Cyg	55379.6589	31087	0.0150	G. Samolyk	0.0001
V388 Cyg	55381.7181	15632	–0.0887	G. Samolyk	0.0001
V401 Cyg	55341.7523	19746	0.0647	K. Menzies	0.0002
V401 Cyg	55355.7380	19770	0.0651	K. Menzies	0.0002
V401 Cyg	55404.6871	19854	0.0655	K. Menzies	0.0001
V401 Cyg	55414.5942	19871	0.0663	K. Menzies	0.0004
V401 Cyg	55439.6528	19914	0.0679	K. Menzies	0.0002
V456 Cyg	55383.7987	11751	0.0462	K. Menzies	0.0001

Table continued on following pages

Table 1. Recent times of minima of stars in the AAVSO eclipsing binary program, cont.

Star	HJD(min) 2400000+	Cycle	O–C (day)	Observer	Standard Error (day)
V456 Cyg	55436.3798	11810	0.0469	Y. Ogmen	0.0000
V466 Cyg	55379.7512	19119	0.0063	K. Menzies	0.0001
V466 Cyg	55441.6758	19163.5	0.0062	K. Menzies	0.0001
V548 Cyg	55450.3757	6090	0.0109	L. Corp	0.0003
V704 Cyg	55336.7783	30484	0.0286	G. Samolyk	0.0005
V704 Cyg	55408.6878	30610	0.0294	K. Menzies	0.0003
V704 Cyg	55436.6521	30659	0.0292	G. Samolyk	0.0004
V1034 Cyg	55379.6742	12735	–0.0011	G. Samolyk	0.0002
W Del	55444.7593	2521	0.0317	G. Samolyk	0.0001
FZ Del	55445.6715	30798	–0.0392	G. Samolyk	0.0001
Z Dra	55268.6870	3996	–0.0271	R. Poklar	0.0001
RZ Dra	55298.6464	20188	0.0506	N. Simmons	0.0002
TW Dra	55436.6844	4026	0.0233	G. Samolyk	0.0001
AI Dra	55261.8149	9985	0.0241	G. Samolyk	0.0001
YY Eri	55259.5679	42544.5	0.1360	G. Samolyk	0.0002
SX Gem	55261.6592	26506	–0.0526	G. Samolyk	0.0001
AF Gem	55271.6380	22605	–0.0677	G. Samolyk	0.0001
SZ Her	55304.8199	16429	–0.0219	G. Samolyk	0.0001
TT Her	55329.7586	16812	0.0380	K. Menzies	0.0001
UX Her	55346.8012	10120	0.0819	G. Samolyk	0.0003
CC Her	55305.8036	9018	0.1973	G. Samolyk	0.0001
LT Her	55345.8105	13459	–0.1213	G. Samolyk	0.0004
V742 Her	55237.7376	24943	0.0367	L. Corp	0.0002
WY Hya	55260.5932	20516	0.0283	G. Samolyk	0.0001
WY Hya	55261.6676	20517.5	0.0287	R. Poklar	0.0002
AV Hya	55277.6485	27223	–0.0945	G. Samolyk	0.0001
DF Hya	55258.6878	37721.5	–0.0137	R. Poklar	0.0001
DF Hya	55263.6467	37736.5	–0.0138	G. Samolyk	0.0001
DF Hya	55279.6815	37785	–0.0134	G. Samolyk	0.0002
DF Hya	55303.6502	37857.5	–0.0136	G. Samolyk	0.0001
DI Hya	55257.6702	39146	–0.0237	G. Samolyk	0.0001
DK Hya	55259.6959	23789	0.0064	G. Samolyk	0.0002
DK Hya	55259.6959	23789	0.0064	R. Poklar	0.0001
DK Hya	55305.6247	23877	0.0061	G. Samolyk	0.0002
SW Lac	55380.8388	31509	–0.1037	G. Samolyk	0.0001
AW Lac	55436.7891	25211	0.1808	N. Simmons	0.0002
AW Lac	55451.6483	25224	0.1829	K. Menzies	0.0002
Y Leo	55259.6650	5826	–0.0163	G. Samolyk	0.0001

Table continued on following pages

Table 1. Recent times of minima of stars in the AAVSO eclipsing binary program, cont.

Star	*HJD(min) 2400000+*	*Cycle*	*O–C (day)*	*Observer*	*Standard Error (day)*
Y Leo	55345.6563	5877	–0.0162	N. Simmons	0.0001
UU Leo	55304.7352	5898	0.1674	C. Hesseltine	0.0003
UU Leo	55336.6516	5917	0.1687	G. Samolyk	0.0005
UV Leo	55273.7372	28051	0.0327	G. Samolyk	0.0002
VZ Leo	55305.6693	22150	–0.0646	G. Samolyk	0.0001
WZ Leo	55279.6004	17160	–2.4808	G. Samolyk	0.0006
XY Leo	55262.3982	35860.5	0.0507	L. Corp	0.0002
XY Leo	55292.3694	35966	0.0497	L. Corp	0.0004
XZ Leo	52397.6218	15115.5	–0.0961	S. Dvorak	0.0004
XZ Leo	53359.8133	17088	0.0379	S. Dvorak	0.0001
XZ Leo	55297.3567	21060	0.2975	L. Corp	0.0020
XZ Leo	55297.3587	21060	0.2995	L. Corp	0.0020
δ Lib	55337.5564	5318	–0.0132	G. Samolyk	0.0008
FL Lyr	55304.8135	7843	–0.0040	G. Samolyk	0.0002
FL Lyr	55437.6827	7904	–0.0022	G. Samolyk	0.0002
AT Mon	55279.5900	14131	0.0084	G. Samolyk	0.0002
BO Mon	55265.5933	5284	–0.0625	K. Menzies	0.0001
V396 Mon	55238.3894	51644.5	–0.0664	L. Corp	0.0002
V508 Oph	55321.8157	29697	–0.0192	K. Menzies	0.0001
V839 Oph	55303.7784	36321	0.2465	G. Samolyk	0.0001
V839 Oph	55379.8546	36507	0.2496	G. Samolyk	0.0003
V1010 Oph	55380.6832	24860	–0.1394	G. Samolyk	0.0005
FZ Ori	55257.6250	28084	–0.0570	G. Samolyk	0.0003
FZ Ori	55261.6251	28094	–0.0567	C. Hesseltine	0.0004
GU Ori	55262.6120	25904.5	–0.0470	G. Samolyk	0.0002
GU Ori	55263.5537	25906.5	–0.0466	K. Menzies	0.0002
TY Peg	55448.7146	4850	–0.3364	G. Samolyk	0.0004
AQ Peg	55438.4813	2562	0.5123	G. Samolyk	0.0003
BB Peg	55416.8077	32233.5	–0.0036	K. Menzies	0.0001
BB Peg	55437.7753	32291.5	–0.0032	G. Samolyk	0.0001
BB Peg	55451.6928	32330	–0.0035	N. Simmons	0.0001
GP Peg	55379.8630	14495	–0.0465	G. Samolyk	0.0002
RT Per	55436.7522	25972	0.0688	G. Samolyk	0.0001
RT Per	55441.8487	25978	0.0689	K. Menzies	0.0001
ST Per	55262.5949	4843	0.2974	G. Samolyk	0.0001
AE Phe	55182.6283	31596.5	–0.0985	G. Samolyk	0.0002
AE Phe	55192.5937	31624	–0.0984	G. Samolyk	0.0002
UZ Pup	55260.7222	13395	–0.0079	G. Samolyk	0.0002

Table continued on following pages

Table 1. Recent times of minima of stars in the AAVSO eclipsing binary program, cont.

Star	HJD(min) 2400000+	Cycle	O–C (day)	Observer	Standard Error (day)
UZ Pup	55282.5817	13422.5	–0.0068	G. Samolyk	0.0005
AV Pup	55271.6457	43307	0.1460	G. Samolyk	0.0001
U Sge	55449.7247	11335	–0.0068	G. Samolyk	0.0001
V1968 Sgr	55381.6596	31178	–0.0148	G. Samolyk	0.0004
AO Ser	55259.7737	24025	–0.0128	G. Samolyk	0.0002
AU Ser	55340.3160	27472	–0.1101	Y. Ogmen	0.0001
CC Ser	55263.8284	34459.5	0.9428	K. Menzies	0.0001
WY Tau	55461.8343	26069	0.0576	K. Menzies	0.0001
EQ Tau	55259.5991	44079	–0.0255	G. Samolyk	0.0001
W UMa	55260.6641	28459	–0.0637	G. Samolyk	0.0001
W UMa	55264.6672	28471	–0.0643	K. Menzies	0.0002
TY UMa	55260.6414	44361.5	0.2808	R. Poklar	0.0002
TY UMa	55262.5940	44367	0.2834	G. Samolyk	0.0002
UX UMa	55259.6969	90643	0.0017	G. Samolyk	0.0001
UX UMa	55279.7572	90745	0.0015	G. Samolyk	0.0001
UX UMa	55283.6908	90765	0.0017	K. Menzies	0.0001
UX UMa	55298.6378	90841	0.0017	G. Samolyk	0.0001
UX UMa	55309.6512	90897	0.0015	G. Samolyk	0.0001
UX UMa	55346.6254	91085	0.0015	G. Samolyk	0.0001
VV UMa	55257.8274	13737	–0.0482	G. Samolyk	0.0001
VV UMa	55262.6395	13744	–0.0477	K. Menzies	0.0001
VV UMa	55273.6360	13760	–0.0493	R. Poklar	0.0003
XZ UMa	55263.6061	7441	–0.1030	G. Samolyk	0.0001
XZ UMa	55280.7185	7455	–0.1031	R. Poklar	0.0001
ZZ UMa	55260.6661	8398	–0.0034	G. Samolyk	0.0002
RU UMi	55303.7201	26113	–0.0137	R. Poklar	0.0001
AH Vir	55262.7789	23184.5	0.2233	K. Menzies	0.0001
AH Vir	55277.6530	23221	0.2229	G. Samolyk	0.0002
AK Vir	55309.6695	10668	–0.0430	G. Samolyk	0.0001
AW Vir	55296.7211	29023	0.0226	R. Poklar	0.0001
AW Vir	55304.6863	29045.5	0.0229	G. Samolyk	0.0001
AZ Vir	55257.7642	32263	–0.0212	G. Samolyk	0.0005
AZ Vir	55271.7507	32303	–0.0213	R. Sabo	0.0002
AZ Vir	55322.6263	32448.5	–0.0220	G. Samolyk	0.0002
BH Vir	55309.6805	14787	–0.0090	G. Samolyk	0.0003
BH Vir	55336.6380	14820	–0.0083	G. Samolyk	0.0003
NY Vir	55240.6163	49668	–0.0071	L. Corp	0.0001
Z Vul	55381.7097	5065	–0.0087	G. Samolyk	0.0001

Table continued on following page

Table 1. Recent times of minima of stars in the AAVSO eclipsing binary program, cont.

Star	*HJD(min) 2400000+*	*Cycle*	*O–C (day)*	*Observer*	*Standard Error (day)*
RS Vul	50266.6900	3899	0.0230	S. Cook	
RS Vul	55429.4220	5052	0.0090	L. Corp	0.0005
AW Vul	55379.8029	11277	–0.0147	G. Samolyk	0.0001
BS Vul	55380.7456	25441	–0.0226	G. Samolyk	0.0004
BU Vul	55437.6562	38496	0.0187	G. Samolyk	0.0001
BU Vul	55439.3613	38499	0.0168	Y. Ogmen	0.0001
CD Vul	55380.6897	13283	–0.0001	G. Samolyk	0.0001

Times of Minima for Several Eclipsing Binaries and New Ephemerides for V569 Lyrae, V571 Lyrae, and V572 Lyrae

A. Marchini
University of Siena Astronomical Observatory, Siena, Italy; and Sezione Stelle Variabili UAI-GRAV; stellevariabili@uai.it

M. Banfi
Nova Milanese Astronomical Observatory, via Cesare Battisti 26, Nova Milanese, Milano 20054, Italy; and Sezione Stelle Variabili UAI-GRAV

M. Cena
Torgnon Astronomical Observatory, Valle d'Aosta, Italy; and Sezione Stelle Variabili UAI-GRAV

G, Corfini
Corfini Astronomical Observatory, Lucca, Italy; and Sezione Stelle Variabili UAI-GRAV

S. Mandelli
Seveso Astronomical Observatory, Seveso, Italy; and Sezione Stelle Variabili UAI-GRAV

G. Marino
Skylive and Gruppo Astrofili Catanesi, Catania, Italy; and Sezione Stelle Variabili UAI-GRAV

R. Papini
San Casciano Astronomical Observatory, San Casciano, Italy; and Sezione Stelle Variabili UAI-GRAV

D. Premoli
Seveso Astronomical Observatory, Seveso, Italy; and Sezione Stelle Variabili UAI-GRAV

S. Santini
Santini Astronomical Observatory, Prato, Italy; and Sezione Stelle Variabili UAI-GRAV

S. Valentini
Marana Astronomical Observatory, Marana di Crespadoro, Italy; and Sezione Stelle Variabili UAI-GRAV

M. Vincenzi
Poggio Ameno Astronomical Observatory, Roma, Italy; and Sezione Stelle Variabili UAI-GRAV

Received December 20, 2010; revised February 22, 2011; accepted February 23, 2011

Abstract We present several CCD minima observations of eclipsing binaries. New ephemerides are given for V569 Lyrae, V571 Lyrae, and V572 Lyrae.

1. Introduction

The accompanying table (Table 2) contains times of minima for fourteen eclipsing binary stars calculated from CCD observations made by participants in the Sezione Stelle Variabili-Unione Astrofili Italiani-GRAV (SSV-UAI-GRAV) Eclipsing Binaries Program. The whole set of data was acquired between July 2005 and July 2010. All the observatories are located in Italy; one is managed by the Physics Department of the University of Siena, while the others are privately operated. The observations were reduced following standard procedures (see next section) and the light curves were analyzed using the Kwee-van Woerden algorithm (Kwee and van Woerden 1956) to determine the times of minimum. This algorithm also provides an error estimate. All the times of minima listed in this paper are heliocentric.

2. Instruments and data reduction

Table 1 shows, for each observer contributing to this study, the instrument and detector used. Frame calibration (dark subtraction and flat field correction) and photometric analysis (differential photometry on each image) were mainly performed using MAXIM-DL and AIP4WIN software packages; in a few cases IRIS and ASTROART were used.

3. Minimum determination

The times of minima, expressed as heliocentric Julian days (Table 2), were computed adopting the KW method (Kwee and van Woerden 1956) mainly using AVE (Barberá 1996) software; PERANSO (Vanmunster 2007) and KWEE, a DOS program available from the AAVSO (2000), were also used on some occasions.

The types of minimum quoted in Table 2 for V569 Lyr and V571 Lyr were deduced according to our updated elements (see below). For the other stars, the type of minimum was deduced by adopting the ephemerides provided by Kreiner (2004).

4. Individual cases: V569 Lyr, V571 Lyr, and V572 Lyr

4.1. V569 Lyr

For V569 Lyr, which is not included in Kreiner's database, only three times of minimum were found in the literature, reported by Diethelm (2001) and Nelson (2002). Diethelm (2001) did not specify the types of his two ROTSE1 minima, while Nelson (2002) assumed his minimum to be primary. These three times of

minimum are consistent with a period of 0.62 day or 1.24 days. Our minima, however, lead us to discard the 0.62-day period.

In order to derive the ephemeris of this star, the linear best fit of the O–C vs. the epoch for the available times of minimum was computed, leaving the initial epoch and period free to vary. Assuming that the primary is the deeper minimum, we obtain the following new ephemeris:

$$T_{min}\,(\mathrm{HJD}) = 2451274.5520\ (\pm\ 0.0045) + 1.2397626\mathrm{d}\ (\pm\ 0.0000018)\ \mathrm{E} \qquad (1)$$

With this ephemeris, the minimum given by Nelson (2002) has to be considered as secondary. Figure 1 shows the O–C diagram obtained by adopting our ephemeris.

Note that O–C of our minima and that of Nelson minima are nearly zero (within the errors), as can be seen in Figure 1. For the ROTSE1 minimum times, the O–C are instead much larger than their errors. At this stage, the data available do not allow us to establish whether the large O–C residuals are due to period variations or whether they are the result of the data quality.

4.2. V571 Lyr

V571 Lyr is not included in Kreiner's database. To study the behavior of the O–C, our data were analyzed together with the only two times of minimum present in the literature (Diethelm 2001).

Our minima are consistent with the period of $\simeq 1.25$ days given by Diethelm (2001), and they turn out to be primary, in accordance with the types of Diethelm's minima. This period is about double that originally reported in the ROTSE1 catalog (Akerlof *et al.* 2000). However, using $p = 0.62$d, it is not possible to justify the secondary type given by Diethelm to one of his two minima.

The linear best-fit of the O–C allows us to greatly improve Diethelm's ephemeris, obtaining:

$$T_{min}\,(\mathrm{HJD}) = 2451303.2009\ (\pm\ 0.0037) + 1.2525883\mathrm{d}\ (\pm\ 0.0000022)\ \mathrm{E} \qquad (2)$$

The O–C diagram obtained with the new ephemeris is shown in Figure 2. Note that the errors given by the KW method are internal formal errors, which are typically underestimated with respect to actual uncertainties (Nelson 2009). This explains why the data scatter is larger than three times the 1-σ error bar, at least for the last points.

4.3. V572 Lyr

Figure 3 shows the O–C diagram for V572 Lyr computed using Kreiner's updated elements, including the two minima retrieved from the literature. The linear fit (dashed line in Figure 3) of our data and the previously published data leads to the following updated ephemeris:

$$T_{min}\,(HJD) = 2452500.8459 + 0.9933045\ E \pm 0.0011 \pm 0.0000007 \quad (3)$$

which is in agreement with the ephemeris reported in Kreiner's database within the errors.

References

AAVSO 2000, KWEE software, AAVSO, Cambridge, MA.
Akerlof, C., *et al.* 2000, *Astron. J.*, **119**, 1901.
Barberá, R. 1996, AVE home page (www.astrogea.org/soft/ave/introave.htm).
Diethelm, R. 2001, *Inf. Bull. Var. Stars*, No. 5060.
Kreiner, J. M. 2004, *Acta Astron.*, **54**, 207 (www.as.up.krakow.pl/ephem).
Kwee, K. K., and van Woerden, H. 1956, *Bull. Astron. Inst. Netherlands*, **12**, 327.
Nelson, R. H. 2002, *Inf. Bull. Var. Stars*, No. 5224.
Nelson, R. H. 2009, private communication.
Vanmunster, T. 2007, PERANSO period analysis software (www.peranso.com).

Table 1. Instruments and detectors.

Observer	*Instrument*	*Detector*
Banfi	Meade LX200 20cm F = 126cm	SBIG ST7E
Cena	Apochromatic William Optics 8cm F = 54cm	FLI Kaf 0402 Me
Corfini	Newton 11cm F = 90cm	CCD UAI-Sony ICX429ALL based
Mandelli	Meade LX200 20–25cm F = 200–250cm	SBIG ST8–ST9
Marchini	Meade LX200 25cm F = 160cm	Starlight Xpress SX-L8
Marino	Apochromatic Takahashi 9cm F = 51cm	SBIG ST8
Papini	Meade LX200 20–25cm F = 200–250cm	SBIG ST8-ST9
Premoli	Meade LX200 20–25cm F = 200–250cm	SBIG ST8-ST9
Santini	Celestron Celestar 20cm F = 200cm	Hisis22
Valentini	Celestron 23cm F = 235cm	FLI-CM9
Vincenzi	Meade LX200 20–25cm F = 200–250cm	SBIG ST8-ST9

Table 2. Times of minima of selected eclipsing binary stars.

Star name	*Time of min. HJD 2400000+*	*Error*	*Type*	*Filter*	*Observer*
TW And	53693.351	0.002	I	V	PRI
OO Aql	53962.3642	0.0004	I	—	MST
	54034.327	0.002	I	V	VST
	54300.392	0.003	I	—	MST
	54656.4111	0.0002	II	V	MST
	54689.3531	0.0002	II	V	MST
	55028.3984	0.0002	II	—	MST
	55031.4389	0.0001	II	V	PDA
GU Cas	53579.459	0.0011	I	V	BMA
	53644.420	0.001	I	V	PRI
	53644.422	0.0031	I	V	BMA
	53706.289	0.002	I	V	BMA
	53706.290	0.003	I	—	MST
	53712.482	0.002	I	V	BMA
	53944.479	0.002	I	V	BMA
	53947.569	0.003	I	—	MST
	53975.4083	0.0004	I	V	PRI
	54278.553	0.004	I	—	BMA
	54306.3941	0.0006	I	—	VST
	54309.4852	0.0003	I	V	BMA
	54405.383	0.001	I	V	VST
	54340.419	0.002	I	V	VST
DO Cyg	53933.430	0.0011	I	—	SSI
YY Del	55118.4198	0.0002	I	—	CGI
IK Her	53983.349	0.004	I	V	VST
V400 Lyr	55021.4022	0.0008	I	—	CGI
	55021.5293	0.0008	II	—	CGI
V569 Lyr	54288.4147	0.0009	I	V	BMA
	55372.588	0.001	II	g	MAR
	55374.448	0.001	I	g	MAR
	55379.4064	0.0004	I	V	MXI
	55382.5059	0.0002	II	V	MXI
V571 Lyr	53932.389	0.002	I	V	BMA
	53937.3933	0.0002	I	—	MST

Table continued on next page

Table 2. Times of minima of selected eclipsing binary stars, cont.

Star name	*Time of min. HJD 2400000+*	*Error*	*Type*	*Filter*	*Observer*
	54299.3881	0.0006	I	—	SSI
V572 Lyr	53894.449	0.004	I	V	BMA
	53897.431	0.001	I	V	BMA
	53899.4171	0.0004	I	—	MST
	53900.4056	0.0007	I	—	SSI
	53901.3978	0.002	I	V	PRI
	53902.4000	0.0004	I	V	PRI
	53955.5439	0.0004	II	—	MXI
	53969.4439	0.0004	II	—	MST
	53970.442	0.002	II	V	PRI
	53971.4324	0.0006	II	—	MST
	53971.4339	0.0003	II	V	MXI
	53971.4339	0.0005	II	V	PRI
	53974.4148	0.0003	II	V	MXI
	53979.3810	0.0007	II	V	PRI
	53980.3745	0.0002	II	V	MXI
	53980.375	0.001	II	V	PRI
	53982.3599	0.0007	II	V	PRI
	53983.3553	0.0002	II	V	PRI
	53984.3481	0.0004	II	V	PRI
	54062.3204	0.0006	I	V	MXI
	54062.3208	0.0006	I	V	VST
	54069.2764	0.0006	I	V	MXI
	54275.3850	0.0007	II	—	MST
	54277.3716	0.0006	II	—	MST
	54338.4596	0.0002	I	V	CEM
	54346.4052	0.0006	I	V	MST
	54354.3518	0.0002	I	V	MXI
	54355.3452	0.0007	I	V	MXI
	54359.3130	0.0004	I	—	MST
	54646.3857	0.0004	I	V	MST
	54648.3733	0.0004	I	V	MST
	54719.3923	0.0003	II	R	MST
	54720.3843	0.0004	II	B	MST
V576 Lyr	53913.4250	0.0003	I	—	MST
	54294.399	0.003	I	—	MST

Table continued on next page

Table 2. Times of minima of selected eclipsing binary stars, cont.

Star name	*Time of min. HJD 2400000+*	*Error*	*Type*	*Filter*	*Observer*
FZ Ori	54093.461	0.002	II	—	MST
	54094.4599	0.0004	I	—	MST
	54116.4557	0.0007	I	V	VST
	54128.459	0.001	I	R	VST
	54135.460	0.002	II	R	VST
	54527.4442	0.0005	II	V	MST
BO Peg	55070.3930	0.0002	I	—	VMA
	55077.3651	0.0001	I	—	VMA
GQ Tau	54438.3654	0.0001	I	V	VST

Observers: BMA = M. Banfi; CEM = M. Cena; CGI = G. Corfini; MAR = G. Marino; MST = S. Mandelli; MXI = A. Marchini; PRI = R. Papini; PDA = D. Premoli; SSI = S. Santini; VST = S. Valentini; VMA = M. Vincenzi.

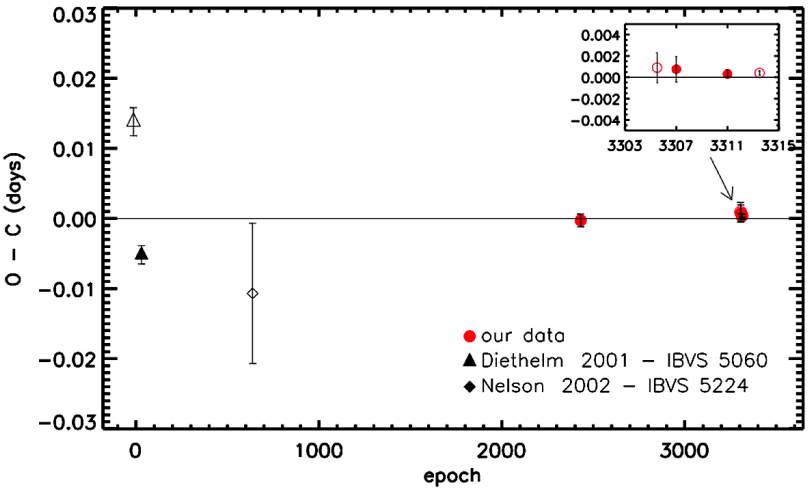

Figure 1. O–C diagram for V569 Lyr. Open symbols for secondary minima.

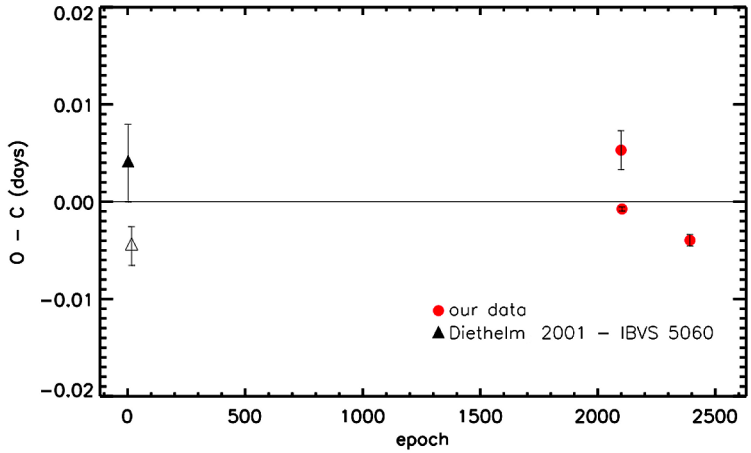

Figure 2. O–C diagram for V571 Lyr. Open symbols for secondary minima.

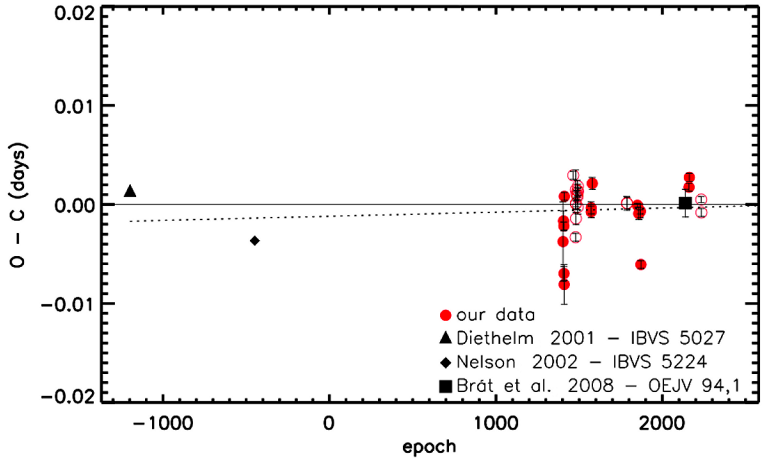

Figure 3. O–C diagram for V572 Lyr. Open symbols for secondary minima.

Searching for Orbital Periods of Supergiant Fast X-ray Transients

Maurizio Falanga
International Space Science Institute (ISSI), Hallerstrasse 6, CH-3012 Bern, Switzerland; mfalanga@issibern.ch

Enrico Bozzo
Roland Walter
ISDC, Geneva Observatory, University of Geneva, Chemin d'Ecogia 16, CH-1290 Versoix, Switzerland

Gordon E. Sarty
University of Saskatchewan, Departments of Psychology and Physics and Engineering Physics, 9 Campus Drive, Saskatoon, Saskatchewan S7N 5A5, Canada; gordon.sarty@usask.ca

Luigi Stella
INAF-Obsservatorio Astronomico di Roma, via Frascati 33, 00040 Monteporzio Catone (Rome), Italy

Received September 2, 2010; revised October 30, 2010; accepted November 16, 2010

Abstract Building on the currently active program of observing High Mass X-ray Binaries (HMXBs), we describe here a challenging extension of the project for experienced AAVSO observers who want to push their observing to the limit. A new subclass of HMXBs, the Supergiant Fast X-ray Transients (SFXTs), have been recently discovered in *INTEGRAL* data and are still poorly understood. In these systems, a neutron star is accreting matter from the strong wind of its supergiant companion (typically of spectral type O–B), resulting in a conspicuous emission of x-ray radiation. At odds with the other previously known HMXBs, the SFXT sources display an extreme variability in x-ray output. The origin of this variability is presently unknown, and has led in the past three years to the suggestion that the SFXT sources might host neutron stars with ultra-strong magnetic fields or supergiant stars with peculiar ultra-dense clumpy winds. Our new program aims at determining the orbital parameters of all the known systems in this class (fifteen objects) in order to distinguish between the different theoretical models proposed to interpret the behavior of the SFXTs.

1. Description of the proposed program and scientific rationale

One of the most important results in high-energy astronomy was the discovery of x-ray binary systems; these systems comprise a compact object

(a white dwarf, a neutron star, or a black hole) and a companion star, typically a main sequence star. In these systems, the compact object (if it is not a white dwarf) is formed during the final stages of the evolution of the binary through a supernova explosion (although a neutron star might also be formed by the accretion, induced collapse of a white dwarf). We consider in the following only the case in which the compact object is a neutron star. The mechanism that makes these binary systems very bright in x-rays is the accretion of matter from the companion star onto the compact object. Due to evolutionary processes, the companion star in these systems tends to lose a conspicuous fraction of its mass through the emission of a strong stellar wind and/or through so called Roche-lobe overflow. The strong gravitational field of the neutron star channels the inflowing matter toward its surface, where the gravitational potential energy is finally converted into electromagnetic radiation. Due to the compactness of the star and the relatively high velocity of the infalling matter (~1000 km/s), most of the radiation is emitted in the x-ray domain (0.1–100 keV). The accretion of matter onto a neutron star is thus a very efficient mechanism for converting gravitational energy into radiation, and it allows astronomers to study the nearby environment of an otherwise invisible compact object.

The study of x-ray emission from neutron star binary systems has proven to be very useful in past years for gaining information into the physics of accretion, the nuclear physics of neutron stars, and electromagnetic phenomena in the presence of a very strong magnetic field (the oldest neutron stars might have magnetic fields lower than 10^8 G, but for young objects the magnetic field can be $> 10^{12}$ G and can reach 10^{15} G in the most extreme cases).

Among the large variety of binary systems with neutron stars, we propose to concentrate on the so-called supergiant high mass x-ray binaries (SgHMXBs). These systems are relatively young ($< 10^7$ years), are mostly distributed near the Galactic plane, and are characterized by circular orbits with relatively short orbital periods (from a few days up to ~30 days). Their companion stars are supergiants of spectral type O or B and they possess strong stellar winds, which are accelerated by the absorption in the wind itself of UV radiation from the star (line-trapping mechanism). Part of the stellar wind is captured and accreted onto the compact object which gives rise to a strong x-ray emission (x-ray luminosities can be up to few 10^{37} erg/s). In a few peculiar systems with very short orbital periods, accretion can also take place through a transient accretion disk that is formed around the neutron star during periods of intense mass loss rate from the supergiant companion. Due to the irregular and intense mass loss rate that characterize the supergiant stars, the majority of the SgHMXBs are persistent bright emitters in x-rays (10^{35}–10^{36} erg/s) and display a typical x-ray variability of a factor 10–50 along the neutron star orbit. Because of the large size of the companion stars, x-ray eclipses are commonly observed in many of the SgHMXBs, thus giving direct evidence of the binary nature of the system. In a large fraction of SgHMXBs, periodic x-ray pulsations are also observed;

these pulsations are due to the beamed radiation that is produced close to the magnetic poles of the accreting NS. The pulsation periods are distributed over a wide range from milliseconds up to few thousand seconds, and are observed to increase and/or decrease over time due to the interaction of the neutron star with the inflowing matter.

Recently, a new subclass of SgHMXBs, collectively termed *Supergiant Fast X-ray Transients* (SFXTs), have been discovered thanks to the x-ray observatory *INTEGRAL*. These sources are composed of an accreting neutron star and a supergiant companion, similar to the classical SgHMXBs (see Figure 1). However, at odds with the classical SgHMXBs, they display a much more pronounced variability in x-rays. SFXTs undergo sporadic outbursts which reach $\sim 10^{37}$ erg/s^{-1} and last only a few hours; they then return to a quiescent state in which the x-ray luminosity decreases by up to a factor of $\sim 10^5$. Optical studies have already provided some detail about the supergiant stars in these systems, and in a few cases x-ray monitoring has been able to determine a rough orbital period (3–50 days) from the recurrence of the outbursts and from the x-ray eclipses (so far only in two sources). In five systems x-ray pulsations have also been discovered which provide the spin period of the neutron stars. All of these measurements have not revealed any peculiarity with respect to the classical SgHMXBs. Given the close similarity between SgHMXBs and SFXTs, the extreme x-ray variability of the latter sources remains, so far, unexplained.

In the past three years, several different models have been proposed in order to interpret the behavior of the SFXT sources. One of these models suggests that the accretion onto the neutron stars takes place from an extremely clumpy wind environment (see, for example, Walter and Zurita Heras 2007). According to this interpretation, the wind of the supergiant star in the SFXT is characterized by the presence of very dense "clumps" of material, which produce short and bright x-ray flares when they are accreted onto the neutron star. In this model, the orbital period of the system fixes the separation of the two stars and thus the probability of having an encounter between the neutron star and the clumps. Eccentric orbits were introduced to explain why the majority of the bursts are observed close to periastron in many SFXTs. Indeed, in an eccentric orbit one should expect that the probability for the neutron star to intercept one of the clumps along its orbit is larger close to the companion at periastron. Other models predict that the magnetic field of neutron stars in SFXTs are extremely high ($\geq 10^{14}$ G), and this field regulates the duration and peak luminosity of the outbursts (Bozzo *et al.* 2008). In this model, the orbital period of the system plays a key role since it fixes the average value of the mass inflow rate that is interacting with the neutron star magnetic field along the orbit, causing the onset of the sporadic outbursts. A third model suggests that neutron stars in SFXTs might have transient accretion disks around them whose formation and extension is also dependent on the orbital period of the system (Ducci *et al.* 2010).

In all the suggested models, the orbital parameters of the SFXT sources play

a fundamental role. Determining the orbital periods of the SFXTs, along with a measurement of their orbital eccentricity, is crucial for distinguishing among the different models to finally unveil the mechanism behind the peculiar x-ray variability of these sources.

2. Scientific objectives and the role of the AAVSO

Due to their unique behavior in x-rays, the SFXTs have gained much interest in the astronomical community over the past five years. This interest is also testified to by the high number of publications dedicated to the SFXTs during this period. However, despite the large amount of x-ray observing time that has been devoted in the past few years to investigate the SFXT sources, the origin of their extreme variability is still a matter of debate. The time is now propitious for beginning an in-depth investigation of these sources in the optical and infrared domain.

Up to now, both deep pointed and long-term monitoring programs using all the available x-ray observatories have been done for a large sample of the SFXT sources, and a systematic long-term optical monitoring of these sources is now required to bring our knowledge in this field a further step forward.

With our proposed program, we aim at investigating, in the optical and infrared domain (*I*, *R*, and *V* bands), the whole sample of the presently confirmed members in the SFXT class (fifteen objects). Useful details on all these sources are provided in Tables 1, 2, and 3. Our immediate objectives are:

- *Identify and measure the magnitudes of the SFXT counterparts in the optical and infrared domain.* Most of the SFXT spectral types have been determined in these energy bands (see Table 3), but some values are still missing (see the cases of, for example, IGR J17354-3255 and IGR J17407-2808). Filling in the missing magnitude values in Table 1 will be useful for improving our knowledge of the nature of the supergiant stars in the SFXT systems which, in turn, will give us further insight into the nature of these objects.

- *Determining, through optical and infrared monitoring, the orbital periods of all the selected candidates.* We are particularly interested in discovering the orbital periods of those sources for which the period is presently unknown. However, providing a confirmation and an improved estimate of the orbital period of those systems for which the period is already known will be useful as well. Indeed, the known orbital periods are still affected by rather large errors and thus do not allow us to predict, with the required accuracy, the time of periastron passage that would allow us to perform follow-up observations at longer wavelength infrared bands (especially the *K* band) and at x-ray wavelengths during different parts of their orbits.

• *Determining the value of the eccentricity of the orbit (if any).* This will be of particular interest in order for us to distinguish among the different models and clarify if there exists a significant difference between the orbital parameters of the SFXTs and the SgHMXBs (which mostly have circular orbits with negligible eccentricities). A measurement of the eccentricity is possible only if a sufficiently detailed (daily observations with relatively small errors on the estimated magnitudes) dataset for each source can be obtained.

• *Measuring the terminal velocity of the stellar wind, calculating the companion OB mass-loss rate, and making radial velocity measurements.* These parameters will be determined by us through spectroscopic observations with large telescopes. As with previous HMXB observations, *AAVSO Special Notices* will be issued to alert observers of the times when the spectroscopic observations are planned. Simultaneous light curve and spectroscopic radial velocity data are useful, for example, to separate periodicity due to pulsations of the primary from periodicity due to orbital motion (Sarty *et al.* 2009).

We remark that, in order to achieve the scientific aims presented above, *the contributions of AAVSO members and observers are critical*, since no single institutional telescope can afford such a large amount of observation time with the time spacing implied by an effective monitoring of the seventeen proposed candidate sources. (Two of the objects listed in the Tables are not SFXTs *per se* but "obscured HMXBs," another class of new HMXBs discovered by *INTEGRAL*. Our objectives for observing the obscured sources are the same as for the SFTXs although the astrophysical models are different.) Here we propose to observe the primary stars in SFXTs, which are generally faint in the visual domain (*V* band) due to the high extinction in the direction of these systems (and absorption intrinsic to the systems as well). For this reason, observations will need to be done in the *I* and possibly *R* bands (see section 3).

3. Feasibility: observing methods

This project extends the observational program for AAVSO observers described by Sarty *et al.* (2007) to the realm of the new class of SFXTs. The complete listing of program SFXTs is given in Tables 1, 2, and 3. The magnitude listing given in Table 1 is especially important to note. In the visual bands, the SFXTs are mostly beyond the reach of amateur-sized telescopes, although at least one, IGR J08408-4503, appears to be bright enough to be observed in the *V* band. Inspection of Table 1 reveals that the determination of two SFXT candidate optical counterparts will comprise the first stage of the observational program. The following stage will be to monitor as deeply and as frequently as possible

all the proposed sources, in order to obtain at least daily estimates of their visual and/or infrared magnitudes and to determine their orbital periods. For this long term light curve monitoring, most of the observing will need to be done in the *I* and possibly *R* bands, where, even then, many objects will be faint. Since the amplitude of any periodicities in the light curves are currently unknown, the highest precision possible is required. This means longer exposures that maximize the signal-to-noise ratio are required as opposed to densely sampled time-series. A goal of 0.01 magnitude precision or better is ideal but this may not be achievable for some of the dimmer sources. However, all data free from systematic error, of any precision, are valuable since so little is known about the optical properties of the SFXTs. For example, the x-ray flares may be accompanied by fairly large amplitude optical flares that would be visible in lower precision data. Some techniques for achieving the highest possible precision are given by Castellano *et al.* (2004) where topics like pixel scale choices (typically two or three pixels across the seeing disk) are discussed. To ensure a homogeneous set of comparison and check stars, standardized observing charts will be posted to:

http://homepage.usask.ca/ges125/AAVSO_HMXB_Charts.html.

With every observer using the same comparison star, or stars for ensemble differential photometry, we hope to reduce the systematic differences between observers. Generally, there should be a suitable comparison star within 10 arc minutes of the SFXT of interest. It will take some preparatory observations with the AAVSO Photometric All-Sky Survey (Henden *et al.* 2009), or some all-sky photometry by others, to define comparison stars having similar magnitude and color to the target SFXT. In the meantime, observers will be able to record useful differential photometry that can be shifted once the comparison star magnitudes are standardized. As with the wider HMXB observing project, observers will submit their reduced data directly to the AAVSO International Database. The authors of this manuscript will then download the data for period analysis, using software such as PERIOD04 (Lenz and Breger 2005), to discover the orbital periods in your data. If we discover periods, or other interesting phenomena such as flares, in your data you will be offered authorship on the resulting discovery paper.

If you are interested in participating in this challenging new observing project, please watch for the *AAVSO Special Notices* and/or contact author G. E. Sarty (AAVSO observer SGE) and M. Falanga.

References

Bamba, A., Yokogawa, J., Ueno, M., Koyama, K., and Yamauchi, S. 2001, *Publ. Astron. Soc. Pacific*, **53**, 1179.

Belczynski, K., and Ziolkowski, J. 2009, *Astrophys. J.*, **707**, 870.

Bird, A. J., Bazzano, A., Hill, A. B., McBride, V. A., Sguera, V., Shaw, S. E., and Watkins, H. J. 2009, *Mon. Not. Roy. Astron. Soc.*, **393**, L11.

Bozzo, E., Falanga, M., and Stella, L. 2008, *Astrophys. J.*, **683**, 1031.

Bozzo, E., Stella, L., Israel, G., Falanga, M., and Campana, S. 2009, in *SIMBOL-X: Focusing on the Hard X-ray Universe,* AIP Conf. Proc., 1126, 319.

Castellano, T. P., Laughlin, G., Terry, R. S., Kaufman, M., Hubbert, S., Schelbert, G. M., Bohler, D., and Rhodes, R. 2004, *J. Amer. Assoc. Var. Star Obs.*, **33**, 1.

Chaty, S., and Filliâtre, P. 2005, *Astrophys. Space Sci.*, **297**, 235.

Chaty, S., Rahoui, F., Foellmi, C., Tomsick, J. A., Rodriguez, J., and Walter, R. 2008, *Astron. Astrophys.*, **484**, 783.

Clark, D. J., Hill, A. B., Bird, A. J., McBride, V. A., Scaringi, S., and Dean, A. J. 2009, *Mon. Not. Roy. Astron. Soc.*, **399**, L113.

Clark, D. J., Sguera, V., Bird, A. J., *et al.* 2010, *Mon. Not. Roy. Astron. Soc.*, **406**, L75.

Coe, M., Fabregat, J., Negueruela, I., Roche, P., and Steele, I. 1996, *Mon. Not. Roy. Astron. Soc.*, **281**, 333.

D'Ai', A., Cusumano, G., La Parola, V., and Segreto, A. 2010, *Astron. Telegram*, No. 2596, 1.

Drave, S. P., Clark, D. J., Bird, A. J., McBride, V. A., Hill, A. B. Sguera, V., Scaringi, S., and Bazzano, A. 2010, *Mon. Not. Roy. Astron. Soc.*, accepted.

Drilling, J. S. 1991, *Astrophys. J.*, Suppl. Ser., **76**, 1033.

Ducci, L., Sidoli, L., and Paizis, A. 2010, astro-ph/1006.3256.

Filliâtre, P., and Chaty, S. 2004, *Astrophys. J.*, **616**, 469.

Halpern, J. P., and Gotthelf, E. V. 2006, *Astron. Telegram*, No. 692, 1.

Halpern, J. P., Gotthelf, E. V., Helfand, D. J., Gezari, S., and Wegner, G. A. 2004, *Astron. Telegram*, No. 289, 1.

Heinke, C. O., Tomsick, J. A., Yusef-Zadeh, F., and Grindlay, J. E. 2009, *Astrophys. J.*, **701**, 1627.

Henden, A. A., Welch, D. L., Terrell, D., and Levine, S.E. 2009, *Bull. Amer. Astron. Soc.*, **41**, 669.

Ibarra, A., Matt, G., Guainazzi, M., Kuulkers, E., Jimenez-Bailón, E., Rodriguez, J., Nicastro, F., and Walter, R. 2007, *Astron. Astrophys.*, **465**, 501.

in't Zand, J., Jonker, P., Mendez, M., and Markwardt, C. 2006, *Astron. Telegram*, No. 915, 1.

Jain, C., Paul, B., and Dutta, A. 2009, *Res. Astron. Astrophys.*, **9**, 1303.

Kennea, J. A., Pagani, C., Markwardt, C., Blustin, A., Cummings, J., Nousek, J., and Gehrels, N. 2005, *Astron. Telegram*, No. 599, 1.

Kinugasa, K., Torii, K., Hashimoto, Y., *et al.* 1998, *Astrophys. J.*, **495**, 435.

Kouveliotou, C., Patel, S., Tennant, A., Woods, P., Finger, M., and Wachter, S. 2003, *IAU Circ.*, No. 8109, 2.

Lenz, P., and Breger, M. 2005, *Commun. Asteroseismology*, **146**, 53.

Levine, A. M., and Corbet, R. 2006, *Astron. Telegram*, No. 940, 1.

Leyder, J. -C., Walter, R, Lazos, M., Masetti, N., and Produit, N. 2007, *Astron. Astrophys.*, **465**, L35.

Lutovinov, A., Revnivtsev, M., Gilfanov, M., Shtykovskiy, P., Molkov, S., Sunyaev, R. 2005, *Astron. Astrophys.*, **444**, 821.

Morris, D. C., Smith, R. K., Markwardt, C. B., Mushotzky, R. F., Tueller, J., Kollman, T. R., and Dhuga, K. S. 2009, *Astrophys. J.*, **699**, 892.
Naik, S., Joshi, V., Vadawale, S. V., and Ashok, N. M. 2010, *Astron. Telegram*, No. 2475, 1.
Negueruela, I., and Schurch, M. P. E. 2007, *Astron. Astrophys.*, **461**, 631.
Negueruela, I., and Smith, D. M. 2006, *Astron. Telegram*, No. 831, 1.
Negueruela, I., Smith, D. M., and Chaty, S. 2005, *Astron. Telegram*, No. 429, 1.
Negueruela, I., Smith, D. M., Harrison, T. E., and Torrejón, J. M. 2006, *Astrophys. J.*, **638**, 982.
Nespoli, E., Fabregat, J., and Mennickent, R. E. 2008, *Astron. Astrophys.*, **486**, 911.
Patel, S. K., Zurita, J., Del Santo, M. *et al.* 2007, *Astrophys. J.*, **657**, 994.
Pellizza, L. J., Chaty, S., and Negueruela, I. 2006, *Astron. Astrophys.*, **455**, 653.
Rahoui, F., and Chaty, S. 2008a, *Astron. Astrophys.*, **492**, 163.
Rahoui, F., Chaty, S., Lagage, P.-O., and Pantin, E. 2008b, *Astron. Astrophys.*, **484**, 801.
Ratti, E. M., Bassa, C., Torres, M. A. P., Kuiper, L., Miller-Jones, J., and Jonker, P. 2010, *Mon. Not. Roy. Astron. Soc.*, **408**, 1866.
Rupen, M. P., Dhawan V., and Mioduszewski, A. J. 2004, *Astron. Telegram*, No. 335, 1.
Sarty, G. E., Kiss, L. L., Johnston, H. M., Huziak, R., and Wu, K., 2007, *J. Amer. Assoc. Var. Star Obs.*, **35**, 327.
Sarty, G. E., Kiss, L. L., Huziak, R., *et al.*, 2009, *Mon. Not. Roy. Astron. Soc.*, **392**, 1242.
Sidoli, L., Romano, P., Ducci, L., *et al.* 2009, *Mon. Not. Roy. Astron. Soc.*, **397**, 1528.
Sguera, V., Bazzano, A., Bird, A. J., *et al.* 2006, *Astrophys. J.*, **646**, 452.
Sguera, V., Hill, A. B., Bird, A. J., *et al.* 2007, *Astron. Astrophys.*, **467**, 249.
Smith, D. M. 2004, *Astron. Telegram*, No. 338. 1.
Smith, D. M., Heindl, W. A., Markwardt, C. B., Swank, J. H., Negueruela, I., Harrison, T. E., and Huss, L. 2006, *Astrophys. J.*, **638**, 974.
Tomsick, J. A., Chaty, S., Rodriguez, J., Foschini, L., Walter, R., and Kaaret, P. 2006, *Astrophys. J.*, **647**, 1309.
Tomsick, J. A., Chaty, S., Rodriguez, J., Walter, R., and Kaaret, P. 2008, *Astrophys. J.*, **685**, 1143.
Tomsick, J. A., Chaty, S., Rodriguez, J., Walter, R., and Kaaret, P. 2009a, *Astrophys. J.*, **701**, 811.
Tomsick, J. A., Chaty, S., Rodriguez, J., Walter, R., Kaaret, P., and Tovmassian, G. 2009b, *Astrophys. J.*, 694, 344.
Torrejón J. M., Negueruela, I., Smith, D. M., and Harrison, T. E. 2010, *Astron. Astrophys.*, **510**, 61.
Walter, R., and Zurita Heras, J. 2007, *Astron. Astrophys.*, **476**, 335.
Walter, R., Zurita Heras, J., Bassani, L., *et al.* 2006, *Astron. Astrophys.*, **453**, 133.
Zurita Heras, J. A., and Chaty, S. 2009, *Astron. Astrophys.*, 493, L1.
Zurita Heras, J. A., and Walter, R. 2004, *Astron. Telegram*, No. 336, 1.

Table 1. Positions and magnitudes of the program SFXTs.

Source	*Coordinates*		*B*	*V*	*R*	*I*	*K*
	R.A.	*Dec.*					
IGR J08408–4503	08:40:47.79	–45:03:30.2[1]	7.8	7.6[2]	—	—	6.8[3]
IGR J16195–4945	16:19:32.20	–49:44:30.7[4]	18.1	17.2	16.4	15.5[5]	11.0[6]
IGR J16207–5129	16:20:46.26	–51:30:06.0[4]	19.8	17.7	15.4	13.6[5]	9.2[7]
IGR J16318–4848*	16:31:48.31	–48:49:00.7[8]	>25.4	>21.1	17.7	16.1[9]	7.6[3]
IGR J16358–4726	16:35:53.8	–47:25:41.1[10]	—	—	—	12.6[3]	—
IGR J16465–4507	16:46:35.26	–45:07:04.6[11]	15.2	—	13.0	—	9.8[12]
IGR J16479–4514	16:48:06.56	–45:12:06.8[11]	—	20.4[13]	—	—	9.8[14]
IGR J17354–3255*	17:35:25	–32:55:18 [11]	—	—	—	—	10.3[3]
XTE J1739–302	17:39:11.58	–30:20:37.6[15]	17.0	14.9	12.9	11.4[16]	7.4[12]
IGR J17407–2808	17:40:42	–28:08:00[17]	—	—	—	—	—
XTE J1743–363	17:43:01.324	–36:22:22.2[18]	—	—	—	—	7.6[19]
IGR J17544–2619	17:54:25.27	–26:19:52.7[20]	14.4	12.7	<11.9	—	8.0[21]
SAX J1818.6–1703	18:18:37.89	–17:02:47.9[22]	—	—	17.2	—	7.9[23]
AX J1820.5–1434	18:20:29.5	–14:34:24[24]	16.5	—	14.7[25]	—	—
AX J1841.0–0536	18:41:00.43	–05:35:46.5[11]	—	—	—	—	8.9[3]
AX J1845.0–0433	18:45:02.1	–04:33:55[26]	16.2	14.0	12.7	11.4	8.9[27]
IGR J18483–0311	18:48:17.17	–03:10:15.54	>25.2	21.9[28]	19.3	15.3[29]	8.6[30]

*[1]Coordinates of the optical counterpart HD 74194 (Leyder et al. 2007). [2]B and V mags from Drilling (1991). [3]K mag from SIMBAD based on identification with 2MASS object listed in Table 3. [4]Coordinates from Chandra (Tomsick et al. 2006). [5]BVRI mags from Tomsick et al. (2006). [6]K mag based on identification with 2MASS J16193220–4944305 (Tomsick et al. 2006). [7]K mag based on identification with 2MASS J16204627–5130060 (Tomsick et al. 2006). [8]Position of optical counterpart identified by Filliâtre and Chaty (2004). [9]BVRI mags from Filliâtre and Chaty (2004). [10]Rahoui et al. (2008b). [11]Coordinates from Simbad based on 2 MASS object listed in Table 3. [12]BRK mags from Smith (2004). [13]Kennea et al. (2005). [14]Chaty et al. (2008). [15]Chandra localization (Smith et al. 2006). [16]VI mags from Negueruela et al. (2006). [17]Sguera et al. 2006. [18]Position of I band optical candidate identified by Ratti et al. 2010. [19]K mag of 2 MASS object (see Table 3) identified by Ratti et al. 2010. [20]Position of optical counterpart identified by Pellizza et al. (2006), see Table 3. [21]BVRK mags from Pellizza et al. (2006); Naik et al. (2010) found K=8.2. [22]Chandra coordinates (in't Zand et al. 2006). [23]RK mags from Negueruela and Smith (2006). [24]Kinugasa et al. (1998). [25]BR mags based on identification given in Table 3 (Negueruela and Schurch 2007). [26]Halpern and Gotthelf (2006). [27]BVRIK mags from Coe et al. (1996). [28]BV mags from Rahoui and Chaty (2008a). [29]Position and RI mags from Sguera et al. (2007). [30]Chaty et al. (2008). *Note that these two sources are not part of the SFXT class. However, given their peculiar behavior in the x–ray domain, we included them in our observational program.*

Table 2. Physical characteristics of the program SFXTs.

Source	*Orbital Period(d)*	*Spin Period(s)*	*Spec Type*	*Remarks*
IGR J08408-4503	24[1]	—	O8.5Ib(f)[2]	5% microvar[3]
IGR J16195-4945	16[4]	—	O, B or A[5]	Near HD 146628[5]
IGR J16207-5129	—	—	B0I[7]	No x-ray period <12 hr[8]
IGR J16318-4848	80[9]	—	sgB[e][10]	Almost edge-on obscuring matter[11]
IGR J16358-4726	—	5871[12]	sgB[e][13]	
IGR J16465-4507	30.32[14]	228[15]	B0.5I[16]/O9.5Ia[17]	
IGR J16479-4514	3.32[18]	—	O8.5Ib[19]	x-ray eclipses[20]
IGR J17354-3255	8.452[21]	—	—	x-ray eclipses[21]
XTE J1739-302	51.47[22]	—	O8.5Iab(f)[23]	
IGR J17407-2808	—	—	—	No Opt Cpt[24]
XTE J1743-363	—	—	late sg or OI[25]	No radio src at 4.9 and 8.5 GHz[26]
IGR J17544-2619	4.926[27]	—	O9Ib[28]	
SAX J1818.6-1703	30[29]	—	O9-B1I[30]	
AX J1820.5-1434	—	152.26[31]	O9.5-B0Ve[32]	
AX J1841.0-0536	—	4.7[33]	B1Ib[34]	
AX J1845.0-0433	—	—	O9Ia[35]	
IGR J18483-0311	18.55[36]	21.05[37]	B0.5Ia[38]	

[1]Based on recurring x-ray flares (Sidoli et al. 2009). [2]Spectral type of HD 74194 as reported in Sidoli et al. (2009). [3]Microvariable (from Hipparcos) with period of 7.8d (Leyder et al. 2007). [4]Based on a model of the fraction of an orbit spent in an x-ray flare (Morris et al. 2009). [5]Tomsick et al. (2006). [6]Possible blended optical source (Tomsick et al. 2006). [7]Based on I-band spectrum (Negueruela and Schurch 2007). [8]Tomsick et al. (2009b). [9]Based on x-ray outburst intervals (Jain et al. 2009). [10]Chaty and Filliâtre (2005). [11]Ibarra et al. (2007). [12]Variable spin (Patel et al. 2007). [13]Rahoui et al. (2008b). [14]Based on x-ray light curves (Clark et al. 2010). [15]Lutovinov et al. (2005). [16]Negueruela et al. (2005). [17]Nespoli et al. (2008). [18]Period based on x-ray light curves (Bozzo et al. 2009). [19]Nespoli et al. (2008). [20]Bozzo et al. (2009). [21]D'Ai' et al. (2010). [22]From x-ray light curve (Drave et al. 2010). [23]Rahoui et al. (2008b). [24]Need to follow up an x-ray outburst with optical observations to identify the counterpart; may be an unusual LMXT (Heinke et al. 2009). [25]Ratti et al. (2010). [26]Rupen et al. (2004). [27]Clark et al. (2009). [28]Pellizza et al. (2006). [29]Based on x-ray outburst intervals (Bird et al. 2009, Zurita Heras et al. 2009). [30]Zurita Heras et al. (2009) and Torrejón et al. (2010). [31]Kinugasa et al. (1998). [32]Belczynski and Ziolkowski (2009). [33]Bamba et al. (2001). [34]Nespoli et al. (2008). [35]Coe et al. (1996). [36]Levine and Corbet (2006), Jain et al. (2009). [37]Sguera et al. (2007). [38]Rahoui et al. (2008b).

Table 3. Name cross references for the program SFXTs.

Source	*Other Names*
IGR J08408-4503	LM Vel, HD 74194, 2MASS J08404780-4503302[1]
IGR J16195-4945	2MASS J16193220-4944305[2]
IGR J16207-5129	2MASS J16204627-5130060, USNO-B1.0 0384-0560875[2]
IGR J16318-4848	2MASS J16314831-4849005[3]
IGR J16358-4726	2MASS J16355369-4725398[4]
IGR J16465-4507	2MASS J16463526-4507045, USNO-B1.0 0448-00520455[5]
IGR J16479-4514	2MASS J16480656-4512068, USNO-B1.0 0447-0531332[6]
IGR J17354-3255	2MASS J17352760-3255544, Possible gamma-ray transient AGL J1734-3310[7]
XTE J1739-302	IGR J17391-3021, 2MASS J17391155-3020380, USNO-B1.0 0596-0585865[8]
IGR J17407-2808	CXOU J174042.0-280724[9]
XTE J1743-363	2MASS J17430133-3622221[10]
IGR J17544-2619	2MASS J17542527?2619526, USNO-B1.0 0636-0620933[11]
SAX J1818.6-1703	2MASS J18183790-1702479, USNO-B1.0 0729-0750578[12]
AX J1820.5-1434	2MASS J18203114-1434193, USNO-B1.0 0754-0489829[13]
AX J1841.0-0536	2MASS J18410043-0535465[14]
AX J1845.0-0433	IGR J18450-0435[15]
IGR J18483-0311	2MASS J18481720-0310168[16]

[1]Identification of HD 74194 with LM Vel and 2MASS J08404780-4503302 is based on SIMBAD *data. [2]Tomsick et al. (2006). [3]Filliâtre and Chaty (2004). [4]Kouveliotou et al. (2003). [5]Zurita Heras and Walter (2004), Nespoli et al. (2008). [6]Walter et al. (2006). [7]Tomsick et al. (2009a). [8]Rahoui et al. (2008b). [9]Chandra counterpart suggested by Heinke et al. (2009); however Tomsick et al., 2008 find no Chandra counterparts. [10]Ratti et al. (2010). [11]Pellizza et al. (2006). [12]Negueruela and Smith (2006). [13]Negueruela and Schurch (2007) but identification is uncertain. [14]Halpern et al. (2004). [15]Halpern and Gotthelf (2006). [16]Sguera et al. (2007).*

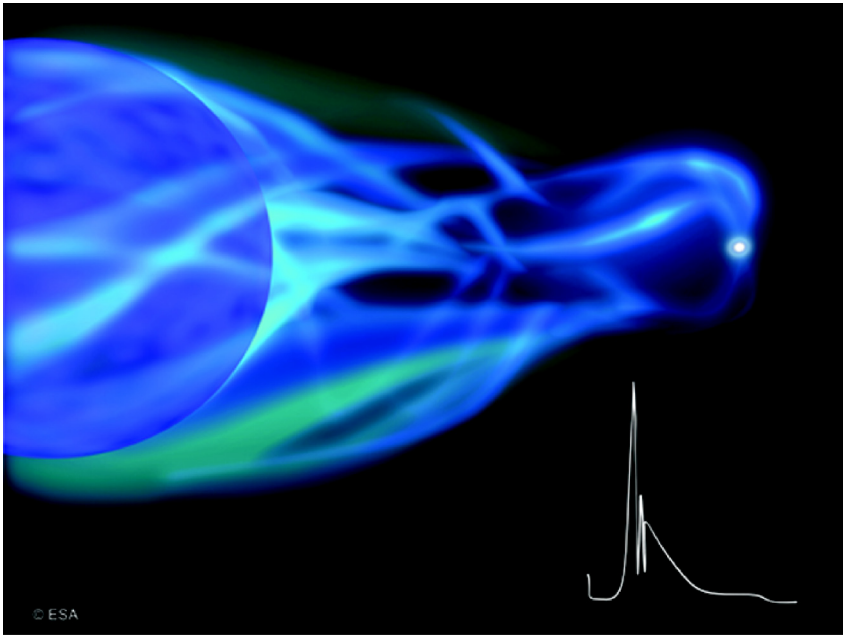

Figure 1. This artist's impression shows a high-mass binary system, composed of a supergiant luminous star (on the left) and a neutron star as the compact stellar object. These supergiant systems show strong and exceptionally fast-rising x-ray outbursts lasting a few hours, hence their name "supergiant fast x-ray transients." A typical x-ray flare light curve is shown at the bottom-right. The discovery story can be found on the ESA Space Science News from 16 November 2005: http://www.esa.int/esaSC/SEM20VJBWFE_index_0.html. *Picture copyright ESA, used with permission.*

Anchoring the Universal Distance Scale Via a Wesenheit Template

Daniel J. Majaess
David G. Turner
David J. Lane
Saint Mary's University, Halifax, Nova Scotia, B3H 3C3, Canada

and

The Abbey Ridge Observatory, Stillwater Lake, Nova Scotia, Canada; dmajaess@ap.smu.ca

Arne A. Henden
AAVSO, 49 Bay State Road, Cambridge, MA 02138; aavso@aavso.org

Tom Krajci
Astrokolkhoz Telescope Facility, Cloudcroft, NM 88317; tom_krajci@tularosa.net
and

Sonoita Research Observatory, Sonoita, Arizona

Received May 4, 2010; revised July 26, 2010; accepted August 16, 2010

Abstract A *VI* Wesenheit diagram featuring SX Phoenicis, δ Scuti, RR Lyrae, and type II and classical Cepheid variables is calibrated by means of geometric-based distances inferred from HST, Hipparcos, and VLBA observations ($n = 30$). The distance to a target population follows from the offset between the observed Wesenheit magnitudes and the calibrated template. The method is evaluated by ascertaining the distance moduli for the LMC ($\mu_0 = 18.43 \pm 0.03\ \sigma_{\bar{x}}$) and the globular clusters ω Cen, M54, M13, M3, and M15. The results agree with estimates cited in the literature, although a nearer distance to M13 is favored (pending confirmation of the data's photometric zero-point) and observations of variables near the core of M15 suffer from photometric contamination. The calibrated LMC data are subsequently added to the Wesenheit template since that galaxy exhibits precise OGLE photometry for innumerable variables of differing classes, that includes recent observations for δ Scuti variables indicating the stars follow a steeper *VI* Wesenheit function than classical Cepheids pulsating in the fundamental mode. *VI* photometry for the calibrators is tabulated to facilitate further research, and includes new observations acquired via the AAVSO's robotic telescope network (e.g., VY Pyx: $\langle V \rangle = 7.25$ and $\langle V \rangle - \langle I \rangle = 0.67$). The approach outlined here supercedes the lead author's prior first-order effort to unify variables of the instability strip in order to establish reliable distances.

1. Introduction

SX Phoenicis, δ Scuti, RR Lyrae, and type II and classical Cepheid variables are useful for establishing distances to globular clusters, the Galactic center, and galaxies (McNamara *et al.* 2000, 2007; Kubiak and Udalski 2003; Pritzl *et al.* 2003; Matsunaga *et al.* 2006, 2009; Majaess *et al.* 2009b, 2009c; Majaess 2009, 2010a, 2010b). However, there is an absence of precise trigonometric parallaxes for nearby type II Cepheids and RR Lyrae variables which would otherwise serve to anchor the standard candles. RR Lyrae is the single member of its class exhibiting a parallax uncertainty ≤ 30% (Table 1). Likewise, κ Pav and VY Pyx are unique among type II Cepheids that feature marginal parallax uncertainties (Table 1). The meagre statistics presently hamper efforts to establish individual zero-points for each variable type, particularly given that the aforementioned calibrators may exhibit peculiarities or multiplicity, or may sample the edge of the instability strip. Variables on the hot edge of the instability strip are brighter relative to objects on the cool edge that share a common pulsation period. Ignoring the distribution of calibrators within the instability strip may subsequently result in biased period-M_v and period-color relations, especially in the absence of viable statistics (Turner 2010).

The aforementioned problems may be mitigated by adopting a holistic approach and calibrating a *VI* Wesenheit diagram featuring SX Phe, δ Scuti, RR Lyrae, and type II and classical Cepheid variables. Anchoring the distance scale via a universal Wesenheit diagram (template) mobilizes the statistical weight of the entire variable star demographic to ensure precise distance determinations. Wesenheit magnitudes are reddening-free and relatively insensitive to the width of the instability strip. The Wesenheit function is defined and discussed by Madore (1982), Opolski (1983, 1988), Madore and Freedman (1991, 2009), Kovács and Jurcsik (1997), Kovács and Walker (2001), Di Criscienzo *et al.* (2004, 2007), and Turner (2010).

In this study, a *VI* Wesenheit template characterizing differing variables of the instability strip is calibrated by means of geometric-based distances (section 2.2) and the pertinent photometry (section 2.1). The calibration is evaluated by establishing distances to the LMC, ω Cen, M54, M13, M3,and M15 (section 2.3).

2. Analysis

2.1. Photometry (calibration)

The lead author has advocated that RR Lyrae variables and Cepheids obey *VI*-based Wesenheit and period-color relations which are comparatively insensitive to metallicity (Udalski *et al.* 2001; Bono 2003; Pietrzynski *et al.* 2004; Majaess *et al.* 2008, 2009b, 2009c; Bono *et al.* 2008; Majaess 2009, 2010a, 2010b), hence the advantage of constructing such a relation. That conclusion is based in part upon a

direct comparison of RR Lyrae variables, type II Cepheids, and classical Cepheids at common zero-points, which offers an opportunity to constrain the effects of chemical composition on their luminosities and intrinsic colors (Freedman and Madore 1996; Udalski *et al.* 2001; Dolphin *et al.* 2001; Majaess *et al.* 2009b, 2009c; Majaess 2009, 2010a, 2010b; Feast 2010, see also the historic precedent outlined in Tammann *et al.* 2008). For example, the distances inferred for the LMC, SMC, IC 1613, and several globular clusters from the aforementioned standard candles agree to within the uncertainties (Majaess *et al.* 2009b; Majaess 2009, 2010b), despite the neglect of metallicity corrections for variable types sampling different temperature, radius, and density regimes. Admittedly, the subject is actively debated (Smith 2004; Romaniello *et al.* 2008; Catelan 2009, and references therein). By contrast there appears to be a consensus that relations which rely on *BV* photometry are sensitive to variations in chemical abundance and a significant break in the period-magnitude relation is apparent (Majaess *et al.* 2009b, and references therein). Consequently, a *VI*-based Wesenheit calibration is developed here.

A notable success of the Hipparcos mission was the establishment of time-series and standardized photometry for bright stars. Hipparcos surveyed the sky in $B_T V_T$ while follow-up surveys such as ASAS and TASS obtained *VI* photometry (Pojmański 2002; Droege *et al.* 2006). Observations from a series of studies by Balona and Stobie (1980a, 1980b, 1983), in addition to data from the aforementioned sources, provide the photometry for the shorter-period calibrators examined (Table 1). Additional observations for VY Pyx and V703 Sco were obtained via the AAVSO's Sonoita (SRO) and Bright Star Monitor (BSM) telescopes (http://www.aavso.org/aavsonet). The SRO features an SBIG STL-1001E CCD (fov: 20' × 20') mounted upon a 35-cm telescope stationed near the town of Sonoita, Arizona. The BSM features an SBIG ST8XME CCD (fov: 127' × 84') mounted upon a 6-cm wide-field telescope located at the Astrokolkhoz telescope facility near Cloudcroft, New Mexico. The AAVSO observations are tied to Landolt (1983, 1992) photometric standards according to precepts outlined in Henden and Kaitchuck (1990) (see also Henden and Munari 2008). The data for VZ Cnc were supplemented by observations taken at the Abbey Ridge Observatory (Lane 2007). *VI* photometry for Benedict *et al.* (2007) Galactic classical Cepheid calibrators was obtained from the catalogue of Berdnikov *et al.* (2000).

The phased light curves for several variables are presented in Figure 1. The relevant photometry (is) shall be available online via databases maintained by CDS, ASAS, TASS, and the AAVSO. The pulsation periods employed to phase the data were adopted from the GCVS (Samus *et al.* 2009a), the AAVSO's VSX archive (http://www.aavso.org/vsx/), and the GEOS RR Lyr survey (Le Borgne *et al.* 2007). Several pulsators display pronounced amplitude variations and are discernably multiperiodic (e.g., AI Vel, V703 Sco,SX Phe, Figures 1 and 2), topics that shall be elaborated upon elsewhere.

2.2. Parallaxes (calibration)

Twenty-four variables with parallaxes measured by Hipparcos and HST are employed to calibrate the *VI* Wesenheit diagram (Table 1). The sample consists of eight SX Phoenicis and δ Scuti variables, four RR Lyrae variables, two type II Cepheids, and ten classical Cepheids. That sample is supplemented by six type II Cepheids detected by Macri *et al.* (2006) in their comprehensive survey of the galaxy M106 (Majaess *et al.* 2009b), which features a precise geometric-based distance estimate (Herrnstein *et al.* 1999). It is perhaps ironic that stars 7.2 Mpc distant may be enlisted as calibrators because of an absence of viable parallaxes for nearby objects. Type II Cepheids within the inner region of M106 were not employed in the calibration because of the likelihood of photometric contamination via crowding and blending (Figure 4, see also Stanek and Udalski 1999; Mochejska *et al.* 2000, 2001; Macri *et al.* 2006; Vilardell *et al.* 2007; Smith *et al.* 2007; Majaess *et al.* 2009b; Majaess 2010b). The stars employed were observed in the outer regions of M106 where the stellar density and surface brightness are diminished by comparison. Extragalactic type II Cepheids are often detected fortuitously near the limiting magnitude of surveys originally aimed at discovering more luminous classical Cepheids, hence the preference toward detecting the longer period (brighter) RV Tau subclass (Majaess *et al.* 2009b).

Parallaxes for several calibrators were sought from the van Leeuwen (2007) catalogue of revised Hipparcos data (Table 1). The parallaxes cited in the study differ from those issued by van Leeuwen *et al.* (2007). The reliability of Hipparcos parallaxes has been questioned because of disagreements over the distance to Polaris and the Pleiades cluster (Turner and Burke 2002; Soderblom *et al.* 2005; Turner *et al.* 2005; van Leeuwen *et al.* 2007; van Leeuwen 2009a, 2009b; Turner 2009, 2010). The Hipparcos parallax for the Pleiades corresponds to a distance of $d = 120.2 \pm 1.9$ pc (van Leeuwen 2009a), whereas HST observations imply $d = 134.6 \pm 3.1$ pc (Soderblom *et al.* 2005). A comparison of stars with both Hipparcos and HST parallaxes indicates that there may be a marginal systemic offset (~5%). However, the statistics are poor. van Leeuwen (2009a, 2009b) argues in favor of the Hipparcos scale and the reader is referred to that comprehensive study.

Tammann *et al.* (2008) questioned the reliability of HST parallaxes for nearby classical Cepheids since the resulting period-magnitude relations inferred from that sample do not match their own functions (Tammann *et al.* 2003; Sandage *et al.* 2004), which were constructed from the best available data at the time and prior to the publication of the HST parallaxes (Benedict *et al.* 2007). Turner (2010) has since revised the parameters for longer-period classical Cepheid calibrators, although continued work is needed and ongoing (survey initiated at the OMM, Artigau *et al.* 2010). The viability of the HST parallaxes is supported by the results of Turner (2010) and Majaess (2010b). A central conclusion of Turner (2010) was that the classical Cepheid period-luminosity relation tied to the HST sample is in agreement with that inferred from cluster Cepheids. Majaess (2010b)

reaffirmed that the slope of the *VI* Wesenheit function inferred from Benedict *et al.* (2007) HST data matches that of precise ground-based observations of classical Cepheids in the LMC, NGC 6822, SMC, and IC 1613 (see Figure 2 in Majaess 2010b). Classical Cepheids in the aforementioned galaxies span a sizeable abundance baseline and adhere to a common *VI* Wesenheit slope to within the uncertainties, thereby precluding a dependence on metallicity (see Figure 2 in Majaess 2010b).

The uncertainty tied to the Wesenheit magnitude for a given calibrator is presently dominated by the parallax and distance uncertainties. Those uncertainties are converted into magnitude space (σ_ω) through the formula:

$$\sigma_\omega \simeq | 5 \log (d + \sigma_\delta) - 5 - (5 \log (d - \sigma_\delta) - 5)| / 2 \quad (1)$$

$$\sigma_\omega \simeq \left| 2.5 \log \left(\frac{d + \sigma_d}{d - \sigma_d} \right) \right| \quad (2)$$

$$\sigma_\omega \simeq \left| 2.5 \log \left(\frac{\pi + \sigma_\pi}{\pi - \sigma_\pi} \right) \right| \quad (3)$$

The uncertainty associated with the Wesenheit magnitudes for type II Cepheids in M106 (σ'_ω) is estimated as:

$$\sigma'_\omega \simeq \sqrt{\sigma_{TII}^2 + \sigma_\omega^2} \quad (4)$$

Where σ_{TII} is the average photometric deviation of type II Cepheids occupying the outer region of M106 from the mean *VI* Wesenheit function. The calibration derived here shall be bolstered by additional and precise parallax measurements. F. Benedict and coauthors are presently acquiring HST parallaxes for important stars such as κ Pav, XZ Cyg, UV Oct, and VY Pyx (Table 1).

2.3. Calibrated Wesenheit diagrams

The calibrating and LMC *VI* Wesenheit diagrams are displayed in Figure 3. The Wesenheit magnitudes were computed as follows:

$$W_{VI,0} = \langle V \rangle - R_{VI} (\langle V \rangle - \langle I \rangle) - \mu_0 \quad (5)$$

$$W_{VI} = \langle V \rangle - R_{VI} (\langle V \rangle - \langle I \rangle) \quad (6)$$

Where R_{VI}=2.55 is the canonical extinction law, although there are concerns with adopting a color-independent extinction law. The Wesenheit magnitudes tied to BN Vul and AD CMi are spurious so the stars were omitted from Figure 3. The cases may be analogous to RT Aur, Y Sgr, or perhaps FF Aql (see Table 1 in van Leeuwen *et al.* 2007). RR Lyrae variables pulsating in the overtone were

shifted by $\log P_f \simeq \log P_o + 0.13$ to yield the equivalent fundamental mode period (Walker and Nemec 1996; Hurdis and Krajci 2010). Figure 3 was plotted with the fundamentalized periods so to illustrate the general continuity across the variable types, however, plotting the uncorrected principal period is preferred so to permit a direct assessment of the pulsation mode.

The distance to a target population follows from the offset between the observed Wesenheit magnitudes and the calibration.

2.3.1. LMC

The resulting distance modulus for the LMC is $\mu_0 = 18.43 \pm 0.03$ ($\sigma_{\bar{x}}$) ± 0.17 (σ). That agrees with the value obtained by Majaess *et al.* (2008) and Majaess (2009), and exhibits smaller uncertainties. Likewise, the estimate is consistent with a mean derived from the NASA/IPAC Extragalactic Database (NED-D) master list of galaxy distances, which features over 300 distances for the LMC (Madore and Steer 2007; Steer and Madore 2010) (http://nedwww.ipac.caltech.edu/level5/NED1D/intro.html and http://nedwww.ipac.caltech.edu/Library/Distances/).

The author's prior estimates were inferred by applying a *VI* Galactic classical Cepheid calibration (Majaess *et al.* 2008) to the LMC photometry of Udalski *et al.* (1999) and Sebo *et al.* (2002). Majaess *et al.* (2008) calibration is based primarily on the efforts of fellow researchers who established classical Cepheids as members of Galactic open clusters (e.g., Sandage 1958; Madore and van den Bergh 1975; Turner 2010) and secured precise trigonometric parallaxes (HST, Benedict *et al.* 2002b, 2007).

The latest OGLE LMC observations indicate that δ Scuti stars exhibit a steeper *VI* Wesenheit slope than classical Cepheids pulsating in the fundamental mode (Figure 3, see also Soszyński *et al.* 2008b; Poleski *et al.* 2010). The pulsation modes of δ Scuti variables may be constrained by overlaying a target demographic—along with RR Lyrae and type II Cepheid variables which are often detected in tandem—upon the calibrated LMC Wesenheit template. SX Phe variables appear toward the shorter-period extension of the δ Scuti regime on the Wesenheit diagram (Figure 3).

2.3.2. M3

The distance to variable stars in globular clusters may be established by comparing the observed Wesenheit magnitudes to the calibrated LMC template, which exhibits extensive statistics and period coverage for innumerable variable types. The distance modulus for M3 from the analysis is: $\mu_0 = 15.12 \pm 0.01$ ($\sigma_{\bar{x}}$) ± 0.20 (σ). That agrees with Harris' (1996) estimate of $\mu_0 \simeq 15.08$. Harris (1996) distances to globular clusters are established from the magnitude of the horizontal branch (http://physwww.mcmaster.ca/~harris/mwgc.ref).

2.3.3. ω Cen

The distance modulus for ω Cen from the aforementioned approach is: $\mu_0 = 13.49 \pm 0.01\ (\sigma_{\bar{x}}) \pm 0.09 (\sigma)$. Estimates in the literature for ω Cen span a range: $\mu_0 \simeq 13.41$ ® 13.76 (van de Ven *et al.* 2006; Del Principe *et al.* 2006). The *VI* photometry characterizing variables in ω Cen was obtained somewhat indirectly (see Weldrake *et al.* 2007). Securing multi-epoch *I*-band observations is therefore desirable to permit a more confident determination of the zero-point, and enable further constraints on the effects of chemical composition on the luminosities of RR Lyrae variables. Stars in ω Cen exhibit a sizeable spread in metallicity at a common zero-point owing to the presence of multiple populations ($-1 \geq$ [Fe/H] ≥ -2.4, Rey *et al.* 2000). Evaluating the correlation between the distance modulus computed for a given RR Lyrae variable and its abundance yields direct constraints on the effects of metallicity (e.g., Majaess 2009).

2.3.4. M13

An analysis of the variable stars in M13 yields: $\mu_0 = 14.09 \pm 0.02\ (\sigma_{\bar{x}}) \pm 0.06$ (σ) (caution warranted, see below). That may agree with the infrared weighted solution of $\mu_0 = 14.25$ by Buckley and Longmore (1992), but the estimate is significantly smaller than the distance modulus for M13 cited by Harris (1996) ($\mu_0 \simeq 14.43$). The observations of M13 are from a series of studies that detected at least four SX Phe variables, five RR Lyrae variables (four RRc and one RRab), and three type II Cepheids (Kopacki *et al.* 2003; Pietrukowicz and Kaluzny 2004; Kopacki 2005). The surveys were conducted as part of renewed efforts to secure multiband photometric parameters for variable stars in globular clusters (Pietrukowicz and Kaluzny 2003; Pietrukowicz *et al.* 2008, see also Sawyer 1939, Clement *et al.* 2001, Samus *et al.* 2009b).

Applying the *VI* RR Lyrae variable period-reddening calibration of Majaess (2010a) to the M13 data yields a mean color excess of: $E_{(B-V)} = 0.06 \pm 0.02\ (\sigma_{\bar{x}})$ (caution warranted, see below). The *VI* RR Lyrae variable period-color relation derived by Pejcha and Stanek (2009) yields $E_{(V-I)} = 0.05 \pm 0.02\ (\sigma_{\bar{x}})$ ($E_{(B-V)} \simeq 0.04$). The estimates are larger than the reddening inferred from the NED extinction calculator for the direction toward M13 ($E_{(B-V)} \simeq 0.02$). The consensus position is that the line of sight toward M13 is unobscured, however the Wesenheit approach is extinction free and independent of that assertion (for the canonical extinction law). Applying the new reddening to previous optical estimates of the cluster's distance modulus would result in a correction of $\Delta\mu_0 \simeq E_{(B-V)} \times R_V \simeq -0.15$ (R_V, Turner 1976), thereby bringing the estimates into closer agreement.

The data for M13 are based on ground and HST photometry, which are challenging to standardize and may therefore be susceptible to a host of concerns related to photometric contamination and floating photometric zero-points (see Saha *et al.* 2006). If the photometry is trustworthy, then the distance and reddening estimates obtained for M13 are reliable. Additional observations are presently being acquired to facilitate that assessment.

2.3.5. M54

The distance modulus derived for M54 is $\mu_0 = 17.04 \pm 0.01\ (\sigma_{\bar{x}}) \pm 0.05\ (\sigma)$. That agrees with Harris' (1996) estimate of $\mu_0 \simeq 17.14$.

2.3.6. M15

The distance modulus for M15 from the analysis is: $\mu_0 \geq 14.82$. Estimates in the literature for M15 span a range: $\mu_0 \simeq 14.69 \rightarrow 14.99$ (Arellano Ferro *et al.* 2006; McNamara *et al.* 2004). Applying the *VI* RR Lyrae variable period-reddening calibration of Majaess (2010a) yields a mean color excess of $E_{(B-V)} \leq 0.12$, matching that cited by Harris (1996). However, the observations suffer from photometric contamination, particularly for stars near the cluster's core where the surface brightness and stellar density increase rapidly (Figure 4). Blending may introduce spurious flux and cause variables to appear brighter (often redder) and hence nearer (Figure 4). Photometric contamination provides a viable explanation for the discrepancy noted in the Bailey diagram describing variables in M15 (see Corwin *et al.*2008).

That contamination was overlooked by the lead author when previously investigating the cluster (Majaess 2009). Other globular cluster photometry should be examined in similar fashion pending the availability of published positional data beyond pixel coordinates. Photometric contamination may bias efforts to construct an RR Lyrae variable period-amplitude-metallicity relation, and may exaggerate the perceived spread of the cluster's main-sequence and red giant branch, thereby mimicking the signature of multiple populations (in certain instances). A trend similar to that displayed in Figure 4 is observed in data for extragalactic Cepheids (Majaess *et al.* 2009b). In an effort to constrain the effect of chemical composition on the luminosities of classical Cepheids, researchers have endeavored to compare the distance offset between classical Cepheids located in the central (metal-rich) and outer (metal-poor) regions of a particular galaxy (e.g., M101, M106, M33). A degeneracy complicates the analysis (photometric contamination) since the stellar density and surface brightness often increase toward the central region. Depending on the circumstances, the effects of metallicity and blending/crowding may act in the same sense and be of similar magnitude (e.g., compare Figures 17 and 18 in Macri *et al.* 2006, see also Macri *et al.* 2001). Furthermore, R (the ratio of total to selective extinction) may also vary as a function of radial distance from the centers of galaxies in tandem with the metallicity gradient. For example, the extinction law characterizing dust properties near the center of the Milky Way is possibly anomalous (Udalski 2003, see Kunder *et al.* 2008 for the dissenting view). As stated earlier, the author has advocated that *VI*-based Cepheid and RR Lyrae variable Wesenheit and period-color relations are comparatively insensitive to metallicity, and thus the offset arises from photometric contamination or another source.

The uncertainties associated with the derived distance modulus and mean color excess for M15 cited above are exacerbated systemically and statistically

by the aforementioned bias (Figure 4). The distance modulus and color excess representing stars near the periphery of the cluster, where the effects of photometric contamination are mitigated, are: $\mu_0 \simeq 15$ and $E_{(B-V)} \simeq 0.06$ (Figure 4). The analysis reaffirms the advantage of adopting a period-magnitude-color approach to investigating RR Lyrae variables, in addition to the approach outlined in Figure 3 or the canonical [Fe/H]–M_v relation. The slope of the Wesenheit function is also an important diagnostic for assessing photometric irregularities (Majaess *et al.* 2009b; Majaess 2010b), and should be assessed in tandem with the establishment of distances via the Wesenheit template (Figure 3).

3. Summary and future research

A *VI* Wesenheit diagram unifying variables of the instability strip is calibrated by means of geometric-based distances inferred from HST, Hipparcos, and VLBA observations (Table 1, Figure 3). The distance modulus for a target population is determined by evaluating the offset between the observed Wesenheit magnitudes and a calibrated template. The approach mitigates the uncertainties tied to establishing a distance scale based on type II Cepheids or RR Lyrae variables individually, since presently there is an absence of viable parallaxes. F. Benedict and coauthors are engaged in ongoing efforts to secure precise parallaxes for a host of variables employed in the calibration (Table 1).

To first order the distance moduli established for the LMC, ω Cen, M54, M13, M3, and M15 via the calibration agree with estimates in the literature (section 2.3). *VI* photometry for variable stars in the globular clusters examined (and LMC) were sought from innumerable sources (Udalski *et al.* 1999; Layden and Sarajedini 2000; Soszyński *et al.* 2003, 2008a, 2008b, 2009; Kopacki *et al.* 2003; Pietrukowicz and Kaluzny 2004; Kopacki 2005; Benkő *et al.* 2006; Weldrake *et al.* 2007; Corwin *et al.* 2008; Poleski *et al.* 2010).

VI photometry for the calibrating set was acquired from the AAVSO's robotic telescope network and other sources (Table 1, section 2.1). This study reaffirms the importance of modest telescopes in conducting pertinent research (Percy 1986, 2007; Welch *et al.* 1995; Szabados 2003; Henden 2006; Paczyński 2006; Genet *et al.* 2009; Pojmański 2009; Udalski 2009; Turner *et al.* 2009), whether that is facilitating an understanding of terrestrial mass extinction events, discovering distant supernovae, aiding the search for life by detecting exoplanets, or anchoring the universal distance scale (e.g., Price *et al.* 2005; Lane and Gray 2005; Charbonneau *et al.* 2009; Majaess *et al.* 2009a).

Lastly, the present holistic approach supercedes the lead author's prior first order and somewhat erroneous effort (Majaess 2009). (SX Phe, RR Lyrae, and type II Cepheid variables may be characterized by a common *VI* Wesenheit function to first order, as noted by Majaess (2009, 2010a), but not to second order (Figure 3).) Yet it is envisioned that the universal distance scale could be further constrained via the current approach by relying on an additional suite of calibrators, namely:

variables in globular clusters that possess dynamically-established distances (e.g., ω Cen and M15, McNamara *et al.* 2004; van de Ven *et al.* 2006); δ Scuti stars in nearby open clusters (e.g., Pleiades, Praesepae, Hyades; Li and Michel 1999); variable stars in clusters with distances secured by means of eclipsing binaries (e.g., Cluster AgeS Experiment); and variables in the Galactic bulge that are tied to a precise geometric-based distance (Eisenhauer *et al.* 2005; Reid *et al.* 2009, bolstered by observations from the upcoming VVV survey; Minniti *et al.* 2010). The resulting *VI* Wesenheit calibration (Figure 3) could be applied to galaxies beyond the LMC, such as the SMC (Udalski *et al.* 1999; Soszyński *et al.* 2002), IC 1613 (Udalski *et al.* 2001; Dolphin *et al.* 2001), and M33 (Sarajedini *et al.* 2006; Scowcroft *et al.* 2009), which feature *VI* observations for population I and II variables. The results of such an analysis would support ongoing efforts to constrain the Hubble constant (e.g., Ngeow and Kanbur 2006; Macri and Riess 2009). However, a successful outcome is contingent upon the admittedly challenging task of obtaining precise, commonly standardized, multi-epoch, multiband, comparatively uncontaminated photometry.

Acknowledgements

DJM is grateful to: G. Pojmański, L. Macri, F. van Leeuwen, F. Benedict, L. Balona, and R. Stobie; TASS (T. Droege, M. Sallman, and M. Richmond); T. Corwin, D. Weldrake, W. Harris, G. Kopacki, P. Pietrukowicz, J. Kaluzny; and OGLE (I. Soszyński, R. Poleski, M. Kubiak, and A. Udalski) whose surveys were the foundation of this study; the AAVSO (M. Saladyga and W. Renz); CDS; arXiv; NASA ADS; I. Steer (NED); and the RASC. T. Krajci, J. Bedient, D. Welch, D. Starkey, and others (kindly) funded the AAVSO's BSM.

References

Alves, D. R., Bond, H. E., and Livio, M. 2000, *Astron. J.*, **120**, 2044.

Arellano Ferro, A., Garcdotlessia Lugo, G., and Rosenzweig, P. 2006, *Rev. Mex. Astron. Astrofis.*, **42**, 75.

Artigau, E., Doyon, R., and Lamontagne, R. 2010, in *Observatory Operations: Strategies, Processes, and Systems III*, ed. D. R. Silva, A. B. Peck, and B. T. Soifer, Proc. SPIE, 7737, 63.

Balona, L. A., and Martin, W. L. 1978, *Mon. Not. Roy. Astron. Soc.*, **184**, 1.

Balona, L. A., and Stobie, R. S. 1980a, *Mon. Not. Roy. Astron. Soc.*, **190**, 931.

Balona, L. A., and Stobie, R. S. 1980b, *Mon. Not. Roy. Astron. Soc.*, **192**, 625.

Balona, L. A., and Stobie, R. S. 1983, *S. Afr. Astron. Obs., Circ.*, **7**, 19.

Benedict, G. F. *et al.*, 2002a, *Astron. J.*, **123**, 473.

Benedict, G. F., *et al.* 2002b, *Astron. J.*, **124**, 1695.

Benedict, G. F. *et al.*, 2007, *Astron. J.*, **133**, 1810.

Benkő, J. M., Bakos, G. A., and Nuspl, J. 2006, *Mon. Not. Roy. Astron. Soc.*, 372, 1657.

Berdnikov, L. N. 2008, VizieR Online Data Catalog, II/285, Sternberg Astron. Inst., Moscow.

Berdnikov, L. N., Dambis, A. K., and Vozyakova, O. V. 2000, *Astron. Astrophys.*, **143**, 211.

Bono, G. 2003, in *Stellar Candles for the Extragalactic Distance Scale*, ed. D. Alloin, and W. Gieren, Lecture Notes Phys. 635, 85.

Bono, G., Caputo, F., Fiorentino, G., Marconi, M., and Musella, I. 2008, *Astrophys. J.*, **684**, 102.

Buckley, D. R. V., and Longmore, A. J. 1992, *Mon. Not. Roy. Astron. Soc.*, **257**, 731.

Catelan, M. 2009, *Astrophys. Space Sci.*, **320**, 261.

Charbonneau, D., *et al.* 2009, *Nature*, **462**, 891.

Clement, C. M., *et al.* 2001, *Astron. J.*, **122**, 2587.

Corwin, T. M., Borissova, J., Stetson, P. B., Catelan, M., Smith, H. A., Kurtev, R., and Stephens, A. W. 2008, *Astron. J.*, **135**, 1459.

Del Principe, M., *et al.* 2006, *Astrophys. J.*, **652**, 362.

Di Criscienzo, M., Caputo, F., Marconi, M., and Cassisi, S. 2007, *Astron. Astrophys.*, **471**, 893.

Di Criscienzo, M., Marconi, M., and Caputo, F. 2004, *Astrophys. J.*, **612**, 1092.

Dolphin, A. E., *et al.* 2001, *Astrophys. J.*, **550**, 554.

Droege, T. F., Richmond, M. W., Sallman, M. P., Creager, R. P., 2006, *Publ. Astron. Soc. Pacific*, **118**, 1666.

Eisenhauer, F., *et al.* 2005, *Astrophys. J.*, **628**, 246.

Feast, M. W. 2010, in *Variable Stars, the Galactic Halo and Galaxy Formation*, Sternberg Astron. Inst., Moscow, 45.

Feast, M. W., Laney, C. D., Kinman, T. D., van Leeuwen, F., and Whitelock, P. A., 2008, *Mon. Not. Roy. Astron. Soc.*, **386**, 2115.

Freedman, W. L., and Madore, B. F. 1996, in *Clusters, Lensing, and the Future of the Universe*, ed. V. Trimble, and A. Reisenegger, ASP Conf. Proc. 88, Astron. Soc. Pacific, San Francisco, 9.

Genet, R. M., Johnson, J. M., and Wallen, V., 2009, *Small Telescopes and Astronomical Research*, Collins Foundation Press, Santa Margarita, CA.

Harris, W. E. 1996, *Astron. J.*, **112**, 1487.

Henden, A. A. 2006, in *Astrophysics of Variable Stars*, ed. C. Sterken, and C. Aerts, ASP Conf. Ser. 349, Astron. Soc. Pacific, San Francisco, 165.

Henden, A. A., and Kaitchuck, R. H. 1990, *Astronomical Photometry*, Willmann-Bell, Richmond, VA.

Henden, A. A., and Munari, U. 2008, *Inf. Bull Var. Stars*, No. 5822, 1.

Henden, A. A., and Sallman, M. P. 2007, in *The Future of Photometric, Spectrophotometric and Polarimetric Standardization*, ed. C. Sterken, ASP Conf. Proc. 364, Astron. Soc. Pacific, San Francisco, 139.

Herrnstein, J. R., *et al.* 1999, *Nature*, **400**, 539.

Hurdis, D. A., and Krajci, T. 2010, *J. Amer. Assoc. Var. Star Obs.*, **38**, 1.

Jacoby, G. H., Morse, J. A., Fullton, L. K., Kwitter, K. B., and Henry, R. B. C. 1997, *Astron. J.*, **114**, 2611.

Kopacki, G. 2005, *Acta Astron.*, **55**, 85.
Kopacki, G., Kolaczkowski, Z., and Pigulski, A. 2003, *Astron. Astrophys.*, **398**, 541.
Kovács, G., and Jurcsik, J. 1997, *Astron. Astrophys.*, **322**, 218.
Kovács, G., and Walker, A. R. 2001, *Astron. Astrophys.*, **371**, 579.
Kubiak, M., and Udalski, A., 2003, *Acta Astron.*, **53**, 117.
Kunder, A., Popowski, P., Cook, K. H., and Chaboyer, B. 2008, *Astron. J.*, **135**, 631.
Landolt, A. U. 1983, *Astron. J.*, **88**, 439.
Landolt, A. U. 1992, *Astron. J.*, **104**, 340.
Lane, D. J., 2007, 96th Spring Meeting of the AAVSO, http://www.aavso.org/aavso/meetings/spring07present/Lane.ppt.
Lane, D., and Gray, P. 2005, *Cent. Bur. Electron. Telegrams*, **224**, 1.
Layden, A. C., and Sarajedini, A. 2000, *Astron. J.*, **119**, 1760.
Le Borgne, J. F., *et al.* 2007, *Astron. Astrophys.*, **476**, 307.
Li, Z. P., and Michel, E. 1999, *Astron. Astrophys.*, **344**, L41.
Macri, L. M., and Riess, A. G. 2009, in *Stellar Pulsation: Challenges for Theory and Observation*, J. A. Guzik and P. A. Bradley, eds., Proc. International Conf., Amer. Inst. Phys. Conf. Proc., 1170, Amer. Inst. Phys., Melville, NY, 23.
Macri, L. M., Stanek, K. Z., Bersier, D., Greenhill, L. J., and Reid, M. J. 2006, *Astrophys. J.*, **652**, 1133.
Macri, L. M., *et al.* 2001, *Astrophys. J.*, **549**, 721.
Madore, B. F., 1982, *Astrophys. J.*, **253**, 575.
Madore, B. F., and Freedman, W. L. 1991, *Publ. Astron. Soc. Pacific*, **103**, 933.
Madore, B. F., and Freedman, W. L. 2009, *Astrophys. J.*, **696**, 1498.
Madore, B. F., and Steer, I. 2007, NASA/IPAC Extragalactic Database Master List of Galaxy Distances, http://nedwww.ipac.caltech.edu/level5/NED1D/intro.html.
Madore, B. F., and van den Bergh, S. 1975, *Astrophys. J.*, **197**, 55.
Majaess, D. J. 2009, arXiv:0912.2928.
Majaess, D. J. 2010a, *Acta Astron.*, **60**, 55.
Majaess, D. J. 2010b, arXiv:1006.2458.
Majaess, D. J., Higgins, D., Molnar, L. A., Haegert, M. J., Lane, D. J., Turner, D. G., and Nielsen, I. 2009c, *J. Roy. Astron. Soc. Canada*, **103**, 7.
Majaess, D. J., Turner, D. G., and Lane, D. J., 2008, *Mon. Not. Roy. Astron. Soc.*, **390**, 1539.
Majaess, D. J., Turner, D. G., and Lane, D. J. 2009a, *Mon. Not. Roy. Astron. Soc.*, **398**, 263.
Majaess, D., Turner, D., and Lane, D. 2009b, *Acta Astron.*, **59**, 403.
Matsunaga, N., Kawadu, T., Nishiyama, S., Nagayama, T., Hatano, H., Tamura, M., Glass, I. S., and Nagata, T. 2009, *Mon. Not. Roy. Astron. Soc.*, **399**, 1709.
Matsunaga, N., *et al.* 2006, *Mon. Not. Roy. Astron. Soc.*, **370**, 1979.
McNamara, B. J., Harrison, T. E., and Baumgardt, H. 2004, *Astrophys. J.*, **602**, 264.
McNamara, D. H., Clementini, G., and Marconi, M. 2007, *Astron. J.*, **133**, 2752.

McNamara, D. H., Madsen, J. B., Barnes, J., and Ericksen, B. F. 2000, *Publ. Astron. Soc. Pacific*, **112**, 202.
Minniti, D., *et al.* 2010, *New Astron.*, **15**, 433.
Mochejska, B. J., Macri, L. M., Sasselov, D. D., and Stanek, K. Z. 2000, *Astron. J.*, **120**, 810.
Mochejska, B. J., Macri, L. M., Sasselov, D. D., and Stanek, K. Z. 2001, arXiv: astro-ph/0103440.
Ngeow, C., and Kanbur, S. M. 2006, *Astrophys. J.*, **642**, L29.
Opolski, A., 1983, *Inf. Bull. Var. Stars*, No. 2425, 1.
Opolski, A. 1988, *Acta Astron.*, **38**, 375.
Paczyński, B. 2006, *Publ. Astron. Soc. Pacific*, **118**, 1621.
Pejcha, O., and Stanek, K. Z. 2009, *Astrophys. J.*, **704**, 1730.
Percy, J. R. 1986, *Study of Variable Stars Using Small Telescopes*, Cambridge Univ. Press, Cambridge, UK.
Percy, J. R. 2007, *Understanding Variable Stars*, Cambridge Univ. Press, Cambridge, UK.
Pietrukowicz, P., and Kaluzny, J. 2003, *Acta Astron.*, **53**, 371.
Pietrukowicz, P., and Kaluzny, J. 2004, *Acta Astron.*, **54**, 19.
Pietrukowicz, P., Olech, A., Kedzierski, P., Zloczewski, K., Wisniewski, M., and Mularczyk, K. 2008, *Acta Astron.*, **58**, 121.
Pietrzynski, G., Gieren, W., Udalski, A., Bresolin, F., Kudritzki, R.-P., Soszyński, I., Szymanski, M., and Kubiak, M. 2004, *Astron. J.*, **128**, 2815.
Pojmański, G. 2002, *Acta Astron.*, **52**, 397.
Pojmański, G. 2009, in *The Variable Universe: A Celebration of Bohdan Paczyński,* ASP Conf. Ser., 403, proceedings of the conference held 29–30 September, 2007, at Princeton University, Princeton, New Jersey, Astron. Soc. Pacific, San Francisco, 52.
Poleski, R., *et al.* 2010, *Acta Astron.*, **60**, 1.
Price, A., *et al.* 2005, *J. Amer. Assoc. Var. Star Obs.*, **34**, 17.
Pritzl, B. J., Smith, H. A., Stetson, P. B., Catelan, M., Sweigart, A. V., Layden, A. C., and Rich, R. M., 2003, *Astron. J.*, **126**, 1381.
Reid, M. J., Menten, K. M., Zheng, X. W., Brunthaler, A., and Xu, Y. 2009, *Astrophys. J.*, **705**, 1548.
Rey, S. -C., Lee, Y. -W., Joo, J. -M., Walker, A., and Baird, S. 2000, *Astron. J.*, **119**, 1824.
Romaniello, M., *et al.* 2008, *Astron. Astrophys.*, **488**, 731.
Saha, A., Thim, F., Tammann, G. A., Reindl, B., and Sandage, A. 2006, *Astrophys. J., Suppl. Ser.*, **165**, 108.
Samus, N. N., Kazarovets, E. V., Pastukhova, E. N., Tsvetkova, T. M., and Durlevich, O. V. 2009b, *Publ. Astron. Soc. Pacific*, **121**, 1378.
Samus, N. N., *et al.* 2009a, VizieR Online Data Catalog, 1, 2025.
Sandage, A. 1958, *Astrophys. J.*, **128**, 150.
Sandage, A., Tammann, G. A., and Reindl, B. 2004, *Astron. Astrophys.*, **424**, 43.

Sarajedini, A., Barker, M. K., Geisler, D., Harding, P., and Schommer, R. 2006, *Astron. J.*, **132**, 1361.
Sawyer, H. B. 1939, *Publ. David Dunlap Obs.*, **1**, 125.
Scowcroft, V., Bersier, D., Mould, J. R., and Wood, P. R. 2009, *Mon. Not. Roy. Astron. Soc.*, **396**, 1287.
Sebo, K. M., *et al.* 2002, *Astrophys. J., Suppl. Ser.*, **142**, 71.
Shobbrook, R. R. 1992, *Mon. Not. Roy. Astron. Soc.*, **255**, 486.
Smith, H. A. 2004, *RR Lyrae Stars*, Cambridge Univ. Press, Cambridge, UK, 166.
Smith, M. C., Wozniak, P., Mao, S., and Sumi, T. 2007, *Mon. Not. Roy. Astron. Soc.*, **380**, 805.
Soderblom, D. R., Nelan, E., Benedict, G. F., McArthur, B., Ramirez, I., Spiesman, W., and Jones, B. F. 2005, *Astron. J.*, **129**, 1616.
Soszyński, I., *et al.* 2002, *Acta Astron.*, **52**, 369.
Soszyński, I., *et al.* 2003, *Acta Astron.*, **53**, 93.
Soszyński, I., *et al.* 2008a, *Acta Astron.*, **58**, 293.
Soszyński, I., *et al.* 2008b, *Acta Astron.*, **58**, 163.
Soszyński, I., *et al.* 2009, *Acta Astron.*, **59**, 1.
Stanek, K. Z., and Udalski, A. 1999, arXiv:astro-ph/9909346.
Steer, I. and Madore, B. F. 2010, NED-D: A Master List of Redshift-Independent Extragalactic Distances, http://nedwww.ipac.caltech.edu/Library/Distances/
Szabados, L. 2003, in *The Future of Small Telescopes In The New Millennium. Volume III—Science in the Shadows of Giants,* T. D. Oswalt, ed., Astrophys. Space Sci. Lib., 289, Kluwer, Dordrecht, 207.
Tammann, G. A., Sandage, A., and Reindl, B. 2003, *Astron. Astrophys.*, **404**, 423.
Tammann, G. A., Sandage, A., and Reindl, B. 2008, *Astrophys. J.*, **679**, 52.
Turner, D. G. 1976, *Astron. J.*, **81**, 1125.
Turner, D. G. 2001, *Odessa Astron. Publ.*, **14**, 166.
Turner, D. G. 2009, in *Stellar Pulsation: Challenges for Theory and Observation*, J. A. Guzik and P. A. Bradley, eds., Proc. International Conf., Amer. Inst. Phys. Conf. Proc., 1170, Amer. Inst. Phys., Melville, NY, 59.
Turner, D. G. 2010, *Astrophys. Space Sci.*, **326**, 219.
Turner, D. G., and Burke, J. F., 2002, *Astron. J.*, **124**, 2931.
Turner, D. G., Majaess, D. J., Lane, D. J., Szabados, L., Kovtyukh, V. V., Usenko, I. A., and Berdnikov, L. N. 2009, in *Stellar Pulsation: Challenges for Theory and Observation*, J. A. Guzik and P. A. Bradley, eds., Proc. International Conf., Amer. Inst. Phys. Conf. Proc., 1170, Amer. Inst. Phys., Melville, NY, 108.
Turner, D. G., Savoy, J., Derrah, J., Abdel-Sabour Abdel-Latif, M., and Berdnikov, L. N. 2005, *Publ. Astron. Soc. Pacific*, **117**, 207.
Turner, D. G. *et al.* 2010, *Mon. Not. Roy. Astron. Soc.*, submitted.
Udalski, A. 2003, *Astrophys. J.*, **590**, 284.
Udalski, A. 2009, in *The Variable Universe: A Celebration of Bohdan Paczyński,* ASP Conf. Ser., 403, proceedings of the conference held 29–30 September, 2007, at Princeton University, Princeton, New Jersey, Astron. Soc. Pacific, San Francisco, 110.

Udalski, A., Soszyński, I., Szymanski, M., Kubiak, M., Pietrzynski, G., Wozniak, P., and Zebrun, K., 1999, *Acta Astron.*, **49**, 223.

Udalski, A., Wyrzykowski, L., Pietrzynski, G., Szewczyk, O., Szymanski, M., Kubiak, M., Soszyński, I., and Zebrun, K. 2001, *Acta Astron.*, 51, 221.

van de Ven, G., van den Bosch, R. C. E., Verolme, E. K., and de Zeeuw, P. T. 2006, *Astron. Astrophys.*, **445**, 513.

van Leeuwen, F. 2007, *Astron. Astrophys.*, **474**, 653.

van Leeuwen, F. 2009a, *Astron. Astrophys.*, **497**, 209.

van Leeuwen, F. 2009b, *Astron. Astrophys.*, **500**, 505.

van Leeuwen, F., Feast, M. W., Whitelock, P. A., and Laney, C. D. 2007, *Mon. Not. Roy. Astron. Soc.*, **379**, 723.

Vilardell, F., Jordi, C., and Ribas, I. 2007, *Astron. Astrophys.*, **473**, 847.

Walker, A. R., and Nemec, J. M. 1996, *Astron. J.*, **112**, 2026.

Welch, D. L., *et al.* 1995, in *Astrophysical Applications of Stellar Pulsation,* R. S. Stobie, and P.A. Whitelock, eds., Astron. Soc. Pacific Conf. Ser., 83, Proc. IAU Colloq. 155 held in Cape Town; South Africa, 6–10 February 1995, Astron. Soc. Pacific, San Francisco, 232.

Weldrake, D. T. F., Sackett, P. D., and Bridges, T. J. 2007, *Astron. J.*, **133**, 1447.

Table 1. Potential calibrators for the Wesenheit template.

Object	*Variable Type*	σ_π/π	*Source VI Photometry*
SX Phe	SX Phe	0.04	van Leeuwen *et al.* 2007 ASAS
V703 Sco	δ Scuti:	0.12	van Leeuwen *et al.* 2007 Balona and Stobie 1983, AAVSO
AI Vel	δ Scuti:	0.03	van Leeuwen *et al.* 2007 Balona and Stobie 1980b, ASAS
VW Ari	SX Phe:	0.07	van Leeuwen *et al.* 2007 TASS
AD CMi	δ Scuti	0.24	van Leeuwen *et al.* 2007 Balona and Stobie 1983, TASS
VZ Cnc	δ Scuti	0.10	van Leeuwen *et al.* 2007 Balona and Stobie 1983, TASS, ARO
RS Gru	δ Scuti:	0.29	van Leeuwen *et al.* 2007 Balona and Martin 1978
V474 Mon	δ Scuti:	0.04	van Leeuwen *et al.* 2007 Balona and Stobie 1980a
RR Lyrae	RR Lyr	0.05	Benedict *et al.* 2002a TASS
UV Oct	RR Lyr	0.33	van Leeuwen *et al.* 2007 ASAS
XZ Cyg	RR Lyr	0.37	van Leeuwen *et al.* 2007 TASS
BN Vul	RR Lyr	0.37	van Leeuwen *et al.* 2007 TASS
VY Pyx	TII Cep	0.09	van Leeuwen *et al.* 2007 AAVSO (this study)
κ Pav	TII Cep	0.12	van Leeuwen *et al.* 2007 Shobbrook 1992, Berdnikov *et al.* 2000
MSB2006 O-38462	TII Cep	0.05	Herrnstein *et al.* 1999 Macri *et al.* 2006
MSB2006 O-07822	TII Cep	0.05	Herrnstein *et al.* 1999 Macri *et al.* 2006
MSB2006 O-11134	TII Cep	0.05	Herrnstein *et al.* 1999 Macri *et al.* 2006
MSB2006 O-28609	TII Cep	0.05	Herrnstein *et al.* 1999 Macri *et al.* 2006
MSB2006 O-29582	TII Cep	0.05	Herrnstein *et al.* 1999 Macri *et al.* 2006

Table continued on next page

Table 1. Potential calibrators for the Wesenheit template, cont.

Object	*Variable Type*	σ_π/π	*Source VI Photometry*
MSB2006 O-31291	TII Cep	0.05	Herrnstein *et al.* 1999 Macri *et al.* 2006
RT Aur	TI Cep	0.08	Benedict *et al.* 2007 Berdnikov *et al.* 2000
T Vul	TI Cep	0.12	Benedict *et al.* 2007 Berdnikov *et al.* 2000
FF Aql	TI Cep	0.06	Benedict *et al.* 2007 Berdnikov *et al.* 2000
δ Cep	TI Cep	0.04	Benedict *et al.* 2002b, 2007 Berdnikov *et al.* 2000
Y Sgr	TI Cep	0.14	Benedict *et al.* 2007 Berdnikov *et al.* 2000
X Sgr	TI Cep	0.06	Benedict *et al.* 2007 Berdnikov *et al.* 2000
W Sgr	TI Cep	0.09	Benedict *et al.* 2007 Berdnikov *et al.* 2000
β Dor	TI Cep	0.05	Benedict *et al.* 2007 Berdnikov *et al.* 2000
ζ Gem	TI Cep	0.06	Benedict *et al.* 2007 Berdnikov *et al.* 2000
l Car	TI Cep	0.10	Benedict *et al.* 2007 Berdnikov *et al.* 2000

Table notes: Unpublished I-band ASAS observations for several calibrators were kindly provided by G. Pojmański (http://www.astrouw.edu.pl/asas/).

There are concerns regarding the photometric zero-point for bright stars sampled in the all-sky surveys (Henden and Sallman 2007; Pojmański 2009).

Colons next to the variable types indicate cases where contradictory designations were assigned in the literature.

Distinguishing between population II SX Phe variables and population I δ Scuti variables on the basis of metallicity alone may be inept granted there are innumerable metal-rich RR Lyrae variables exhibiting [Fe/H] $\geq$ –0.5 (e.g., Feast et al. 2008).

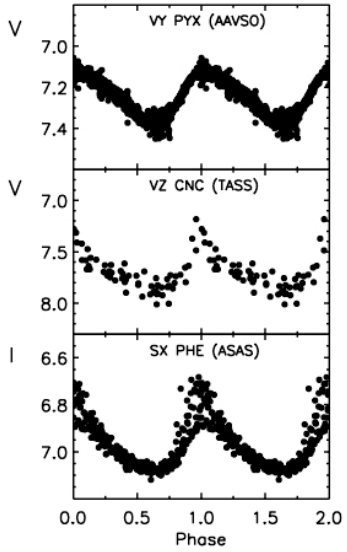

Figure 1. Light curves for a subsample of the objects studied here. Data for the type II Cepheid VY Pyx were obtained via the AAVSO's robotic telescope network. An analysis of that photometry yields the following mean parameters for VY Pyx: $\langle V \rangle = 7.25$ and $\langle V \rangle - \langle I \rangle = 0.67$. VZ Cnc and SX Phe are multiperiodic, and thus the scatter exhibited is only tied in part to photometric uncertainties (Figure 2).

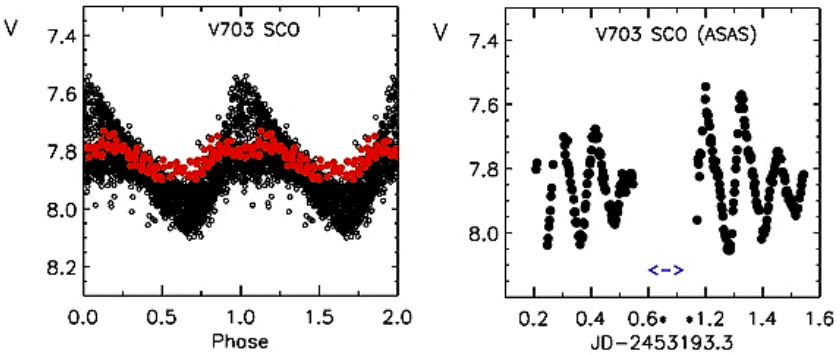

Figure 2. Several variables employed in the calibration (Table 1) are discernably multiperiodic and exhibit pronounced amplitude variations, as exemplified by observations of V703 Sco. Observations for V703 Sco were obtained via the AAVSO's robotic telescope network (overlaid dots) and ASAS. No prewhitening was performed.

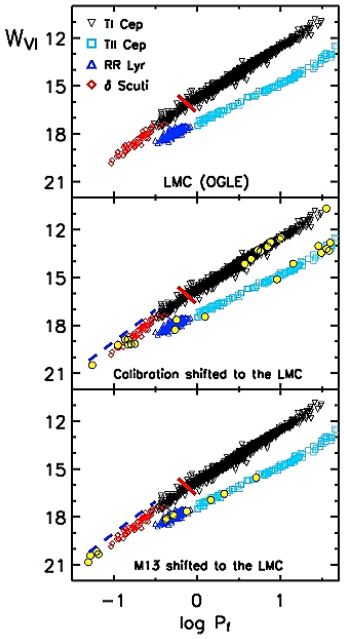

Figure 3. A *VI* Wesenheit diagram characterizing a subsample of the examined data. The distance to the LMC is secured by evaluating the offset from the calibration (middle panel, circles; the size of the datapoints is representative of the uncertainties). The Wesenheit magnitudes of variable stars in globular clusters (e.g., M13, bottom panel, circles) may be compared to the LMC template to derive the zero-point. The dashed line indicates the position of uncorrected δ Scuti stars pulsating in the overtone (see Poleski *et al.* 2010). A break in the classical Cepheid relation near $\log P_f \simeq -0.15$ (short slanted line) may define the δ Sct/Cep boundary (see also Figure 6 in Soszyński *et al.* 2008b, $\log P \simeq -0.3$).

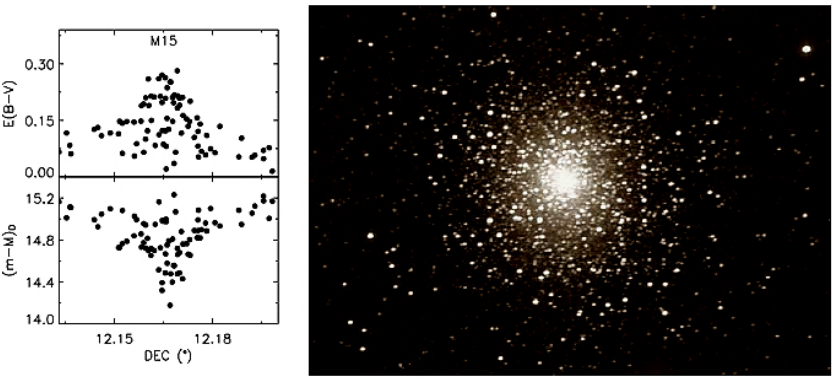

Figure 4. Variables near the core of M15 suffer from photometric contamination. The surface brightness and stellar density increase rapidly toward the core, thereby increasing the likelihood of contamination. Plot on left indicates the distance moduli and color excess for RR Lyrae variables computed via the calibrations of Majaess *et al.* 2009 and Majaess 2010a. Image on right is M15 from the ARO (Lane 2007). M15 is crucial since it is among the most metal-poor Galactic clusters and hosts a planetary nebula (Jacoby *et al.* 1997; Alves *et al.* 2000; Turner *et al.* 2010).

Edward A. Halbach 1909–2011

Gerard Samolyk
P.O. Box 20677, Greenfield, WI 53220; gsamolyk@wi.rr.com

Received April 13, 2011; accepted May 18, 2011

Abstract Edward A. Halbach (1909–2011) was a dedicated, lifelong member of the AAVSO and the Milwaukee Astronomical Society. His service to these organizations, and his valuable contributions to variable star astronomy, are described.

1. Introduction

On March 20, 2011, the longest-term member of the AAVSO and the Milwaukee Astronomical Society (MAS) passed away just short of his 102nd birthday. Ed Halbach is the most significant member in the history of the MAS and a valued and loyal member of the AAVSO. In fact, Ed was one of the most significant amateur astronomers of the twentieth century.

Figure 1. Ed Halbach at the MAS recording box for variable star observations, about 1935. Note AAVSO blueprint charts in side panel.

2. Early years

When Ed Halbach graduated from college and began his engineering career, he looked for an activity to occupy his free time. He felt that most hobbies were way too passive. However in 1932, Ed saw an advertisement in the *Milwaukee Journal* announcing the formation of an astronomical society. Here Ed found an activity into which he could channel his energy.

Ed joined the AAVSO in 1934 and started observing variable stars using the AAVSO's blueprint charts (Figure 1) and a 13-inch reflector located in the backyard of MAS founder Luverne E. Armfield. Ed would continue to observe variables for the next seventy-one years, making 100,715 visual observations. The AAVSO and the MAS were also active in observations of meteors during that time.

In 1936, construction of the MAS observatory began in New Berlin, Wisconsin. Ed would play a key role in this project. At the height of the

depression there was little money available, so the members passed the hat and managed to collect $100 that was used to purchase some used lumber. One of Ed's many talents was the ability to obtain donated material for observatory construction projects (as he used to say, "you need to know how to scrounge"). Concrete for the pier and steel for the dome were obtained.

In 1942, Ed took on the job of observatory director, a position he would hold for the next thirty-five years. During the Second World War, Ed ran an optics shop in the "monastery" building to produce prisms for bombsights. This qualified MAS members for extra gas-ration coupons for observatory access, but observatory use was down significantly during the war.

During this time Ed also served on the AAVSO Council (1940–1943), as 2nd Vice President, and as Chairman of the AAVSO's Auroral Committee (1940–1948). In 1947, Ed was involved in the formation of the Astronomical League and served as the first president of that organization.

Ed married Jane Roth in 1942. They enjoyed sixty-five years together before Jane passed away in 2007. Despite all of Ed's astronomical activities, he always found time for his family. He designed and built a camping trailer so he could take Jane and their six children on cross country trips.

During the 1940s, amateur astronomers became involved in studying the relationship among solar events, aurora, and the magnetic field of the Earth. By comparing observations of solar flares, aurora, and ground currents, Ed was able to predict interruptions in power and communications caused by solar events. This work enabled power companies to prevent interruptions of this type. The MAS was part of a network of astronomers coordinating observations of these phenomena. Cornelius Prinslow, Bill Albrecht, and Ed Halbach, all of the MAS, were featured in an article on the subject in a 1949 issue of *National Geographic*.

Figure 2. Ed Halbach engaged in Project Moonwatch work, 1958.

In the late 1940s and 1950s, Ed became involved in an Air Force project using solar eclipse timings to link the North American datum with the coordinate grids of other continents. This work took him on eclipse expeditions all over the world. The result of much of this work has remained classified to this day.

With the dawn of the space age, the Smithsonian Astrophysical Observatory recruited amateur astronomers to help with tracking satellites in a project called

Moonwatch (Figure 2). Ed got the MAS involved and modified the "monastery" building at the MAS observatory with a pier and slide-off roof to house three satellite tracking telescopes. (The building then became known as the satellite shed). As a result of this work, the MAS predicted and observed the reentry of Sputnik IV in 1962.

Observations of lunar occultations had been going on for decades, but it was not until the mid-1960s that computers became fast enough to accurately predict lunar grazing occultations. Ed got involved with this program at the start. In the process he designed and oversaw the construction of a two-mile cable-and-chart recorder system to facilitate easy recording of these observations. In the early 1970s he led a project to design the 10-inch portascopes, which allowed us to bring larger aperture telescopes to these events. These telescopes were also heavily used in the observation of eclipsing binary and RR Lyr stars from the 1970s through the 2000s. Ed received the Astronomical League Peltier award for his work in lunar occultations.

3. Ed's legacy

In 1977, Ed and Jane decided to retire and move to Estes Park, Colorado. The house that Ed had designed included a rooftop observatory with a 16-inch cassegrain telescope on a modified Springfield mount. He would spend much of his retirement working on this project (Ed always needed to have a project to tinker with). While working on this telescope, Ed used a portable 10-inch telescope in his backyard to continue his occultation and variable star observing.

In addition to Ed's observing, Ed and Jane enjoyed extensive world travel during their retirement. Ed also did volunteer work with Habitat for Humanity. He continued this work until he was well into his 90s.

There are many facets to Ed's legacy. His engineering talent and creativity were at the genius level. He could find an economical solution to almost any problem. His innovations kept the MAS observatory thriving through the depression and a world war. He designed and crafted the drives and setting circles on both A and B telescopes that are still in use today. Those domes continue to function after decades of use.

Ed always looked for opportunities for amateurs to contribute to the science of astronomy and related fields. His energy and enthusiasm was contagious. In 1988, Ed received the AAVSO Merit Award for his long service to that organization.

A significant part of Ed Halbach's legacy was his role as a mentor to other observers. In 1933, Ed met a high school student named Bill Albrecht. Ed took Bill under his wing and it was the start of a close friendship that lasted for over three-quarters of a century. Over the decades that followed, several generations of observers as well as a few professional astronomers were mentored by Ed. At

the 2003 spring meeting of the AAVSO, Ed received the William Tyler Olcott Distinguished Service Award in acknowledgement of this effort. At the same meeting (Figure 3), his wife Jane was credited for "putting up with Ed" during more than sixty years of marriage.

I was a high school student when I first met Ed Halbach. As a young member of the Milwaukee Astronomical Society, I quickly got involved in observatory construction projects. One of the first observing projects Ed got me involved in was grazing lunar occultations, chasing moon shadows all over Wisconsin and northern Illinois. One night Ed gave me my first experience with variable stars. As he was showing me how to observe long period stars, I asked him how many he observed per hour. He told me that he normally observed about fifteen stars per hour but when he had "help" from people like me he got about four. He was always interested in getting new observers started.

Finally, in 1974 came a night that impacted my life. Ed came out to the MAS observatory with a copy of the *AAVSO Circular*. He said "There's an article in here about something called eclipsing binary stars. Let's see what we can do with them." I have been observing EB stars ever since.

In 1980 I took over Ed's old position as observatory director for the MAS. Throughout Ed's retirement we maintained a close friendship and continued to swap information about observing projects. The MAS site always was a special place for both of us; in 2003 Ed made his last visit. I gave him a tour of the new observatories that had been built. He was impressed with the designs of the new sheds and the CCD equipment—it showed how much observing has changed in a single human lifetime.

Figure 3. Jane and Ed Halbach at the AAVSO's 2003 Spring Meeting.

Abstracts of Papers and Posters Presented at the 99th Annual Meeting of the AAVSO, Held in Woburn, Massachusetts, October 29–30, 2010

The AAVSO Centennial Calendar

Elizabeth O. Waagen
AAVSO Headquarters, 49 Bay State Road, Cambridge, MA 02138; eowaagen@aavso.org

Abstract In celebration of the AAVSO Centennial, we have created *A Century of Variable Star Observing: 1911–2010*, a 13-month, full-color calendar that showcases the AAVSO and the people who have made it the dynamic institution it is today.

The 2010 Eruption of U Scorpii

Ashley Pagnotta
3102 Brook Grove Drive, Kingwood, TX 77345; pagnotta@phys.lsu.edu

Abstract We report on the 2010 eruption of the recurrent nova U Scorpii. This outburst was predicted in 2005 and discovered independently by AAVSO observers Barbara G. Harris and Shawn Dvorak on 28 January 2010 as a result of a monitoring program coordinated by our group at LSU in conjunction with the AAVSO. The eruption lasted approximately 64 days, over the course of which more than 35,000 pre-arranged and serendipitous observations were made in all wavelengths from radio to x-ray. We present multi-wavelength light curves (UBVRIJHKby+UV+x-ray) of the entire eruption which show the overall speed of the event, the expected first plateau, the unexpected second plateau, and the return to quiescence. As anticipated, the onset of the optical plateau coincided with the turn-on of the supersoft x-ray emission and the re-emergence of the eclipses. Our comprehensive coverage shows fine-scale phenomena as well, such as flares of up to 0.5 magnitude in amplitude during the initial fast decline which are as yet unexplained and late aperiodic dips (distinct from the well-known eclipses) that are likely caused by accretion disk geometry.

The Latest Results on Accreting Pulsating White Dwarfs

Paula Szkody
Department of Astronomy, University of Washington, Seattle, WA 98195; szkody@astro.washington.edu

Abstract In the last few years, ground- and space-based data on the dozen known accreting pulsating white dwarfs present in cataclysmic variables have produced some surprising results. These include the finding that the instability strip is wider than for non-accreting white dwarfs and that the pulsations can disappear. One of the reasons for the disappearance is the heating of the white dwarf following a dwarf nova outburst, which moves it out of the instability strip. We will show our results from following three systems after their outbursts (GW Lib, V455 And, and SDSS0745+45) and how these objects differ in resuming their pre-outburst pulsation characteristics.

Analyses of "Peculiar" W Virginis Stars in the Milky Way

Doug Welch
100 Melville Street, Dundas, ON L9H 2A3, Canada; welch@physics.mcmaster.ca

Grant Foster
146C Mechanic Street, Westbrook ME 04092; twistor9@gmail.com

Abstract We describe the analysis of light curve data for several candidate "peculiar W Virginis" stars in the field population of the Milky Way. Soszynski *et al.* (2008, 2010) have reported results for the Type 2 Cepheid population from OGLE-III. One of their important findings was a division of the W Vir variables into "regular" and "peculiar" subtypes. The latter are characterized by higher luminosities and a different light curve morphology. Furthermore, the fact that approximately 25% of the sample of "peculiar" W Vir stars were found to be in eclipsing systems suggested that all such stars were in binaries. The orbital periods of the eclipsing or ellipsoidal variations were found to be 10–20 times the pulsation period. Pulsation periods for "peculiar" W Vir stars were found to be between 4 and 10 days in the LMC and between 4.4 and 17.7 days in the SMC, although a claim that such behavior was present in longer-period RV Tau stars was also made. Identifying Milky Way counterparts to "peculiar" W Vir stars would have many potential benefits. The most obvious one is proximity, which allows radial velocity and spectral analysis with intermediate-size telescopes. The number of known or suspected W Vir stars in the Milky Way is large and growing. It would be surprising if there had been no evidence for such behavior in Milky Way stars to date—even if a subclass had not been identified—and indeed it is the case that several stars with similar propertied have been identified. In this paper, we report the time-series analyses of Milky Way "peculiar" W Vir candidates from AAVSO, ASAS-3, MACHO, and SuperWASP photometry in addition to noting binary orbit parameters for the candidates, when known.

RS Sge Observations and Preliminary Analyses

Jerry Horne
3055 Lynview Drive, San Jose, CA 95148; jhorneva@hotmail.com

Abstract New *V-, B-, Ic-,* and *R*-band photometry of RS Sge were obtained using AAVSOnet telescopes and the author's own equipment. Analysis of these new observations allowed a comparison with other previously published observational data. RS Sge was confirmed to be an RVb Tauri type star, showing the characteristic multiple periodic nature of such stars. Observations indicated a fundamental period of 79 days with a longer amplitude modulation of 1,174 days. While RS Sge was being monitored almost nightly for more than 120 days, no eclipses were observed.

Revisiting the Unnamed Fleming Variables

Kristine Larsen
Physics and Earth Sciences, Central Connecticut State University, 1615 Stanley Street, New Britain, CT 06053; larsen@ccsu.edu

Abstract In a 1998 article in *JAAVSO*, Dorrit Hoffleit brought attention to fourteen of the nearly 300 variables directly discovered by Williamina Fleming or discovered under her direction at the HCO. These fourteen stars had not been given permanent designations in the *General Catalogue of Variable Stars* at the time of Hoffleit's article. In the intervening twelve years since the publication of her study, a number of these stars have been further observed, both by AAVSO members and automated telescopes (such as Hipparcos). This poster will revisit these fourteen stars and update their status as variable stars.

Multiple Spiral Branches on Late AGB Stars

Qian Wang
Lee Anne Willson
Department of Physics and Astronomy, Iowa State University, Ames, IA 50011; wqinisu@iastate.edu; lwillson@iastate.edu

Abstract We present some 1-D hydrodynamical models that are capable of generating ring structures around evolved stars. In these models, the pulsation of the star initiates the flow and generates shock waves from a static atmosphere. A secondary period is introduced by an orbiting companion. It creates a series of shocks with different strength. The most energetic one collects all the weak shocks, forming super shocks around the star. The most interesting results are period coupling between pulsation period and orbiting period and multiple spiral

arms in the far zone (>100AU). In the near zone (~100AU), the strong shocks greatly alter the density and temperature structure. This study enriches the possible mechanisms for the morphology of proto-planetary nebulae.

Visual Observations of δ Cephei: Time to Update the Finder Chart

David Turner
Saint Mary University, Department of Astronomy and Physics, Halifax, Nova Scotia, B3H 3C3, Canada; turner@ap.smu.ca

Abstract The current AAVSO finding chart for δ Cephei continues to reflect the notion that visual eye estimates need to refer to reference stars for which the cited visual magnitudes on the Johnson *V* system have been adjusted for a color correction to the eye *V*-system reflecting what is typical of the "average" AAVSO observer. The correction for the best AAVSO observers, however, appears to be negligible, given that the collected phased eye estimates of δ Cep over the past decade (or more) follow a light curve that is greatly suppressed in amplitude from that displayed for Johnson *V*-band data. The author has previously (1999) advocated the use of a modified finder chart for δ Cep that doubles the number of suitable reference stars and eliminates the problem of a suppressed light amplitude in the light curve. As shown here, light curves generated with such a finder chart are also more suitable for studies of period changes in Cepheids like δ Cep using O–C analyses.

Scientific Literacy of Adult Participants in an Online Citizen Science Project

Aaron Price
AAVSO Headquarters, 49 Bay State Road, Cambridge, MA 02138; aaronp@aavso.org

Abstract Citizen Science projects offer opportunities for non-scientists to take part in scientific research. Scientific results from these projects have been well documented. However, there is limited research about how these projects affect their volunteer participants. In this study, I investigate how participation in an online, collaborative astronomical citizen science project can be associated with the scientific literacy of its participants. Scientific literacy is measured through three elements: attitude towards science, belief in the nature of science, and competencies associated with learning science. The first two elements were measured through a pre-test given to 1,385 participants when they joined the project and a post-test given six months later to 125 participants. Attitude towards science was measured using nine Likert-items custom designed for this

project, and beliefs in the nature of science were measured using a modified version of the Nature of Science Knowledge Scale. Responses were analyzed using the Rasch Rating Scale Model. Competencies were measured through analysis of discourse occurring in online asynchronous discussion forums using the Community of Inquiry framework, which describes three types of presence in the online forums: cognitive, social, and teaching. Results show that overall attitudes did not change, $p = 0.225$. However, there was significant change towards attitudes about science in the news (positive) and scientific self efficacy (negative), $p < 0.001$ and $p = 0.035$ respectively. Beliefs in the nature of science exhibited a small, but significant increase, $p = 0.04$. Relative positioning of scores on the belief items did not change much, suggesting the increase is mostly due to reinforcement of current beliefs. The cognitive and teaching presence in the online forums did not change, $p = 0.807$ and $p = 0.505$ respectively. However, the social presence did change, $p = 0.011$. Overall, these results suggest that multi-faceted, collaborative citizen science projects can have an impact on some aspects of scientific literacy. Using the Rasch Model allowed us to uncover effects that may have otherwise been hidden. Future projects may want to include social interactivity between participants and also make participants specifically aware of how they are contributing to the entire scientific process.

Leon Campbell and His Fifty Years at Harvard College Observatory

Thomas R. Williams
1750 Albans Road, Houston, TX 77005; trw@rice.edu

Abstract In traditional AAVSO historiography, Leon Campbell is presented as the first AAVSO Recorder, serving from 1915 to his retirement in 1949. Archival research provides a far more complex story about Campbell's engagement with AAVSO and variable star astronomy over that extended period. In this paper, Campbell's thirty-five years of support for the AAVSO in both informal and formal capacities will, instead, be set in the context of his full time employment on the staff of the Harvard College Observatory.

Artificial Intelligence (AI) Approaches for Analyzing Automatically Zillions of Eclipsing Binary Light Curves

Edward F. Guinan
Astronomy Department, Villanova University, Villanova, PA 19085; edward.guinan@villanova.edu

Abstract Major advances in observing technology promise to vastly increase discovery rates of eclipsing binaries (EBs) as well as other types of variable stars.

For example, missions such as the Large Synoptic Survey Telescope (LSST), the Panoramic Survey Telescope and Rapid Response System (Pan-STARRS), Gaia, and the AAVSO Photometric All-Sky Survey (APASS) are expected to yield hundreds of thousands (even millions) of new variable stars and eclipsing binaries. Current personal interactive (and time consuming) methods of determining the physical and orbital parameters of eclipsing binaries from the current practice of analyzing their light curves will be inadequate to keep up with the overwhelming influx of new data. At present, the currently-used methods require significant technical skill and experience; it typically takes 2 to 3 weeks to model a single binary. We are therefore developing an Artificial Intelligence / Neural Network system with the hope of creating a fully automated, high throughput process for gleaning the orbital and physical properties of EB systems from the observations of tens of thousands of eclipsing binaries at a time. The EBAI project — Eclipsing Binaries with Artificial Intelligence —aims to provide estimates of principal parameters for thousands of eclipsing binaries in a matter of seconds. Initial tests of the neural network's performance and reliability have been conducted and are presented here. Several practical applications also will be presented. This research is supported by the National Science Foundation: Research at Undergraduate Instituions (RUI) Program Grant AST-0507542.

A Web Interface for the DASCH Photometry Database

Edward J. Los
7 Cheyenne Drive, Nashua, NH 03063

Abstract DASCH is "Digital Access to a Sky Century at Harvard," the effort to digitize approximately 530,000 astronomical plates in the Harvard College Observatory collection. We currently have over 900,000,000 magnitude estimates from the 10,000 plates that we have scanned. This paper presents our web photometry interface which allows access to all of our light curves and their underlying scanned images.

A Variable Star Database for the iPhone / iPod Touch

John N. Rachlin
Mark G. McGettrick
260 Winter Street, Holliston, MA 01746; john@diatomsoftware.com

Abstract We present a database of variable stars for the iPhone / iPod Touch mobile platform. In the past 10 years, astronomical and biomedical research has been transformed by the ubiquitous availability of data repositories, and the commensurate opportunities for statistical analysis and data-mining. In order to make such databases accessible to mobile users, we have developed an

application framework that allows us to "mobilize" datasets onto the Apple iOS platform. This framework includes the ability to query the data, sort results, and view the details of individual records. For astronomical applications, we have also developed specific extensions to support object visibility based on the observer's geographical location and date/time. We demonstrate the platform using the International Variable Star Index (VSX) database.

Simple Pulse Width Modulation (PWM) LED Source for Linearity Testing of DSLR Camera Sensor

Helmar G. Adler
40 Mohawk Street, Danvers, MA 01923; eagle.astro@gmail.com

Abstract To create meaningful photometry data knowledge of the linearity performance of the sensor in use (e.g. CCD or CMOS-array) is essential. The emergence of embedded controllers makes it possible—even for the hobbyist — to build fairly low-cost, highly controlled devices with capabilities that can be utilized to make light sources with pulse-width modulated LEDs. A simple system, comprised of a laptop computer, an embedded controller with an LED, and a few additional parts will be shown. Experiences and data regarding linearity testing of the source itself and, subsequently, characterization of a Canon DSLR camera with the source, will be shown. The technique can easily be extended to other sensors. The camera is currently used to take photometry data of epsilon Aurigae.

Solar Astronomy: Plasma Motion Detection At Radio Frequencies

Rodney Howe
3343 Riva Ridge Drive, Fort Collins, CO 80526; ahowe@frii.com

Abstract This article discusses a study of solar plasma motion with a radio receiving system designed to detect plasma motion-riven microwaves, and the initial radio systems analysis to understand the receiving characteristics. A phenomenon of interest in solar astronomy is the increase in temperature from the solar photosphere to the solar corona. This study examines a testable hypothesis for how to measure the different altitudes via a temperature scale of the transition zone (between photosphere and corona) of the sun. When we choose the appropriate frequencies—ones close to the surface, 11.7 GHz, and one above the 2km transition breakpoint at 12.2 GHz—we can test for a couple of possible phenomena: (1) at Extremely Low Frequencies (ELF), we see a Doppler shifting in the phase of plasma motions, and (2) in a polarized recording of data we can measure electromagnetic waves in both electric and magnetic components. The temperatures being measured at 11.7 GHz are approximately

15,000 Kelvin and the temperature at 12.2 GHz is approximately 17,000 Kelvin. The plasma motions between these two temperatures should be a measure of the thermal Doppler motion in the solar plasma as phase differences between the two frequencies.

The Water Tank Observatory

John Pazmino
979 East 42nd Street, New York, New York 11210; john.pazmino@ferc.gov

Abstract New York is still at times written-off as a place for a credible astronomy observatory. It is the ideal place for observing by remote methods, yes, but not for direct observation of the stars in the very sky of the City. This is false myth, and it will be more forcibly so in the next few years. You see, we're planning and designing a new observatory on Manhattan. It will probe supernovae, active galactic nuclei, blackholes, quasars, neutron stars. It will collect data every bit as worthy as from similar observatories in the best of other locations. What's more, to a level unheard of before, this facility taps into an urban resource never intended for astronomy. In fact, the targets mentioned above didn't exist in our profession when this resource began construction some 130 years ago. What about luminous graffiti, or light pollution? The emissions captured by this observatory are in a region of energy that has no competition from terrestrial emissions. It's the energy of the cosmic wind, the flux of atomic nuclei propelled at near lightspeed and crashing into air molecules. We capture the fragments of the collisions and construct the original incoming nucleus. One method of detecting the cosmic wind, or rain from the shower of debris, is by slowing the particles in water and monitoring the resulting Cerenkov emission. Several cosmic rain observatories use this technique, such as the Pierre Auger Observatory in Argentina. We can't in New York build such a facility from scratch—our landscape isn't right for that, apart from the fanatical costs. In a historymaking episode in astronomy that bonds the Stars to the City, we found an alternative, one that literally sits on your roof.